DEVELOPMENT OF AN ION TRAP MASS SPECTROMETER FOR ELEMENTAL ANALYSIS

by

J. A. BERNARD DAIGLE

B. Sc. Chemistry, Université du Québec à Trois-Rivières, 1982

M. Sc. Sciences de l'Environnement, Université du Québec à Trois-Rivières, 1985

A THESIS SUBMITTED IN PARTIAL FULFILLMENT OF
THE REQUIREMENTS FOR THE DEGREE OF
DOCTOR OF PHILOSOPHY

in

THE FACULTY OF GRADUATE STUDIES

Department of Chemistry

We accept this thesis as conforming
to the required standard

THE UNIVERSITY OF BRITISH COLUMBIA

February 1990

In presenting this thesis in partial fulfilment of the requirements for an advanced degree at the University of British Columbia, I agree that the Library shall make it freely available for reference and study. I further agree that permission for extensive copying of this thesis for scholarly purposes may be granted by the head of my department or by his or her representatives. It is understood that copying or publication of this thesis for financial gain shall not be allowed without my written permission.

Department of Chemistry

The University of British Columbia
Vancouver, Canada

Date April 26, 1990

Abstract

Mass spectrometry is a widely used technique for the performance of elemental analysis: not only does it provides excellent limits of detection for a large number of elements, but it is also able to provide information about the isotopic distribution of the analyte. The radio-frequency quadrupole ion trap is a relatively new design of mass spectrometer, which offers the ability to confine charged particles for extended periods of time in a well defined volume by applying a radio-frequency oscillating voltage to an arrangement of three electrodes. A mass analysis of the trapped ions can be obtained by selectively extracting the ions from the cavity of the trap, where they can be detected by an electron multiplier. Despite its unique capabilities, to date the applications of the ion trap mass spectrometer have mostly been restricted to gas chromatography detection. Until recently, there have been very few attempts to use it for any other types of routine analysis.

Our interest lies in the development of an instrument capable of performing a complete mass spectrometric elemental analysis of small volume liquid samples (a few μL) at trace or ultra-trace concentration levels. The ability of the ion trap to accumulate ions in its cavity and to provide an entire mass spectrum of these ions in a single scan of the radio-frequency oscillating voltage applied between the electrodes, makes it a very interesting candidate for the ultra-trace analysis of small size samples. However, to perform an analysis on a sample with the ion trap the sample must first be vaporized; and if an elemental analysis is required, the sample will also have to be atomized. The graphite furnace atomizer used in atomic absorption spectroscopy offers a number of advantages which make it potentially useful for this purpose: it has a high transport efficiency of the analyte from liquid or solid state to the vapour phase, the ionization of the analyte in the furnace is very low (as required by the ion trap) and it handles small volume samples very well. A graphite furnace ion

trap mass spectrometer was designed to fulfil the need of having instrumentation capable of multielemental mass spectrometric analysis of small volume samples containing traces of the analytes of interest.

This document contains a description of the principles of operation of the ion trap as well as a detailed description of the instrument actually built. Data are presented in order to assess the capabilities of the instrument, as well as some of the problems encountered with it. The results obtained with the graphite furnace ion trap mass spectrometer allow us to conclude that the proposed design is not appropriate for the performance of elemental analysis, but is appropriate for mass spectrometric study of low boiling point compounds which can interfere with atomic absorption analysis: it is calculated that these compounds could be analysed at the ppm level.

Promising results obtained with a set up in which the analyte is vaporized directly into the cavity of the ion trap through laser ablation are also presented. These limited results show the potential of this methodology for direct elemental analysis of solid samples.

TABLE OF CONTENTS

LIST OF TABLES

LIST OF FIGURES

ACKNOWLEDGMENT

The development of the instrumentation described in this document would have been impossible without the dedication and the workmanship of the people working in the Mechanical Engineering department and the Electronic shop of UBC Chemistry department. Special recognition has to be given to the work of M. W. Vagg from the mechanical shop for the painstaking work done on the ion trap and to M. Carlisle from the electronic shop for the development and maintenance of the electronic components required to operate the ion trap. We also acknowledge the work done by C. G. Gill mainly on the development of the laser set up used in the laser ablation of samples in the ion trap cavity.

Special thanks to L. L. Burton for reviewing the manuscript of this thesis and for the many suggestions made to improve it.

Many thanks to Dr. M. W. Blades who has been an inspiration for the entire duration of my stay in his laboratory.

The author also acknowledges financial support by "Le fond FCAR pour l'avancement de la recherche et le développement de chercheurs" during part of this project.

Finally, my wife has to be thanked for the patience she showed waiting for the completion of the work I had set myself to accomplish.

LIST OF SYMBOLS

a = acceleration (m s^{-2})

a_x = parameter of Mathieu's equation (dimensionless)

C_{2s} = Parameter of Mathieu's equation

e = elementary charge ($1.6021*10^{-19}$ C)

E = electric field (kg m s^{-2} C^{-1})

E_o = time dependent factor of the field equation (kg m s^{-2} C^{-1})

E_x = component of the electric field corresponding to the "x" co-ordinate of the ion trap (kg m s^{-2} C^{-1})

E_y = component of the electric field corresponding to the "y" co-ordinate of the ion trap (kg m s^{-2} C^{-1})

E_z = component of the electric field corresponding to the "z" co-ordinate of the ion trap (kg m s^{-2} C^{-1})

F = force (kg m s^{-2})

F_r = force applied to an ion along the "r" axis (kg m s^{-2})

F_z = force applied to an ion along the "z" axis (kg m s^{-2})

m = mass of an ion (kg)

q_x = Parameter of Mathieu's equation (dimensionless)

r = "r" cylindrical co-ordinate of position (as measured from the centre of the ion trap) (m)

r_o = radius of the ring electrode of the ion trap (m)

t = time (s)

u = position of an ion inside the ion trap (m)

U = DC potential applied between the ring electrode and the two end cap electrodes (V)

V = amplitude of the RF voltage applied between the ring electrode and the two end caps (V)

x = "x" cartesian co-ordinate of position (as measured from the centre of the ion trap) (m)

y = "y" cartesian co-ordinate of position (as measured from the centre of the ion trap) (m)

z = "z" cartesian or cylindrical co-ordinate of position (as measured from the centre of the ion trap) (m)

z_o = Half the distance that separates the two end cap electrodes of the device (m)

γ = Constant appearing in the field equations (dimensionless)

λ = Constant appearing in the field equations (dimensionless)

ξ = Parameter of Mathieu's equation (radians)

σ = Constant appearing in the field equations (dimensionless)

ϕ = Potential inside the trap (V)

ϕ_0 = Potential applied between the electrodes of the ion trap (V)

Ω = Frequency of the RF voltage applied to the ion trap (radians s^{-1})

CHAPTER I

INTRODUCTION

1.1 - Mass Spectrometry:

Throughout the history of science, advances in our understanding of the world has been inexorably linked to the apparition of new technologies allowing us to probe the world for new information. At the beginning of the twentieth century a preponderance of evidence finally forced all but the most skeptical into accepting the atomic theory of matter. During this time new technology was developed to separate and identify ions according to their mass-to-charge ratios, allowing for the verification of the existence of isotopes of the same element. Soon after this discovery researchers measured the natural abundance of the isotopes of all naturally occuring elements; it marked the beginning of the science of mass spectrometry. With these instruments the sample, which must be in the vapour state, is ionized and the different ions produced are separated according to the ratio of their mass and the number of elementary charges they have acquired during the ionization process. The techniques used to separate the ions can be divided into four major categories of instruments: sector, quadrupole, time-of-flight and Fourier Transform Ion Cyclotron Resonance (FT-ICR) mass spectrometers. Before exploring the operation and potential of the quadrupole ion trap mass spectrometer a brief summary of the principles of operation of the various categories of mass spectrometers will be given.

The sector instruments, which were the first to be used for mass spectrometry, achieve separation of the ions by passing them through a magnetic field. These instruments consist of an ion source, an acceleration stage, a large magnet to enable a separation of the ions and a charged particle detector. The ions are first accelerated to a given energy; they are then made to enter a magnetic field which causes them to take on circular paths that allow for their separation (lighter ions have paths with smaller radii and heavier ones have paths with larger radii). A detector positioned at a given position in the exit plane of the instrument will detect ions of a given mass-to-

charge ratio. Since the radius of curvature of the path of the ions will also be a function of the initial accelerating voltage, a complete mass spectrum can be obtained by varying the accelerating voltage so that each ion of interest will fall on the detector at different times. Another way to obtain a mass spectrum with this type of instrument is through the use of a multidetector system [1].

Quadrupole instruments rely on the stability of the various paths taken by the ions inside a radio-frequency oscillating electric field to separate them on the basis of their mass-to-charge ratios. An oscillating radio-frequency voltage is applied between the electrodes of the instrument; ions entering the electric field created in the instrument will have either a stable trajectory through the field or an unstable trajectory that will project them against one of the electrodes or outside the instrument: only ions with stable trajectories will be able to reach the detector. There are two main types of quadrupole instruments: the quadrupole mass filter and the radio-frequency quadrupole ion trap. In the case of the mass filter, a complete mass spectrum can be obtained by allowing only ions of a given mass-to-charge ratio to pass through the quadrupole, and thus reach the detector; by successively changing the operating conditions of the instrument one can measure the signal from the various species present in the sample.

The time-of-flight (TOF) mass spectrometers work on the principle that ions having different mass-to-charge ratios will take different lengths of time to travel through a field free region, after having all been accelerated through the same voltage. Ions are injected into the device over a very short period of time (μs) to avoid the time spread caused by differences in the initial positions of the ions. The ions will all reach the detector at different times (which makes this instrument very sensitive). The entire process of sampling the gas, ionizing the analyte, separating the ions and detecting them is very fast compared with other MS methods and constitutes one of the advantages of TOF mass spectrometers.

The Fourier Transform Ion Cyclotron Resonance (FT-ICR)[2] mass spectrometer is an ion trapping device. The trapping of the ions is achieved in a cubic cell through the use of a magnetic field and a constant electric field. By applying a voltage pulse to two of the plates of the cell, the ions inside the cavity are excited and accelerated in a spiral path. At the end of the excitation pulse all ions will be cycling with the same radius, but with a frequency dependant upon their mass-to-charge ratio. The rotation of the ions produce a so-called signal current[3] on two of the plates of the cubic cell which are used as detectors. This current is measured and a Fourier transform of this signal produces a mass spectrum. This instrument is unsurpassed as far as resolution and mass range covered are concerned.

Mass spectrometry has developed into a methodology capable of identifying and quantifying the presence of gaseous analytes with high precision and accuracy. Many different analyte sources may be used (GC, plasma, laser ablation, etc.) and the ionization of the analyte can be accomplished in several different manners (electron impact ionization, chemical ionization, photoionization, etc.). There are methodologies which improve our ability to identify unknowns in a sample: mass spectrometry/mass spectrometry (MS/MS) is a technique by which an ion of unknown composition, initially produced and separated in a mass spectrometer, is further fragmented, and a spectrum of the resulting fragment ions can then be taken and used to obtain more information about the structure of the parent ion. MS/MS analysis can be accomplished in space by putting two or more mass analysers in series with a fragmentation cell in between them, or in time by using an ion trapping device.

The device we have chosen to develop into an inorganic mass spectrometer is the radio-frequency quadrupole ion trap which belongs to the family of quadrupole instruments. It offers a number of interesting features which allow it to be developed into an instrument capable of ameliorating the acquisition of the information required for samples that are difficult and costly to analyse with the present technology.

1.2 - History of the Quadrupole Ion Trap Mass Spectrometer:

The 1989 physics Nobel prize has recently been awarded to three scientists including W. Paul and H. G. Dehmelt. They received their prize for the work they have done on the development of ion trapping technology and for the pioneering work they have done on trapped ions. The Nobel prize awarded to these two men is not only a reward for their exceptional work in the field of ion trapping, but is also a recognition of the importance of the instrument they developed to modern science. Early in his work on trapped ions Dehmelt was convinced of the importance of the development of the devices capable of ion trapping; in 1967 he wrote:

> "Experimental attempts to approach the ideal of isolated atomic systems floating at rest in free space for unlimited periods and free from any undesired outside perturbations appears to be worthwhile for a variety of reasons". [4]

At the beginning of the 1950's work accomplished by physicists on strong focussing fields [5] triggered the interest of Wolfgang Paul at the University of Bonn. In a paper published in 1953 [6] Paul and his co-workers showed the usefulness of strong focussing fields to separate ions using a path stability method. During the development of the quadrupole mass filter Paul and his team discovered that a different electrode geometry from the one used in the mass filter was possible. This geometry had the interesting characteristic of applying the focussing field to a charged particle from all directions in space, effectively trapping at its centre all ions having mass-to-charge ratios which allow them to have stable trajectories within the device

(under the working conditions of the instrument). Paul and his many collaborators went on to develop the theory and the instrumentation relating to the quadrupole instruments. Their work lead to the introduction of the monopole mass filter by von Zahn in 1963 [7] and to the development of the QUISTOR (QUadrupole Ion STORe) by Fisher in 1959 [8]. Fisher was the first to describe the use of this device as a mass spectrometer. At this same time Wuerker et al. [9, 10] were using the radio-frequency quadrupole ion trap to study stored microparticles. There are many different appellations for this instrument other than the original (QUISTOR): of these, the ion trap, ion trap detector and ion trap mass spectrometer are the most commonly encountered.

Quadrupole instrumentation revolutionised the field of mass spectrometry by providing the scientific community with compact, low cost, simple instruments that did not require the use of magnetic fields and which also allowed fast scan rates. They also provided scientists with an instrument having the never-before-seen capability to confine charged particles in a well defined volume for extended periods of time, without the use of a magnetic field. The appearance of the trapping instruments triggered the development of new experiments such as the one performed by Dehmelt on the RF spectroscopy of stored ions in 1962 [11]. The ion trap has also been used as an ion reservoir for conventional mass spectrometer [12] and quadrupole mass filters [13]. The ion trap has also been used to study the kinetics of ion/neutral reactions [14], which has led to the use of chemical ionization as a method to produce the ions to be trapped [13]. A remarkable series of experiments were reported in the late 1970s when Neuhauser and his colleagues monitored the presence of barium ions trapped in the centre of a quadrupole radio-frequency ion trap using laser induced fluorescence [15, 16, 17]. This work has led to the observation of a single trapped barium ion as well as to the cooling of ion clouds to a fraction of a degree Kelvin [18, 19, 20, 21].

But, it was only in 1980 that the first application of the ion trap as a tool with the potential to be developed into a routine analytical instrument was developed by Armitage and March [12]; they used it as a detector for gas chromatography. However, due to problems related to the extraction of the ions trapped inside the QUISTOR the device was not developed into a commercially available instrument until, in 1983, Stafford and his co-workers at Finnigan MAT came up with a new and simple method to acquire the mass spectrum of an entire set of ions trapped in the device. Ions of a wide range of mass-to-charge ratio are first trapped in the cavity of the device, they are subsequently extracted selectively from the trap according to their mass-to-charge ratio, and detected by an electron multiplier. The selective extraction of the ions is performed simply by ramping up the amplitude of the oscillating voltage applied between the electrodes of the device. This method was formally presented in a paper published in 1984 [22]. This improvement to the operation of the ion trap quickly caused it to develop into an easy to operate, easy to maintain, relatively inexpensive detector for gas chromatography readily available on the market. Since then, the appearance of various techniques to manipulate the ions trapped inside the ion trap cavity has led to the development of a powerful instrument capable of providing a mass spectrum of the ions present in the trap, performing MS^n analysis and selectively inducing chemical reactions involving ions of a particular mass-to-charge ratio. It has become a very useful instrument for investigating the nature of particular, or of probing unknown, ion/molecule reactions.

Recently the research and development on the ion trap has mainly focussed on improving the resolution, sensitivity, and mass range, and providing the capability to trap externally produced ions [12]. However, to our knowledge, no attempts have been made to use the ion trap in the field of elemental analysis even though the particular features of the instrument make it a good candidate for such development: any analyte that can be vaporized, efficiently transfered to the ion trap and ionized inside the

cavity is a good candidate to be mass spectrometrically analysed with this instrument. In 1987 [23] we proposed to use the ion trap as a pre-concentration chamber and mass spectrometer for performing elemental analysis on small volume samples containing trace levels of analyte. Recently, a paper has been published [24] describing the laser desorption of organic molecules attached to a probe inserted in the cavity of the ion trap, leading the way to the development of an instrument using ion trapping/laser ablation elemental analysis of solid samples. This indicates that there is interest in the development of applications other than that of a gas chromatography detector for this instrument.

The potential of the ion trap has not yet been fully exploited and this instrument may become a centre of attention for the development of instrumentation capable of performing multielemental mass spectrometric analysis on samples that were previously considered difficult to analyse. It has the potential of providing lower limits of detection and higher resolution at a lower cost than the presently available instrumentation.

1.3 - Ion Trapping:

The geometry of the electrodes of the quadrupole radio-frequency ion trap has the same origin as those of the quadrupole mass filter. In the case of the mass filter the instrument consist of four rods installed in pairs parallel to each other, whereas in the case of the ion trap only three electrodes are used (see figure 1.1). One of the electrodes has a "doughnut" shape and is called the ring electrode; the other two are of identical shape to each other and are known as the end caps. The trapping field is created by imposing a radio-frequency potential between the ring electrode and the two end caps. A number of conditions have to be met in order to trap a charged particle in this device (conditions which will be presented and explained in chapter 2).

When ions meeting these conditions are created within the cavity of the device they are trapped, accumulated and can be retained for long periods of time (up to days in some cases).

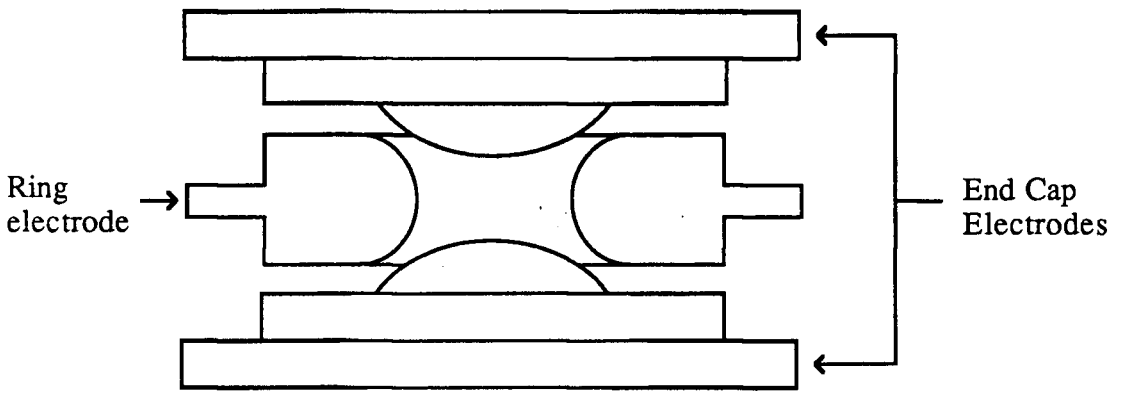

Figure 1.1: Ion trap assembly. Trapping of ions is achieved by applying a radio-frequency oscillating voltage between the two end cap electrodes and the ring electrode.

There are instruments other than the three electrode quadrupole ion trap which are capable of ion trapping. They can be divided into active trapping instruments and passive trapping instruments. The active instruments all use oscillating voltages applied to different arrangements of electrodes to trap the charged particles. The passive instruments rely on constant magnetic or electric fields (or both) to confine the ions. The field created in the three electrode radio-frequency quadrupole ion trap has been approximated by devices made of wire mesh [25] and by less than ideal electrode geometries to produce trapping fields: cylindrical traps [26, 27, 28, 29,30] as well as traps made with spherically shaped electrodes [31] have been used successfully. A hexapole cell has also been described by Todd and Lawson [32]. Other devices have been designed to contain ions in a much larger space; these instruments use electrode

designs similarly to the ones found in the quadrupole mass filter, but the rods are bent into the shape of a circle [33] or a "race track" [34]. There also exists a six-electrode trap using six planar sheets of metal between which RF voltages are applied to create a trapping field [34].

In the category of the passive trapping devices one can find the orbiton [35] which uses an electrostatic field to contain the ions, the omegatron which uses both a magnetic and an electric field to contain the ions while an RF oscillating field is used to stimulate their cyclotron motion and detect them [35]. The Penning trap [12] uses an electrode assembly similar to that of the ion trap but instead of using an oscillating electric field it uses both a DC electric field and a magnetic field to trap the ions. The cubic cell[36] used in ion cyclotron resonance mass spectrometers [37] and Fourier Transform Ion Cyclotron Resonance mass spectrometers [38] is made of six rectangular plates (a magnetic field and a DC electric field are used to confine ions in the device). The electron beam trap can trap the positive ions created within the beam in a potential well formed by its space charge [35].

Of all these trapping devices the cubic cell used in the FT-ICR mass spectrometer and the radio-frequency quadrupole ion trap have stimulated the most interest in the field of analytical chemistry. The FT-ICR mass spectrometer has evolved into one of the most powerful instruments of modern mass spectrometry. The resolution obtained with this instrument is second to none in the field of mass spectrometry [39].

The ion trap mass spectrometer cannot compete with the resolution obtained with the FT-ICR instruments. However, it offers two advantages over the FT-ICR instruments. The ion trap does not require the presence of a magnetic field to confine the ions and its cost is relatively low: the price of an ion trap detector can be as low as 50,000 dollars. The ion trap is also very versatile: it can use many methods of ion creation such as electron impact ionization, chemical ionization and photoionization.

The instrument can be operated in such a way that only ions with a given mass-to-charge ratio will be contained, or it can be operated so that ions of widely different mass-to-charge ratios will be contained. It also offers MS/MS capabilities. The motion of ions of a given mass-to-charge ratio can be thermalized so as to induce a reaction between these particular ions and neutrals present in the system. From a set of many different trapped ions the instrument is able to expel ions of a given mass-to-charge ratio from its cavity without losing the other ones. With the commercial instrumentation available now, ion detection is done externally with an electron multiplier, but approaches such as Fourier transform and spectroscopic methods are currently being developed to detect the presence of the ions without removing them from the trap [12].

The instrument is very compact: in all cases the mass spectrometer and ion detector make up only a very small part of the instrument; the vacuum system and the electronics occupy a much larger volume than the ion trap itself. The ion trap also offers the possibility of studying negative ions as well as positive ones.

There are limitations to the possibilities that the ion trap can offer. The ion density that can be contained in the trap is around 10^6 cm^{-3} [40, 12], which may impose limits on the dynamic range of the instrument. There is also the fact that ions must be created within the cavity of the ion trap. Although there is much work being done in the field of externally created ion trapping, a practical methodology has not yet been developed. The upper mass range that can be analysed using the "mass selective instability" mode of operation of the instrument (generally adopted on these devices) is limited by the voltage output of the RF power supply to the ring electrode. Some new scanning methodologies are currently being considered for solving this problem [12]. Ion/neutral reactions can also pose a major problem if a high pressure inside the ion trap container is used or if long storage times are required [41]. There is also the difficulty of producing the hyperboloid surfaces forming the electrodes. If only very

short storage times are required, imperfections in the electrodes can be tolerated; but if long storage times are required, imperfections in the trapping field caused by manufacturing flaws are experienced by the trapped ions at every cycle of their trajectories causing the rapid loss of ions from the trap.

1.4 - Ion Trap, Applications and Possibilities:

Today's most important application of the ion trap is its use as a mass spectrometer in a GC/MS system. The "Ion Trap Detector" sold by Finnigan MAT is dedicated solely to this application, while their more versatile "Ion Trap Mass Spectrometer", although capable of using other sources of sample, is also mostly used as a sophisticated detector for gas chromatography. The two instruments have been used (GC-ITD and GC-IMS) in applications ranging from pollutant identification and monitoring to research on biological molecules [12]. The ion trap has also been used as an ion reservoir for conventional sector instruments and quadrupole mass spectrometers. Todd et al. [13] have shown that when chemical ionization is employed, the ion trap can be used at much lower pressures than is possible with most conventional chemical ionization cells. Their experiments involved the use of the ion trap to study chemical ionization by accumulating the charged products of the studied reactions. The ions stored in the trap were then pulsed out of it to a quadrupole mass filter to produce a mass spectrum of the reaction products.

The idea to use the ion trap as a holding tank and to detect the ions externally was first presented in a paper by Dawson and Whetten [42] in 1967. In their experiments they trapped ions of a given mass-to-charge ratio for a period of time before pulsing them out of the trap, where they were then detected by an electron multiplier positioned outside one of the two end caps. By repeating the process while slightly changing the value of the trapping parameters so ions of a slightly different

mass-to-charge ratio would be trapped, they were able to obtain mass spectra of the background gas present in their system.

This same idea of trapping ions in the cavity of the trap and detecting them outside the instrument is still the most common method of using the ion trap mass spectrometer. The main improvement over the original idea is in the methodology used to withdraw the ions from the device. The method now used was developed by Stafford et al. [22] and involves the trapping of ions with mass-to-charge ratios covering a broad range of values. The detection is then accomplished by selectively extracting the ions according to their mass-to-charge ratio; a complete mass spectrum of the many ions present in the trap can be obtained in a single scan of the RF potential applied between the electrodes. This method of obtaining mass spectra will be explained in detail in chapter 3. This improvement of the operation of the ion trap makes the acquisition of a complete mass spectrum of the ions present in the trap much easier and much faster.

The ion trap has also been extensively used to study ion/neutral reactions [12, 43, 44]. Since the reacting ions are trapped until they react or until they are withdrawn from the trap (and since the charged reaction products can be trapped as well) this instrument is very useful for the study of such reactions [45, 46]. The next step in using the ability of the ion trap to contain the charged products of a chemical reaction between an ion and a neutral particle is to transform the neutral analyte of interest into an ion using a chemical ionization reaction. This technique was first used by Bonner et al. in 1972 [13]. This technology has continued to evolve and today's instrumentation offers the possibility to use both electron impact and chemical ionization as a means of creating the ions to be trapped. There are also reports showing the possibility of using photoionization as a means to create the analyte ions [47, 48, 49].

The ion trap also offers the possibility of performing MS^n analysis [12]. In this technique the original analyte is ionized and fragmented while the trapping conditions are set so ions of a single mass-to-charge ratio are trapped. The trapping conditions are then restored to values allowing the trapping of ions of a wide range of mass-to-charge ratios. The single mass ions still trapped can be fragmented by an electron beam and a mass spectrum of the ions created by the fragmentation can then be obtained (or if further information is required on one of the ions produced during this second fragmentation period the trapping conditions can be changed to allow only the ion of interest to remain in the trap; these ions can be fragmented again with the electron beam and a mass spectrum can be obtained). This procedure can be repeated "n" times. The limitation on the number of times this procedure can be repeated comes from the fact that the number of ions left in the trap diminishes at every step until the number of ions present after a fragmentation is not sufficient to produce a detectable signal.

Because of its unique capabilities the ion trap has been used in a number of very exciting experiments not directly involving its operation as a mass spectrometer. Amongst these experiments the most exciting are certainly those aimed at studying only a few atomic ions present in the cavity of the device. From the early work done by Newhauser, Dehmelt, Hohenstatt, Toschek and others in the late 1970's and at the beginning of the 1980's [14, 17-21, 50-57] concerned with the trapping and observation of the lowest possible number of ions at the centre of the ion trap, to the studies of the ordering of cooled ions in a crystal like arrangement at the centre of the device [58, 59], ion trapping devices (mainly the Penning trap and the RF quadrupole ion trap) have allowed scientists to obtain information not previously available. Optical observation of a single trapped ion has been achieved [18, 19, 50, 51, 60], ions have been cooled to a few thousandth of a degree Kelvin [51] and quantum jumps have been observed for a single trapped mercury ion [60]. Most of these observations are done using the

following procedure: the atoms of interest are initially produced in an oven located near by the trap; the atoms produced by the oven migrate and some of them are ionized and trapped. A laser beam passing through the centre of the trap and tuned at a frequency corresponding to a transition of the ion of interest excites the trapped ions to a higher level and the fluorescence from this ion is observed. Work done by Newhauser and his co-worker using this technique has led to the visual observation of a single barium ion [18, 19].

Most of the recent interest in the development of the ion trap has focused on the achievement of lower limits of detection, higher resolution, wider mass range coverage, better accuracy and precision, MS^n capability, mass selective extraction of ions and mass selective thermalization of ions. The development of new fields of applicability of the device in the analytical laboratory has been limited to the study of relatively volatile analytes, however the characteristics of the ion trap make it applicable to much wider variety of analysis. Furthermore, to date the use of the ion trap mass spectrometer has been limited to the study of organic materials, although mass spectrometry is widely used in inorganic analysis as a detector for inductively coupled plasmas, spark sources, glow discharges and laser ablation [61], the quadrupole ion trap mass spectrometer has not yet been utilized in inorganic mass spectrometry. But, its ability to accumulate analyte makes it a potential candidate for elemental analysis of low concentration, small size samples: a situation often encountered in inorganic analysis.

The requirements for performing an analysis with an ion trap are that the sample can be atomized, carried efficiently to the cavity of the trap (or be atomized into the cavity of the trap) and ionized at the centre of the cavity (it is believed by the author that the current technology for trapping externally produced ions has not yet reached a level from which it can be used in a routine instrument, it is still at the developmental stage). The only requirements for the instrumentation used to vaporize

the sample are that it does so efficiently and, if possible, is free from chemical interferences. The analyte should also emerge from the vaporization stage as a neutral, and not as an ion, so that it can be trapped. If a transfer line is required between the source of analyte and the ion trap the line should allow for an efficient transfer of the analyte and should not induce chemical changes during the transfer. The work done by Heller et al. [24] and by the author of this document shows that vaporization of a sample directly into the cavity of an ion trap is a very efficient way for obtaining the analyte in the trap. Although only laser ablation has been used so far, thermo-electrical vaporization is potentially an interesting candidate for the vaporization of sample directly into the cavity of the ion trap. As mentioned earlier, the ionization step can also be accomplished by many different means: electron impact ionization, chemical ionization or photoionization could all be used. The operator could also have the choice of detection methods for the trapped ions. The most commonly employed method of detection consists of extracting the ions from the trap and detecting them using an electron multiplier. The extraction of the ions can be carried out by applying a voltage pulse to the end cap electrodes to pulse out the ions; this method is used mostly when ions of a single mass-to-charge ratio are trapped. They can also be extracted using the "mass selective instability" [22] method of extraction. Moreover, analytical chemistry could greatly benefit from the exploration of applications of the ion trap which do not imply its use as a mass spectrometer. The work done by Neuhauser and his colleges [18, 50] on the fluorescence of trapped ions may certainly inspire the use of this device as an ultra-trace analysis instrument using fluorescence as a means of detection of the ions. Other methods of in-situ detection such as Fourier transform methods [12] may also develop into usefull methodologies to detect the trapped ions.

The ion trap could also be developed into a detector capable of catering to many sources of analyte at the "flick of a switch". For example, an ion trap could serve as a

mass spectrometric detector for a gas chromatograph, as a liquid chromatograph, as a source of atoms and for laser ablation system. It could also be used as a preconcentration cell: an analyte present at ultra trace levels in a sample could be carried to the cavity over a long period of time to build up its concentration in the trap. This would allow for higher sensitivity and lower limits of detection. Although the ion trap has been used for many interesting applications, there are still many situations where its ion trapping capabilities could be used to obtain information about a sample with more ease than with existing instrumentation.

1.5 - Graphite Furnace:

The graphite furnace, which is used as an atom reservoir for atomic absorption spectroscopy, provides the analyst with one of the most sensitive techniques available for elemental analysis today (figure 1.2). The instrument is made of a carbon tube (or cup) in which a small sample (in the μL range) is deposited; resistance heating of the graphite tube is used to dry, ash and vaporize the sample. The graphite tubes are coated with pyrolitic graphite to prevent migration of the liquid sample into the walls of the tube. The vaporization/atomization stage of the experiment is generally performed at temperatures ranging from 2000 - 3000 ^{o}C. The percentage of analyte atoms being ionized during the atomization step is generally low (this will differ according to the element studied) because of the relatively high electron density in the graphite tube [62].

The success of graphite furnace atomic absorption spectroscopy comes from its high efficiency in transporting the analyte to the analytical area and the long residence time of the analyte in the analytical zone of the instrument. These two features provide very high sensitivity and low limits of detection. The residence time of the analyte in the analytical zone varies between approximately 0.1 and 0.6 s [63, 64]. In

comparison, the residence time of the analyte in the analytical zone of a standard flame is of the order of 10 ms [64] and in an ICP it is around 1 ms.

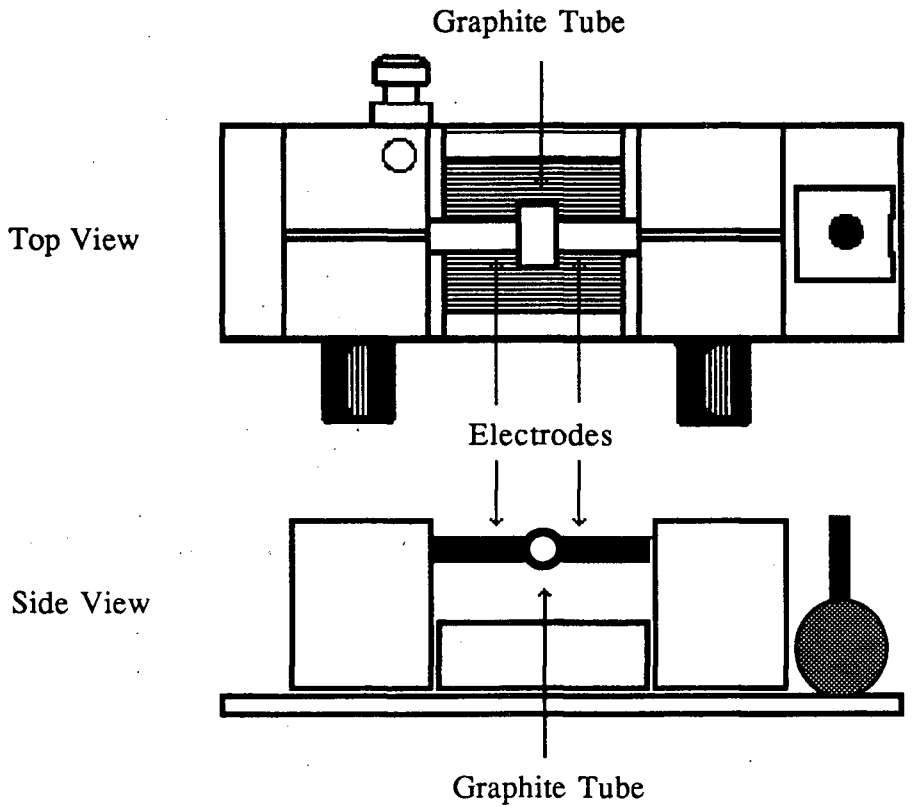

Figure 1.2: Diagram of a graphite furnace.

Mass spectrometric studies of the vapour produced in a graphite furnace have helped in the understanding of the various vaporization mechanisms [65-68]. There have been no reports on the utilization or development of an instrument coupling the graphite furnace atomizer with a mass spectrometer to perform routine analytical analysis.

Despite the advantages offered by the graphite furnace for elemental analysis it is not exempt of problems, the most important being chemical interferences (mainly

the formation of analyte-containing molecules more volatile than the atomic analyte) . The importance of this problem can be seen by the emphasis placed by the manufacturers on the use of chemical modifiers for graphite furnace analysis (Spring atomic absorption workshop 1989, Varian, 1989). There has been a massive amount of work on chemical interferences in graphite furnaces. One of the interesting ways which has been used to study these interference is the mass spectrometric approach; in these studies the graphite furnace is placed in a vacuum in front of a mass spectrometer, where it is heated. The vapour escaping from the furnace is sampled and analysed by the spectrometer. Generally a quadrupole mass filter is used to perform the mass analysis, therefore for each firing of the graphite furnace the mass spectrum obtained covers a narrow mass range.

The use of mass spectrometry to study the vaporization of analyte from the graphite furnace allows one to identify and quantify the interference problems encountered in graphite furnace atomic absorption. These experiments have shown the formation of carbide, the vaporization of molecular species, the formation of oxides and the vaporization of the furnace material during the heating process. Observing the vaporization products as a function of the temperature has allowed researchers to witness the disappearance of the analyte through the formation of low boiling point molecular species early in the heating stage. They could also observe the thermal decomposition of molecular species into atomic species when the temperature inside the graphite reached high enough values. The use of this methodology has also helped in the understanding of the effect of matrix modifiers [69] which either convert the analyte into a more stable compound having a higher boiling point (allowing the elimination of the formation of volatile molecules between the analyte and the interferent) or convert the interferent into a more volatile form (so that it can be eliminated from the system before the atomization of the analyte) [70].

1.6 - Graphite Furnace/Ion Trap Mass Spectrometer:

The ion trap was chosen to develop into an inorganic mass spectrometer because it was believed that some problems commonly encountered in elemental analysis could be best resolved if an instrument capable of trapping the analyte was available. The difficulties we wanted to address with the development of this instrument were the mass spectrometric analysis of small volume liquid samples, the analysis of elements present at ultra-trace levels in solution and the direct mass spectrometric analysis of solid samples.

The choice of the graphite furnace as the source of analyte for the ion trap mass spectrometer, to address the two first difficulties listed above, comes from the following characteristics of the graphite furnace: it has the ability to handle small sample volumes, it has a very high efficiency of transforming the sample from the liquid state to vapour, it provides a relatively long residence time of the vaporized analyte in the furnace and it produces a low percentage of ionized analyte species.

Although there have been reports of the transfer of analyte from electro-thermal vaporizers [71] to a plasma, the situation faced in the development of our instrument is quite different. The graphite furnace and the sampling interface must be positioned in such a way that air will be excluded so as to avoid the oxidation of the vapour emerging from the graphite furnace and the entrance of air into the mass spectrometer enclosure. The ion trap is not able (in practical cases) to trap ions which have been produced outside the cavity, so the analyte cannot be channelled to the mass spectrometer using electrostatic fields; only mass flow due to the difference in pressure between the ion trap enclosure and the graphite furnace is available for mass transport. The vapour produced at high temperature in the graphite furnace will tend to condense rapidly if it encounters cold surfaces. The design of the interface should take this into consideration: it should be short and ideally the analyte should have a

straight path between the source and the mass spectrometer. The analyte should also be carried as close as possible to the centre of the ion trap where the ionization and the trapping efficiencies are the highest. For practical reasons there should also be a way to stop the flow of gas entering the ion trap container. The increase in pressure inside the trap container during the sampling of the analyte must be kept low enough to prevent damage to the detector. All these considerations were taken into account in the development and construction of the instrument described in chapter 3.

The development of an ion trap mass spectrometer coupled with a graphite furnace could also lead to improved research facilities for the study of vaporization processes in graphite furnaces. The characteristics making the ion trap an attractive instrument for this purpose are its ability to accumulate the ions before the mass spectrometric analysis is performed and the fact that it produces spectra covering a wide mass range of ions in a single scan.

1.7 - Laser Ablation/Ion Trap Mass Spectrometry:

During our survey of the possible methods of producing elemental vapour and transfering it to the ion trap for mass spectrometric analysis, we looked at the possibility of performing laser ablation on a solid sample positioned inside the cavity of the ion trap. This would solve the problem of having to dissolve solid samples before performing elemental analysis on them. Although this idea occured early into the project it was only toward the end of the project that the equipment and the know-how were available for the development of the experimental set up. The potential offered by a laser ablation ion trap mass spectrometer comes from the direct sampling possibilities of laser ablation, the multielemental capability of the mass spectrometer

and the ability to obtain isotopic information on the ions produced with a single laser pulse. The system is also potentially very efficient in the transport of analyte to the analytical zone. Laser ablation is an effective way to analyse solid samples, both for bulk properties and for micro-analysis of local attributes of the material - the laser makes possible the vaporization, excitation and ionization of the solid material. Laser ablation mass spectrometry has been used as an analytical method since the appearance of the laser in the early 1960's. Most of the instrumentation now available in the field of laser ablation mass spectrometic analysis is based on time-of-flight mass analysis [61] or on large instruments using photoplate detectors to obtain a wide mass range capability for analysing most of the ions produced by the laser beam [72]. Laser ablation mass spectrometry offers its user the ability to perform multielemental analysis on conducting or non-conducting solid samples with detection limits of about 0.01 to 0.1 ppm [73]. The sample preparation for such analysis is minimal, and this is an important advantage over techniques such as ICP-MS.

The advantage offered by the ion trap in laser ablation analysis comes from the fact that ions can be trapped and accumulated in the cavity of the ion trap before analysis, which could lead to improved limits of detection. The various ion manipulation techniques available with the ion trap allow the analyst to accumulate some of the low level analytes of interest over many laser pulses, while ions coming from the bulk of the material would not be accumulated. A laser ablation mass spectrometer built with an ion trap would also be a much more compact instrument than those currently available.

The ion trap mass spectrometer has also been used in laser desorption mass spectrometric analysis of organic materials [24]. Heller et al. modified an "Ion Trap Detector", manufactured by Finnigan MAT, to enable the insertion of a probe through the ring electrode, inside the cavity of the ion trap. The instrument was further modified to allow the passage of the laser beam through the ring electrode, across the

cavity onto the probe. They noticed that at higher laser powers the larger amount of material desorbed from the probe caused saturation of the trap. They clearly demonstrated the potential of this instrument for laser desorption mass spectrometric analysis.

1.8 - Scope of This Thesis:

The motivation behind the development of this project came from the belief that the use of the ion trap as a mass spectrometer, or as an ion reservoir in other types of analysis, could provide new technology to solve analytical problems that are presently difficult or very costly to solve. The problem of most interest to us was the mass spectrometric analysis of trace level elements in small size samples (in the μL range). At the present moment, graphite furnace atomic absorption spectroscopic methods offer some answer to this problem, but it is only a single element method so that if the amount of sample is limited one has to choose which element is the most important to be analysed. Although other methods of performing ultra-trace multielemental analysis on small sample volumes are being developed [74, 75], the ion trap offers the advantage of not only giving a complete multielemental analysis of the small sample volume, but also of providing information about the isotopic distribution of the elements present in the sample.

Another purpose for the ion trap that was originally planned was its use as an ion reservoir to concentrate analytes for the subsequent performance of fluorescence spectroscopy on them; this technique could be developed into a method of analysis capable of measuring very low levels of analytes. Although this is one of the areas in which this laboratory wants to develop instrumentation in the future, it was beyond the scope of this work to fulfil this task.

The thesis presented here constitutes the presentation of the work done in the first step of a long term project. It will first present the principle of ion trapping with a quadrupole ion trap as well as the system designed and built in our laboratory; it will also present data demonstrating the capability of the ion trap mass spectrometer, as well as data aimed at improving the understanding of the behaviour of the mass spectrometer. A chapter presenting the results obtained during the attempts at performing elemental analysis using a graphite furnace/ion trap mass spectrometer system and a laser ablation/ion trap mass spectrometer is also included. In the last section the conclusions drawn from our work will be outlined along with some of the future avenues that this project should take. Improvements to this instrumentation which could be of some importance to the development of inorganic ion trap mass analysis will be discussed.

CHAPTER II

THEORY

2.1 - Introduction:

The theory relating to the trapping of ions in quadrupole ion traps has been amply described in the literature. For a complete description of the theory a recent text edited by March and Hughes [12] is recommended.

Trapping of the ions in the quadrupole radio-frequency ion trap is accomplished by the creation (inside the device) of an electric field which imposes a force on the ions present in the cavity which increases in proportion to the distance from the centre of the trap. The doughnut shaped ring electrode and the end cap electrodes have hyperboloid shaped surfaces that impose a geometry to the electric field that permits the long storage times. This chapter will present a general description of the quadrupole field created in an ion trap as well as the equations describing the motion of the ions in the trap and a description of the field found in the device constructed in this laboratory.

2.2 - The Spatial Description of the Quadrupole Field:

The derivation of the equations describing the spatial distribution of the quadrupole field and the geometry of the electrodes assumes that the system is operated in the classical way, with a potential ϕ_o being applied to the ring electrode and $-\phi_o$ applied to the end cap electrodes.

Quadrupole instruments are built with a geometry which imposes a strong focussing field on the charged particles. In the Cartesian coordinate system, the linear dependence of the field on the position in the device can be expressed as:

$$E = E_o(\lambda x + \sigma y + \gamma z) \qquad (1)$$

where $x = y = z = 0$ defines the centre of the trap and λ, σ and γ are constants of the system and E_o is a time dependent factor. The force applied by the field on a singly charged particle is given by:

$$F = m\,a = eE \qquad (2)$$

and, as indicated by equation *(1)*, this force becomes greater as the charged particle moves away from the centre of the field. Application of the Laplace condition, $\nabla E = 0$, yields the following relationship between the constants of equation *(1)*:

$$\lambda + \sigma + \gamma = 0 \qquad (3)$$

In the case of the mass filter equation *(3)* is satisfied by:

$$\lambda = -\sigma \qquad \text{and} \qquad \gamma = 0 \qquad (4)$$

For the quadrupole ion trap equation *(3)* is satisfied by:

$$\lambda = \sigma \qquad \text{and} \qquad \gamma = -2\sigma \qquad (5)$$

An instrument built with these specifications will have symmetry around the "z" axis. The form of the potential that has to be applied can be found by integration of the field since:

$$E_x = -\frac{\partial \phi}{\partial x} \qquad E_y = -\frac{\partial \phi}{\partial y} \qquad E_z = -\frac{\partial \phi}{\partial z} \qquad (6)$$

and:

$$E = E_x + E_y + E_z \qquad (7)$$

so the potential "ϕ" is obtained by integrating equation *(1)*. We obtain:

$$\phi = \frac{-1}{2} E_o(\lambda x^2 + \sigma y^2 + \gamma z^2) \qquad (8)$$

For the quadrupole ion trap, for which equation *(5)* applies, when using $\lambda = 1$, we obtain:

$$\phi = \frac{-1}{2} E_o(x^2 + y^2 - 2 z^2) \qquad (9)$$

In the xz plane ($y = 0$) the resulting equation is :

$$\phi = \frac{-1}{2} E_o(x^2 - 2z^2) \qquad (10)$$

This equation can be used to obtain a two dimensional diagram of the equipotential lines created by the electric field of the radio-frequency quadrupole ion trap. Figure 2.1 presents a diagram of the equipotential lines inside an ion trap.

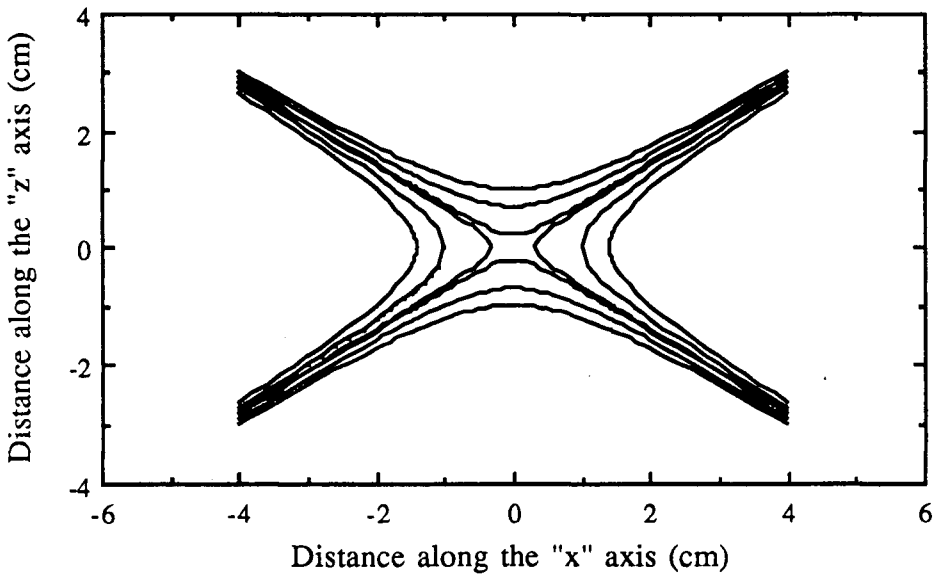

Figure 2.1: Diagram of the equipotential lines in the radio-frequency quadrupole ion trap.

2.3 - The Geometry of the Electrodes:

To produce the quadrupole field described in the previous section, the surface of the electrodes of the trap must have a geometry following the hyperboloid shape of the equipotential lines of the field described by equation *(10)*. Since the instrument will have rotational symmetry about the "z" space axis, we can express our equations in cylindrical coordinates. Equation *(9)* becomes:

$$\phi = \frac{-1}{2} E_o (r^2 - 2z^2) \qquad (11)$$

where "r" is the distace from the centre of the trap along the x, y plane of the device. We can express equation *(11)* as a function of the potential ϕ_o applied between the electrodes (the relationship between E_o and ϕ_o can be found by considering the situation at the position $r = r_o$ (r_o is the radius of the ring electrode), $z = 0$):

$$\phi = \frac{\phi_o}{r_o^2} (r^2 - 2z^2) \qquad (12)$$

One way to obtain a field with zero force applied, at all times, to the ions positioned at the centre of the device is to set the relationship between the radius of the ring electrode, r_o, and the distance between the two end caps, z_o, to:

$$r_o^2 = 2z_o^2 \qquad (13)$$

The equations describing the surface of the three electrodes can be derived from equation *(12)*. At the surface of the ring electrode we have:

$$\phi = \phi_o \qquad (14)$$

In this situation equation *(12)* becomes:

$$\frac{r^2 - 2z^2}{r_o^2} = 1 \qquad (15)$$

and at the surface of the end cap electrodes we have:

$$\phi = -\phi_o \qquad (16)$$

so we can write:

$$\frac{r^2 - 2z^2}{r_o^2} = -1 \qquad (17)$$

Equations *(15)* and *(17)* describe the surface of the electrodes. These equations describe a one sheet hyperbole (for the ring electrode) and a two sheet hyperbole (for the end cap electrodes). Figure 2.2 shows a two dimensional diagram of the electrodes of the ion trap. These curves are rotated about the "*z*" axis to produce the surfaces of the electrodes.

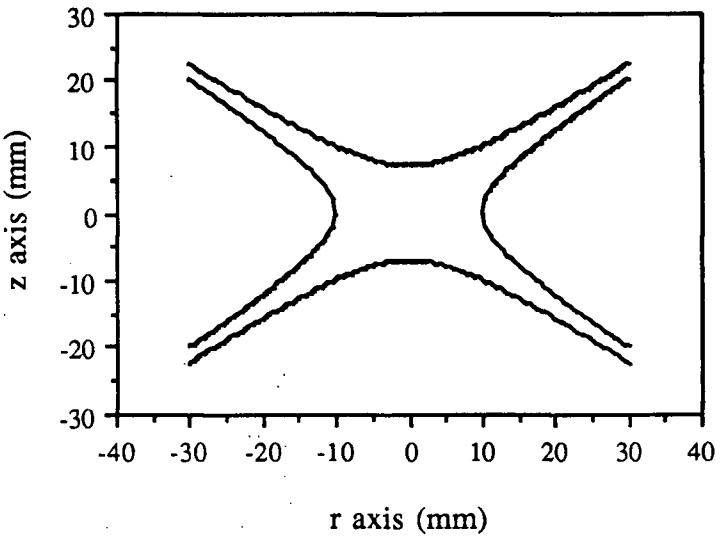

Figure 2.2: Two dimensional diagram showing the curves used to create the electrode surfaces for the ion trap.

2.4 - Ion Motion in the Radio Frequency Quadrupole Ion Trap:

The force applied to a singly charged ion positioned in the ion trap is given by equation *(2)*:

$$F = ma = eE$$

As the field is the variation of the potential in the trap we can write (as described by equation *(6)*):

$$E = -\frac{\partial \phi}{\partial r} - \frac{\partial \phi}{\partial z} \qquad (18$$

The potential in the trap is given by equation *(12)*:

$$\phi = \frac{\phi_o}{r_o^2}(r^2 - 2z^2)$$

where ϕ_o is the potential applied between the electrodes. This potential can be made to consist of a DC component and a radio-frequency voltage:

$$\phi_o = U + V\cos \Omega t \qquad (19)$$

where U is the DC component of the potential, V is the amplitude of the RF component of the potential and Ω is the frequency of the oscillating RF potential. The partial derivatives of equation *(12)* for both the "r" and the "z" directions show the decoupling of the motion of the ions in the two directions. Therefore, to describe the motion of an ion in the "r" direction we can write:

$$F_r = m\frac{\partial^2 r}{\partial t^2} = \frac{-2er}{r_o^2}(U - V\cos\Omega t) \qquad (20a)$$

while in the "z" direction we have:

$$F_z = m\frac{\partial^2 z}{\partial t^2} = \frac{4ez}{r_o^2}(U - V\cos\Omega t) \qquad (20b)$$

These two equations can be rewritten as:

$$\frac{\partial^2 r}{\partial t^2} + \frac{2er}{m r_o^2}(U - V\cos\Omega t) = 0 \qquad (21a)$$

and

$$\frac{\partial^2 z}{\partial t^2} - \frac{4ez}{m r_o^2}(U - V\cos\Omega t) = 0 \qquad (21b)$$

We now define:

$$\xi = \frac{\Omega t}{2} \qquad (22)$$

We can also write:

$$\frac{d}{dt} = \frac{d\xi}{dt}\frac{d}{d\xi} = \frac{\Omega}{2}\frac{d}{d\xi} \qquad (23)$$

and:

$$\frac{d^2}{dt^2} = \frac{d\xi}{dt}\frac{d}{d\xi}\left(\frac{d}{dt}\right) = \left(\frac{d\xi}{dt}\frac{d}{d\xi}\right)\left(\frac{d\xi}{dt}\frac{d}{d\xi}\right) = \frac{\Omega^2}{4}\frac{d^2}{d\xi^2} \qquad (24)$$

Now equations *(21a)* and *(21b)* can be rearranged into:

$$\frac{\partial r^2}{\partial \xi^2} + \frac{8e}{m r_o^2 \Omega^2}(U - V\cos 2\xi)\, r = 0 \qquad (25a)$$

$$\frac{\partial z^2}{\partial \xi^2} - \frac{16e}{m r_o^2 \Omega^2}(U - V\cos 2\xi)\, z = 0 \qquad (25b)$$

These equations are of the same type as the so-called Mathieu's equation, the Canonical form of which is:

$$\frac{\partial u^2}{\partial \xi^2} + (a_u - 2q_u \cos 2\xi)\, u = 0 \qquad (26)$$

Where "u" represents "r" or "z". The "a" and "q" parameters of Mathieu's equation can be written for the quadrupole ion trap system, as:

$$a_r = \frac{8eU}{m^2 r_o^2 \Omega^2} \qquad a_z = \frac{-16eU}{m^2 r_o^2 \Omega^2} = -2a_r \tag{27}$$

and:

$$q_r = \frac{4eV}{m^2 r_o^2 \Omega^2} \qquad q_z = \frac{-8eV}{m^2 r_o^2 \Omega^2} = -2q_r \tag{28}$$

Mathieu's equation has two types of solution: stable and unstable. For an ion of mass "m" in a trap with a given radius r_o of its ring electrode, one has to choose the values of "V", "U" and "Ω " in such a way so as to obtain a stable solution of the equation and thus the trapping of the ions.

2.5 - Solution to Mathieu's Equation:

The solution to Mathieu's equation can be expressed as the sum of two series expansions:

$$u(\xi) = \alpha' e^{\mu\xi} \sum_{-\infty}^{\infty} C_{2s} e^{2is\xi} + \alpha'' e^{-\mu\xi} \sum_{-\infty}^{\infty} C_{2s} e^{-2is\xi} \tag{29}$$

This equation has two types of solutions: if the value of "u" increases without limit when "ξ " is increased to infinity the solution is said to be unstable; if "u" remains finite when "ξ" is increased to infinity the solution is said to be stable. α' and α'' are constants of integration which depend on the initial values of position (u) and velocity ($\dot{u}$) of the particle and on the phase (ξ_o) of the RF potential. The coefficients C_{2s} depend on "a" and "q". μ can be written as:

$$\mu = \propto + i\beta \tag{30}$$

If $\propto \neq 0$ then the value of either $e^{\mu\xi}$ or $e^{-\mu\xi}$ will tend to infinity when "ξ" tends to infinity, but if "μ" is purely imaginary, the solution is stable since

$$e^{i\beta} = \cos\beta + i\sin\beta \tag{31}$$

and

$$|\cos\beta + i\sin\beta| = 1 \qquad (32)$$

The values giving stable solutions to Mathieu's equation have been tabulated. When these values are plotted in the "a" and "q" dimensions they form what is known as a stability diagram [76]. The stability diagram shows the areas where the "a" and "q" values give stable solutions to Mathieu's equation. For practical purposes only the area bounded by "a_o" and "b_1" [76] is used in quadrupole devices. In the case of the ion trap the motion of an ion needs to be bounded in both "r" and "z" directions so the values of "a_r", "a_z", "q_r" and "q_z" must all fall within the stable region of the stability diagram. To obtain the stability diagram which applies to the ion trap we must plot the stability areas for both directions of motion of the ions. The fact that $a_z = -2a_r$ and $q_z = -2q_r$ has to be taken into account in drawing the diagrams.

The boundary of the stability diagram can be calculated using the following equations [76]:

$$a_o = \frac{-1}{2}q^2 + \frac{7}{128}q^4 - \frac{29}{2304}q^6 + \frac{68687}{18874368}q^8 + 0(q^{10}) \qquad (33)$$

and

$$b_1 = 1 - q - \frac{1}{8}q^2 + \frac{1}{64}q^3 \frac{1}{1536}q^4 - \frac{11}{36864}q^5 + \frac{49}{589824}q^6 + \frac{55}{9437184}q^7$$

$$- \frac{265}{113246208}q^8 + 0(q^9) \qquad (34)$$

These equations apply only if $|q|$ is small. Figure 2.3 presents a stability diagram, for the ion trap, in the "a" and "q" dimensions. Since "a" and "q" are proportional to "V" and "U" through equations (27) and (28) we can also plot the stability diagram in the "V" and "U" dimensions (Figure 2.4) (assuming given values for "r_o" and Ω). When the stability diagram is drawn in the "V" and "U" dimensions we obtain a different stability diagram for all ions having different mass to charge ratios.

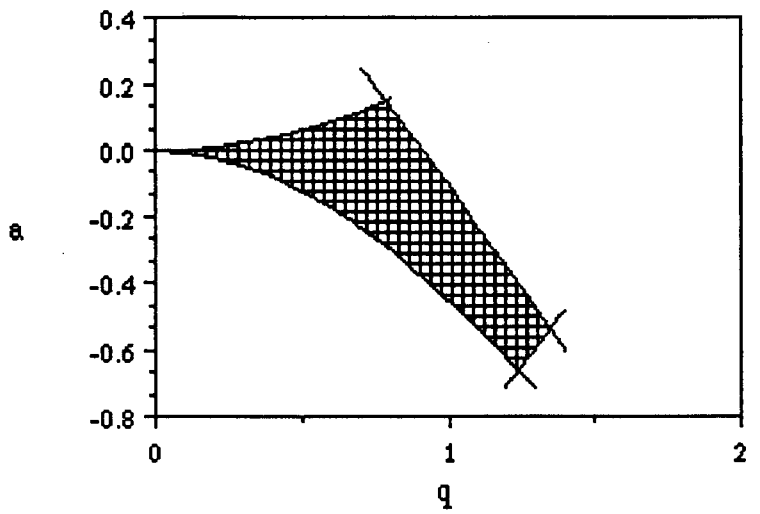

Figure 2.3: Stability diagram in the "a" and "q" dimensions.

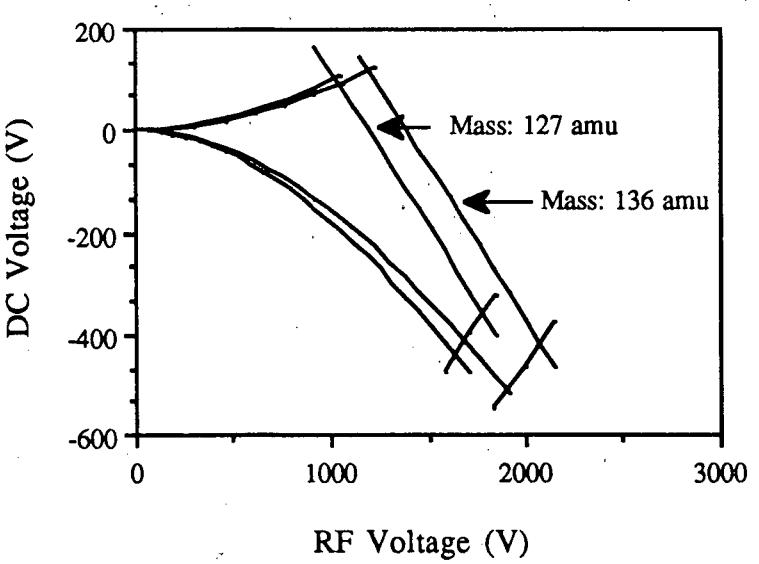

Figure 2.4: Stability diagram in the DC/RF voltage dimensions.

2.6 - Field Derivation For the System Used:

The field description presented in section 2.1 is a general description of quadrupole fields created in quadrupole ion trap instruments. But, since the potential described by equation *(19)* can be applied between the electrodes of the trap in many different ways, special considerations must be given to the particular case encountered in our system. There are three basic ways in which the potential may be applied between the electrodes. Firstly, "ϕ_o" may applied to the ring electrode and "$-\phi_o$" to the end cap electrodes, secondly "ϕ_o" may be applied only to the ring while the end caps are grounded and lastly we may apply only the RF component of "ϕ_o" to the ring electrode while the DC component of "ϕ_o" is applied to the end cap electrodes. The system used in this study has the RF component of "ϕ_o" applied to the ring electrode only while the end cap electrodes are grounded. The DC component of the voltage described by equation *(18)* is completely eliminated. Equation *(11)* can then be written in a more general form:

$$\phi = k r^2 - 2 k z^2 + c \qquad (35)$$

(remember that "ϕ" is obtained by the integration of "E"). At the surface of the ring electrode we have $\phi = \phi_o$ so we can write:

$$\phi(r_o,0) = \phi_o = k r_o^2 + c \qquad (36)$$

and at the surface of the end cap electrodes we have:

$$\phi(0,z_o) = 0 = -2k z_o^2 + c \qquad (37)$$

If we substract the two last equations we obtain:

$$\phi_o = k r_o^2 + 2k z_o^2 \qquad (38)$$

Given that:

$$r_o^2 = 2z_o^2 \qquad (39)$$

We can write:

$$k = \frac{\phi_o}{2\, r_o^2} \qquad (40)$$

And from equation *(36)*:

$$c = \frac{\phi_o}{2} \qquad (41)$$

So we can finally write:

$$\phi = \frac{\phi_o}{2\, r_o^2}(r^2 - 2\, z^2) + \frac{\phi_o}{2} \qquad (42)$$

This implies that the potential at the origin of the device does not have a constant zero value, the potential at the centre of the device follows the potential applied to the ring electrode . The resulting field inside the trap has the same shape as the one presented in figure 2.1, except that its strength is reduced by half compared to the field obtained when applying "ϕ_0" to the ring and "$-\phi_0$" to the end caps. The motion of the ions will be the same as that described in section 2.3 since (from equation *(2)*):

$$F = m\, a = eE$$

and (from equation *(6)*):

$$E = -\frac{\partial \phi}{\partial y} - \frac{\partial \phi}{\partial z}$$

The value of the constant term in equation *(42)* does not appear in the equations of motion. However the values of the parameters of Mathieu's equation ("a" and "q") will be changed because the factor of 1/2 in equation *(42)* is carried through the

equations of motion. Furthermore, because the end cap electrodes are kept at ground potential and no DC potential is applied to the ring electrode, the parameter "a" of Mathieu's equation will be equal to zero. We now have:

$$a_r = \frac{4eU}{m r_o^2 \Omega^2} = 0 \qquad a_z = \frac{-8eU}{m r_o^2 \Omega^2} = -2a_r = 0 \qquad (43)$$

and:

$$q_r = \frac{2eV}{m r_o^2 \Omega^2} \qquad q_z = \frac{-4eV}{m r_o^2 \Omega^2} = -2q_r \qquad (44)$$

These equations indicate that the trap will be operated along the "$a = 0$" axis of the stability diagram. To trap an ion with a given mass to charge ratio, the RF voltage and the RF frequency will have to be chosen to give a "q" value, for the ion, lower than 0.91.

CHAPTER III

EXPERIMENTAL

3.1 - Introduction:

At the time this project was started, Finnigan MAT was already manufacturing the Ion Trap Detector, which was intended to be used as a gas chromatograph detector. This instrument was the only reasonably priced ion trapping device available on the market. After a careful examination of the capabilities and potential of the gas chromatography detector system, it was concluded that both the mechanical and electronic modifications required by this device to meet our needs were too extensive to warrant its purchase. It was then decided to build the ion trap mass spectrometer system as well as the various interfaces needed for our studies, using the facilities available in the chemistry department.

This chapter presents the system designed and built in our laboratory, namely the radio-frequency quadrupole ion trap, the sample introduction systems, the modifications made on the electronic components to satisfy our requirements, and the computer hardware and software used. Some details of the operation of the ion trap system will be described to give the reader an understanding of the way this system was operated. The experimental set up used for the graphite furnace experiments and the laser ablation experiments will also be described.

3.2- Ion Trap Container and Vacuum System:

The experimental set up used to contain the ion trap and provide the required vacuum needed for these studies has been sketched in figure 3.1. The ion trap container is positioned just above a butterfly valve which allows the isolation of the ion trap container from the vacuum system. Between the butterfly valve and the diffusion pump is a Peltier cooled baffle which prevents the backstreaming of the diffusion pump oil into the ion trap assembly. The pumping system itself consists of a

diffusion pump and a fore pump. The seals used between the different components of the system are Viton co-seals 0-rings. In the following sub-sections the details of these various system components will be described in more detail.

3.2.1 - Ion Trap Container:

The ion trap container is made of stainless steel; its dimensions are shown in figure 3.2. There is one optical port built into the container, the window of which is made of quartz; this port was used to allow a laser beam into the trap for the laser ablation studies reported in this thesis. There are two openings in the container for the introduction of gases. A background gas may be introduced into the container through a Granville-Phillips variable leak valve on one side of the can. The interface between the ion trap and the external source of analyte is positioned opposite from the background gas inlet. The sample coming through this interface is brought directly into the cavity of the ion trap through a 1 mm internal diameter stainless steel tube, connecting directly to the ring electrode of the trap assembly. To ensure electrical insulation of the interface tube from the ring electrode a Vespel™ connector is placed between the sampling tube and the ring electrode. From this point a 1 mm hole drilled through the ring carries the analyte to the centre of the trap. Figure 3.3 shows how the connection between the sampling tube and the ring electrode is made. Another similar connection to the ring electrode has been made to allow the operator to introduce the background gas directly into the ion trap, if required.

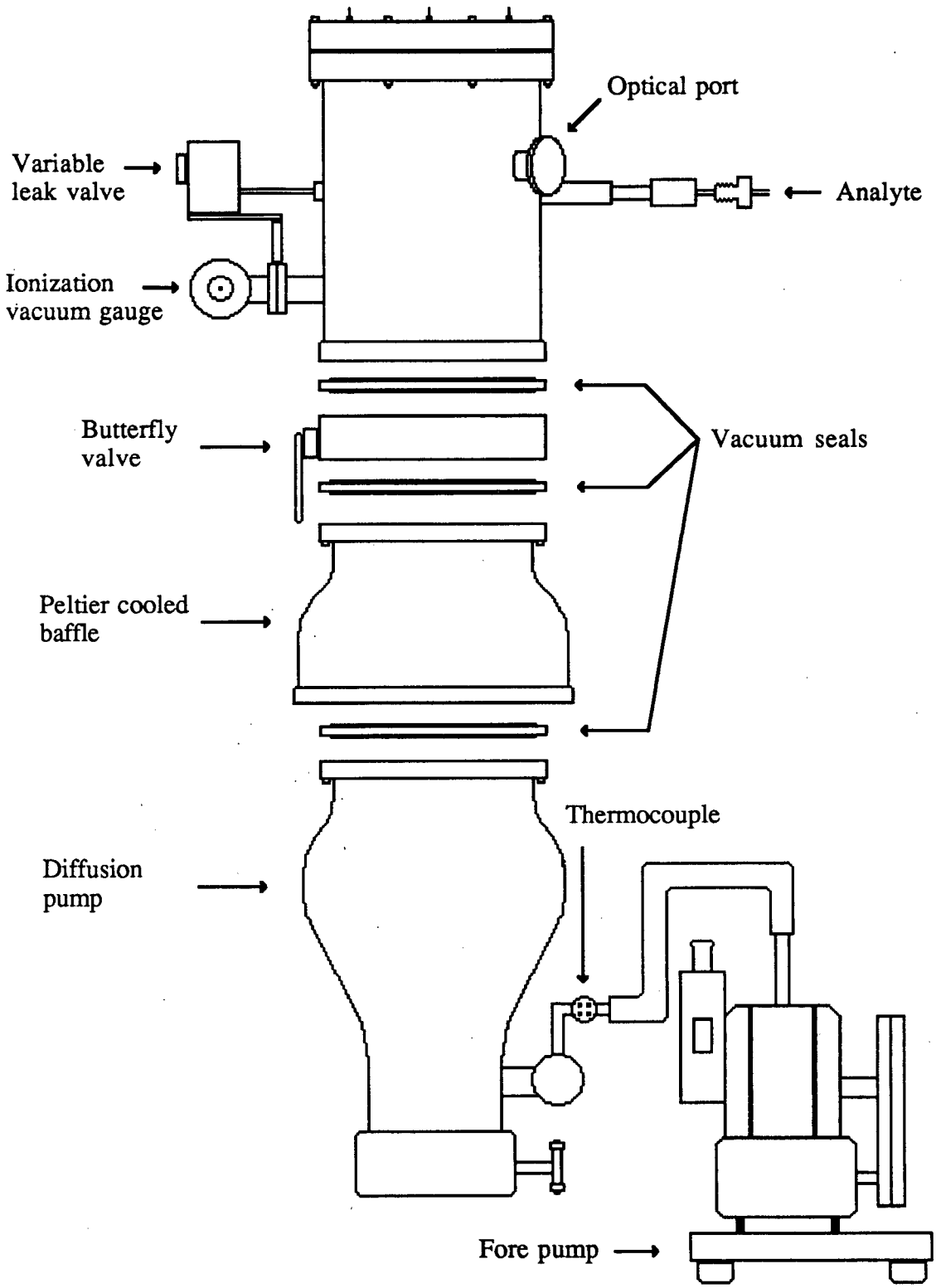

Figure 3.1: Experimental set up for the quadrupole radio-frequency ion trap mass spectrometer.

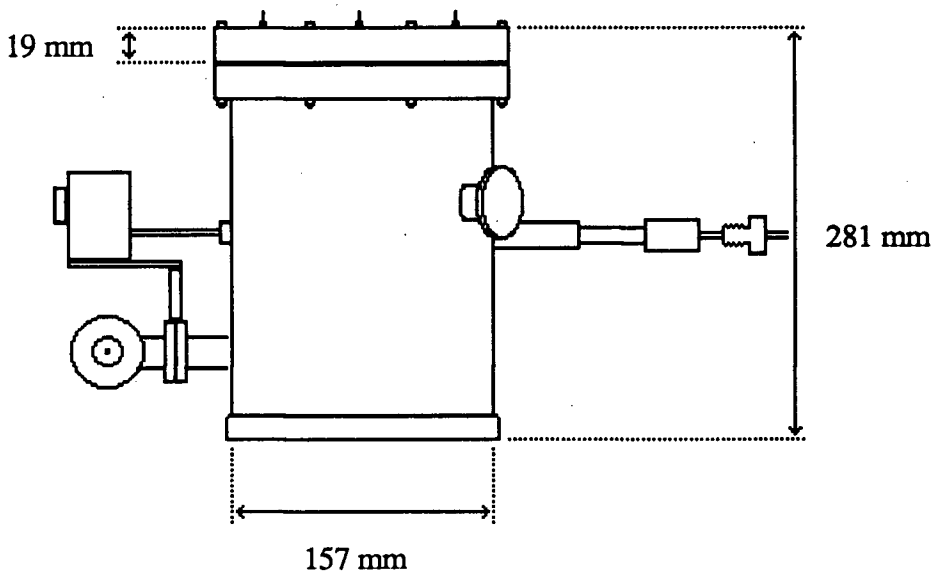

Figure 3.2: Ion trap container dimensions. The ion gauge and the background gas inlet are attached on the left side of the container, while on the right is the analyte sample inlet. The optical port is positioned between these two inlets.

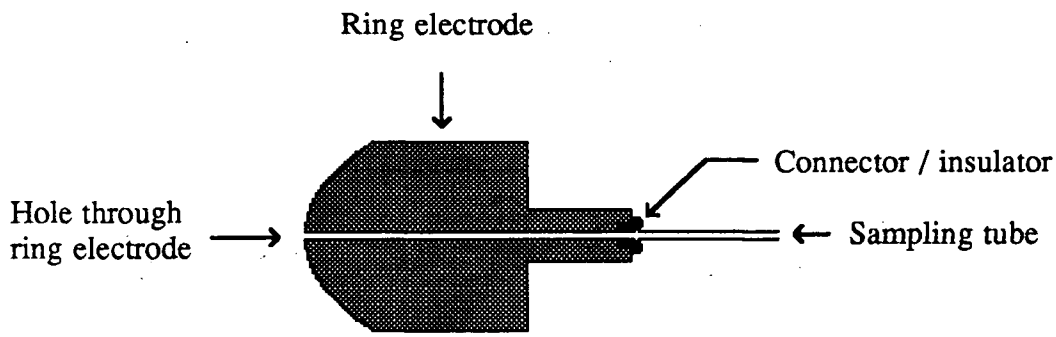

Figure 3.3: Connection between the sampling tube and the ring electrode. The Vespel connector insures electrical insulation between the tube and the ring electrode.

A special interface was machined to allow the passage of the sampling tube from atmospheric pressure to the high vacuum that exists inside the ion trap container. Figure 3.4 presents a schematic diagram of this interface. The most important part of the interface is a Teflon™ ring that is compressed around the stainless steel tube and squeezed against the back wall of the interface to produce the

high vacuum seals required. The sampling tube passes through the teflon spacer with minimal clearance. When the metal fitting is screwed in place it compresses the teflon spacer and a high vacuum seal is created between the spacer and the tube; at the same time the teflon spacer is squeezed against the back wall of the interface creating a high vacuum seal there as well.

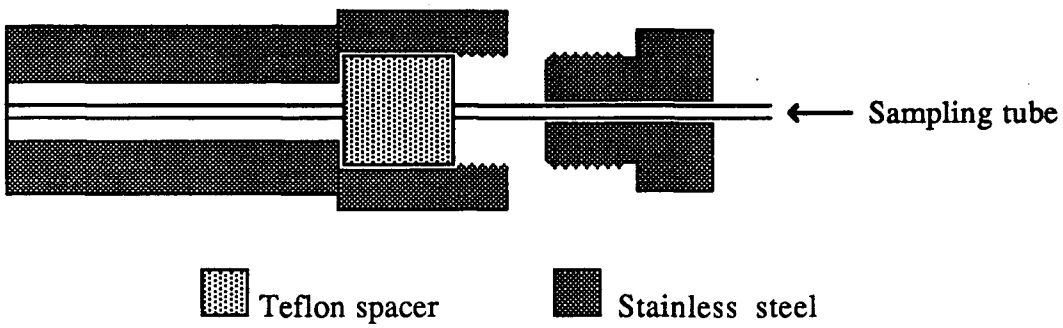

Figure 3.4: Interface used to pass the sampling tube from atmospheric pressure to the high vacuum of the ion trap container.

The electrical connections from the components of the ion trap assembly to the outside electronic instrumentation are made through fourteen electrical feed-through connectors installed in the top of the container (see figure 3.5). Inside the ion trap container bare copper wires are used to connect the different components of the trap to the electrical feed-throughs of the lid. Ceramic beads assure electrical insulation of these wires from other parts of the system. The electrode assembly is held together with three plastic studdings; Vespel spacers are used between the electrodes to assure proper spacing. Three plastic studs are screwed in tapped holes in the top end cap and attached from the electrode assembly to a metal plate positioned half-way between the lid of the container and the trap assembly. Three stainless steel screws connect this plate to the lid of the container. Stainless steel spacers are used between the metal plate and the lid, while Vespel spacers are used between the top

end cap electrode and the half-way metal plate. The ion trap is removed from its container simply by taking off the lid.

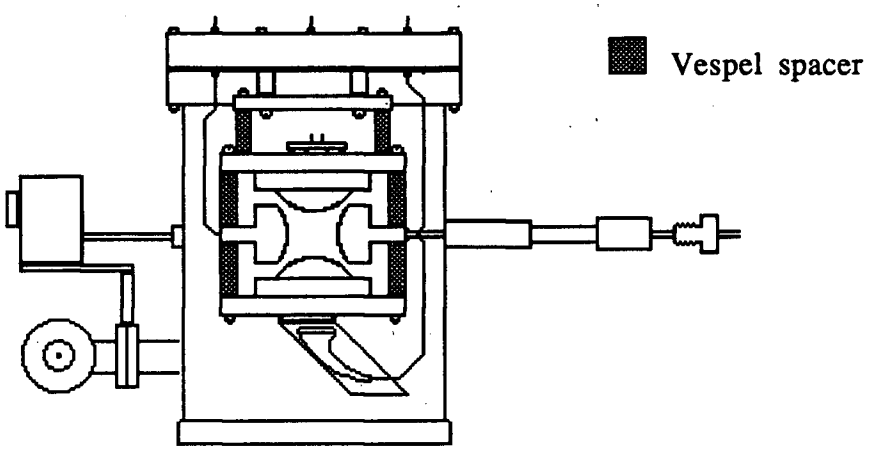

Figure 3.5: The ion trap in its container. The ion trap occupies most of the volume inside the container. The electrical connections to the ion trap are made through fourteen electrical feed-throughs in the cover of the can. The ion trap is easily removed from the container since it is attached to the cover of the can.

3.2.2 - Vacuum System:

In order to achieve the low pressure required in the ion trap container an Edwards (Crawley, England) Diffstak model 100/300 diffusion pump was used. The rated pumping speed, in air, for this pump is 280 l s^{-1}. This pump has a fluid capacity of 125 ml and its heater loading is 0.65 kW. The fluid used in this pump, Santovac 5, was obtained from Varian (Lexiton, MA). This fluid was chosen to avoid the back streaming problem associated with the use of other diffusion pump oils. Despite the use of Santovac 5 in our diffusion pump, after long periods of operation, an oily deposit on the ion trap assembly could be noticed. Therefore, it was decided to place a Peltier

cooled baffle between the diffusion pump and the butterfly valve. The baffle is an Edwards model number DCB 100. The lowest temperature attainable with this piece of equipment is -25 ^{o}C when it is fed with 14 A at 8 V. Because of the limitation of the power supply available to power this Peltier cooler (a Pek Inc (Sunnyvale, CA) model number 401A Short Arc Power Supply) only 8 A at 4 V were supplied to the cooler. The temperature of the baffle under these conditions was 0 ^{o}C. The floor pump used to back up the diffusion pump is a Welch Scientific Company (Skokie, IL) Duo seal vacuum pump model 1397.

To allow access to the ion trap without shutting the vacuum system down completely an Edwards quarter swing valve (model QSB 100) was placed between the ion trap container and the baffle (see figure 3.1). This valve, which has a "butterfly" type construction, is rated to have a conductance of 700 Ls^{-1}. The lowest pressure attainable with the system described is 1.0 * 10^{-7} torr.

3.2.3 - Pressure Metering System:

The pressure inside the ion trap container was monitored using a Varian (Lexington, MA) model 880 Digital Ionization Gauge Controller equipped with a Varian number 531 thermocouple vacuum gauge and a Varian model 564 broad range ionization gauge tube.

When the vacuum system is first started the controller monitors the pressure with the thermocouple gauge. The thermocouple gauge is located between the floor pump and the diffusion pump (see figure 3.1). As long as the pressure at this point does not drop below a preset value (in our case this value was set at 10^{-3} torr) the controller keeps the ionization gauge off. When the pressure has fallen below the threshold, the controller turns on the ionization gauge which then reads the pressure

inside the trap container. The ionization gauge is located on the side of the ion trap container (see figure 3.1). The pressures reported in this work were collected from this pressure meter and are presented without any correction.

It should be noted that the ionization gauge could not be operated at the same time as the channeltron electron multiplier because the light emitted by the ionization gauge was found to saturate the channeltron, the position of the channeltron in the container is such that it will detect the light emitted by the ionization gauge.

3.3 - The Ion Trap:

The entire ion trap assembly is made of three principal parts: the electrode assembly, the electron gun and the detector. The electrode assembly itself consists of three pieces: two end cap electrodes and one ring electrode. The electron gun used to create the ions is attached to the top end cap electrode; it is in fact encased in the top end cap. The ion detector, a channeltron electron multiplier, is attached to the bottom end cap electrode. Each of these three units will be described in more detail in the following sub-sections.

3.3.1 - The Electrode Assembly:

The three electrode assembly is presented, with its dimensions, in figure 6. The electrodes, which were made of 304 stainless steel, were machined according to the following equations:

End Caps:

$$\frac{r^2 - 2z^2}{r_o^2} = 1 \qquad (1)$$

Ring:

$$\frac{r^2 - 2z^2}{r_o^2} = -1 \qquad (2)$$

Equation *(1)* and *(2)* may be written as:

$$r^2 - 2z^2 = r_o^2 \qquad (3)$$

$$r^2 - 2z^2 = -r_o^2 \qquad (4)$$

The equation describing the relationship between the radius of the ring electrode and the separation of the two end caps is:

$$r_o^2 = 2z_o^2 \qquad \text{(equation } 13 \text{ in chapter 2)}$$

It was chosen to build the ion trap with a ring electrode radius of 10 mm. This sets the separation between the end caps electrodes to 14.14 mm (a "z_o" value of 7.07 mm).

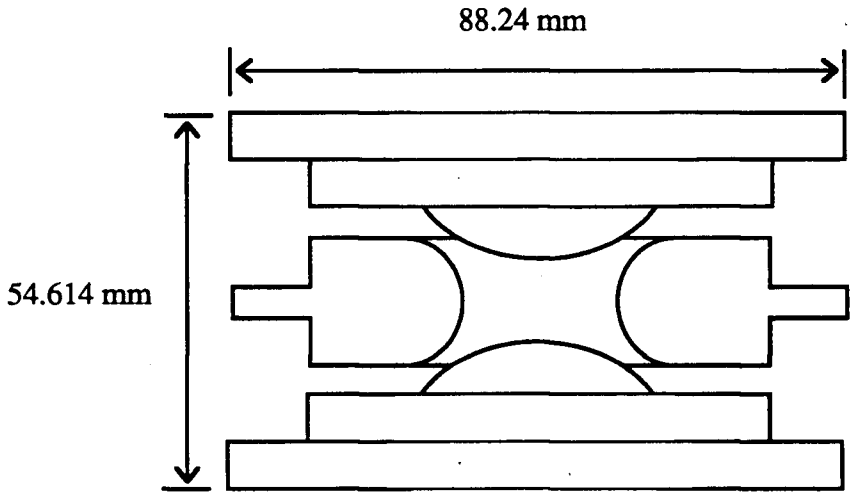

Figure 3.6: Dimensions of the ion trap assembly.

Since the chemistry department's mechanical engineering shop does not have access to a computer controlled lathe, the hyperbolic surfaces of the electrodes had to be machined by manually moving the cutter in small increments in both directions of motion of the cutter. Two computer programs were written to compute the exact positions of the cutter to create the proper shapes for the ring electrode and the end cap electrodes. These two programs are presented in appendix I. Figure 3.7 shows a schematic diagram of the two types of electrodes, the ring and the end cap, and gives their dimensions. The electrodes were first machined leaving their surface roughly machined. The final surfaces were then machined to obtain the finest surface possible (given the limitation of the equipment available) and were finally hand polished with Green and Red Rouge to obtain a highly polished finish. Figure 3.8 present a pseudo three dimensional representation of the electrode assembly.

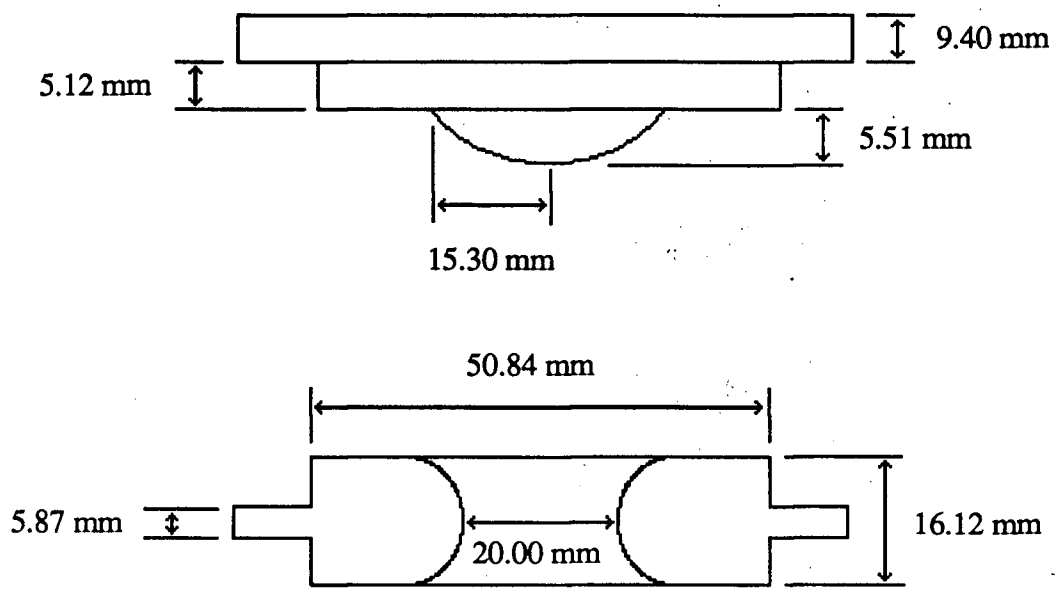

Figure 3.7: Dimensions of the electrodes of the ion trap. The top electrode is an end cap electrode. The bottom one is the ring electrode.

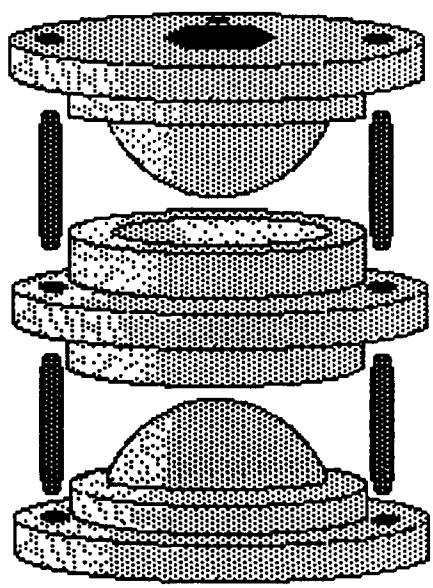

Figure 3.8: Pseudo three dimensional representation of the ion trap.

3.3.2 - The Electron Guns:

Two designs were used for the electron gun during the development of the instrument. A schematic diagram of the first set up is presented in figure 3.9 and the second in figure 3.10. The filament of the electron gun is a 0.007 inch diameter "V" shaped rhenium wire. It is attached to a Vacumetrics Inc (Ventura, CA) filament mount. Between the filament and the ceramic plate of the holder a metal plate was attached to one of the posts of the holder (see figure 3.11). The metal plate was added after the deposition of rhenium on the ceramic holder was found to cause the soldering of the filament holder to the metal ring holding it in place. This seems to happen due to the accumulation of electrons at the ceramic surface during operation, creating an electric field which attracts positively charged ions. Since a certain amount of rhenium evaporates from the hot surface of the filament and is ionized in the electron gun, the metal coating found on the ceramic holder is probably rhenium.

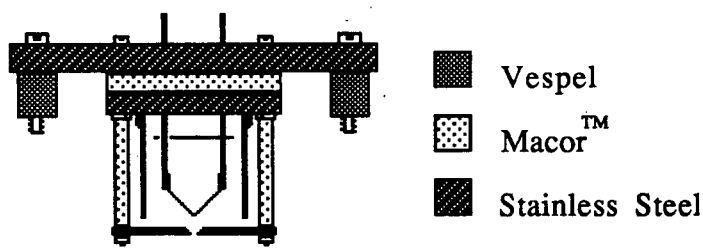

Figure 3.9: First electron gun set up. Macor™ was used to insulate those parts of the electron gun which contact, or are closely located, to the ring around the filament. It was found that the heat produced by the filament was damaging other type of insulator whereas Macor™ is a ceramic material which can easily withstand the heat produced by the filament.

The first electron gun assembly was quite complex. The main reason for the relative complexity of the electron guns used in ion trap mass spectrometry is the fact that the electron beam has to be pulsed. An intense pulse of incoming electrons is needed for a short time during the ionization stage of the experiment, but for the remaining stages of the experiment the electron beam must be off. In the first set up, the filament attached to its holder was enclosed in a grounded metal ring; this was done to avoid the problem of having the insulating material charged by electrons. The metal ring was separated from the main stainless steel holder of the assembly by a sheet of Macor™ which assure electrical insulation between the ring and the main metal holder. This machined piece of Macor™ also kept the filament holder tightly in place The ensemble formed by the metal ring, the filament holder and the Macor™ sheet was fastened to a main metal holder. In this position the filament tip was at the same height as the edge of the ring electrode. A metal plate was then positioned very closely (within 0.5 mm) to the metal ring surrounding the filament, acting as a gate for the electron beam. A 1 mm hole was drilled in the centre of this plate to allow for the passage of the electrons. Macor™ spacers were used to position the plate at the proper height and to ensure electrical insulation between the ring electrode and the metal plate. The details of the operation of this electron gun will be given in section 3.6.2.

The second electron gun assembly was much simpler than the first. Two main modifications were made: firstly, the metal plate used as a gate for the electron beam was totally eliminated (as well as the system holding it in place), secondly, the ring electrode surrounding the filament was extended. In this set up the filament tip was positioned about 7 mm away from the edge of the ring electrode. The main difference between the two electron guns is their operation, this will be discussed in detail in section 3.6.2.

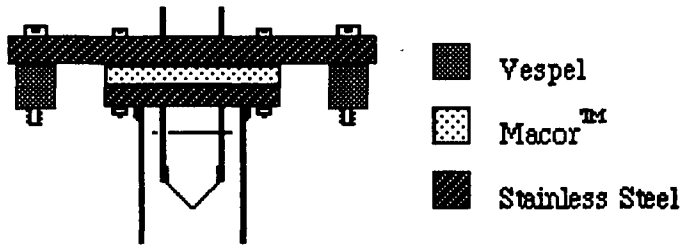

Figure 3.10: Second electron gun set up. Modifications in the electronics associated with the electron gun enabled significant simplification of the electron gun design, resulting in better performance.

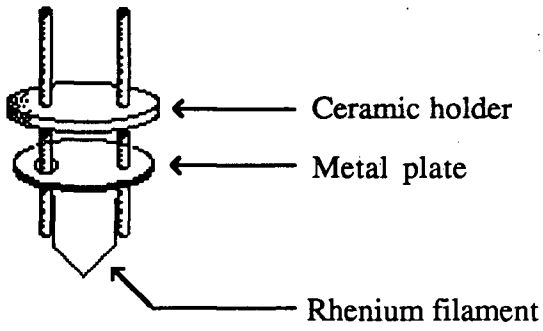

Figure 3.11: Electron gun filament holder. The assembly is made of a commercially available ceramic holder, a "V" shaped rhenium wire,and a metal plate to prevent charging of the ceramic holder by stray electrons.

3.3.3 - The Detector:

The device used to detect the ions as they are expelled from the trap is a Gallileo Electro-Optics Corp (Sturbridge, MA) model number 4870 channeltron electron multiplier. Figure 3.12 is a schematic diagram of the manner in which the channeltron is attached to the bottom end cap of the device. The channeltron mount had to be modified to position the opening of the channeltron directly along the "z" axis of the trap. Some of our experiments showed an important mass dependence of the

collection efficiency of the channeltron when its opening was positioned off axis from the incoming stream of ions. In all our experiments the channeltron was used in the analog mode. The voltage applied to the detector varied between 1700 and 2000 V. For most experiments this value was set at 1800 V.

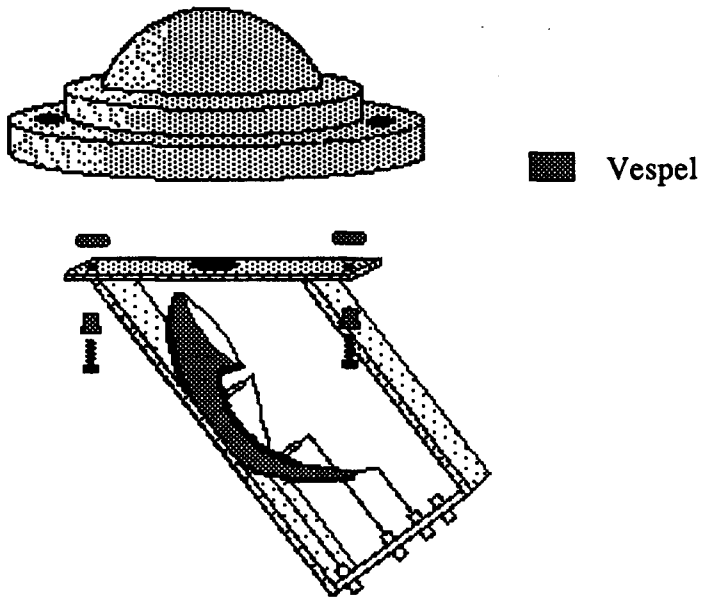

Figure 3.12: Channeltron attachment to the bottom end cap of the ion trap. The entrance to the channeltron is positioned along the "z" axis of the device.

3.4 - Interfacing the Ion Trap With External Sources of Analyte:

Interfacing the ion trap to an outside source of analyte can be quite troublesome. The basic problem is that we are trying to transfer the analyte efficiently, from a system at relatively high pressure (compared to the ion trap container) to a container at a much lower pressure. One limitation we face is that the manufacturer of the channeltron electron multiplier recommends that it not be used at

pressures higher than 10^{-5} torr. A pressure above this value, according to them, could create an arc inside the detector, destroying it. For analytes with high vapour pressures a very simple system (described in detail in the next section) was put in place, whereby the analyte flows continuously towards the ion trap at a slow rate. This allowed both electron impact ionization and chemical ionization studies to be performed.

The transfer of analyte evaporated from a graphite furnace to the ion trap poses an entirely different set of problems. First, the sample comes out of the graphite furnace for only a short time. Second, the sample emerges from the graphite furnace at high temperature, and will have the tendency to condense easily on the surfaces it encounters. Third, the atmosphere surrounding the graphite furnace must be controled so that the gas flowing to the ion trap will not interfere with the experiment we wish to perform. Also, the amount of material entering the ion trap container must be limited to avoid damage to the detector but, the pressure difference between the ion trap container and the graphite furnace container should be as large as possible in order to obtain efficient mass transfer of the analyte from the graphite furnace to the ion trap. To satisfy some of these requirements an interface was built in which the graphite furnace is kept under low pressures. In this system, the flow of gas to the ion trap is totally cut off until the experiment is ready to begin. Section 3.3.2 describes this interface in more detail.

3.4.1 - Interface for the Study of High Vapour Pressure Analytes:

The interface used to introduce organic solvents into the ion trap is presented in figure 3.13. The sampling tube which connects directly into the ring electrode of the ion trap assembly was connected to a Granville-Phillips Co (Boulder, CO) variable leak valve. This leak valve limits the amount of material entering the trap. The gas

introduced into the trap was sampled from the head space of a container half filled with the analyte of interest. A flow of helium bubbling in the liquid sample assured the exclusion of air from the sample container, and served to introduce the desired amount of helium into the trap. The main problem associated with the use of this interface is memory effects. The interface works well if one is interested in introducing the same analyte into the trap over long periods of time, however changing from one analyte to another requires several hours of heating the transfer line and the leak valve to eliminate completely the presence of the first analyte.

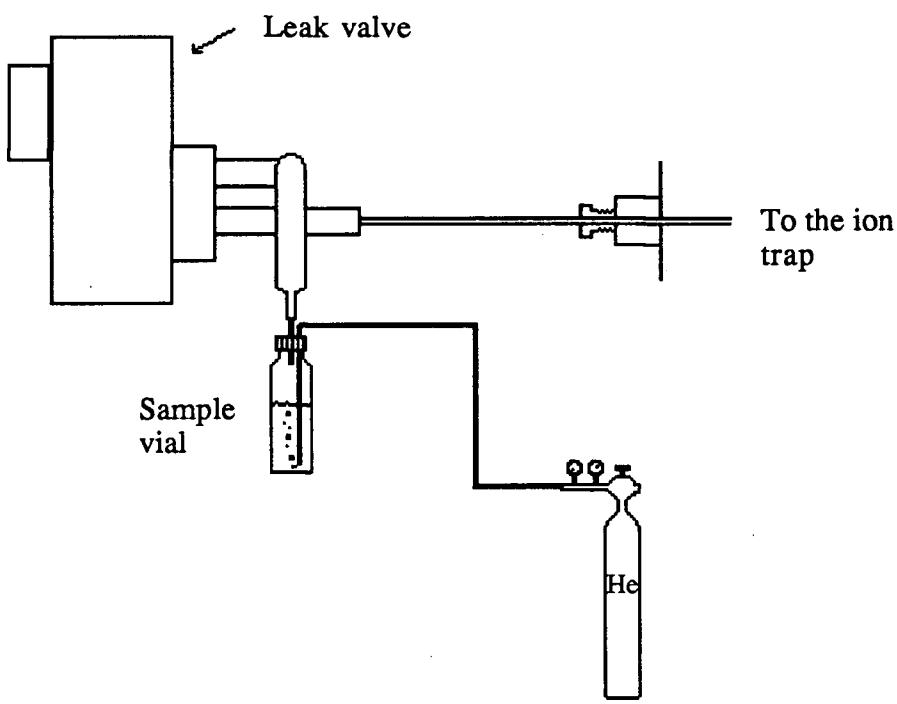

Figure 3.13: Interface to ion trap for high vapour pressure analytes.

3.4.2 - Interface with the Graphite Furnace:

The interface used to transfer the analyte evaporated from the graphite furnace to the ion trap mass spectrometer is made of a 1 mm internal diameter stainless steel tube. The connection between the sampling tube and the ring electrode has been presented in figure 3.3 of this chapter. To insulate the ion trap container when a new sample is put in the graphite furnace, a General Valve corporation (Fairfield, NJ) model number 9-405-900 high speed solenoid valve was put in the line between the graphite furnace container and the ion trap container. The minimum response time of this valve is 2 ms. The power supply used to drive this valve was built at UBC Chemistry department's electronic shop. To pass the sampling tube from atmospheric pressure to the lower pressure of the graphite furnace container, an interface similar to the one shown in figure 3.4 was used. The valve suffers one important shortcoming which diminishes the transport efficiency of the high temperature atomic vapours: it does not have a "straight through" design. This probably caused the loss of a large part of the material evaporated from the graphite furnace through condensation on the inside walls of the valve. Figure 3.14 shows the design of the interior of this valve.

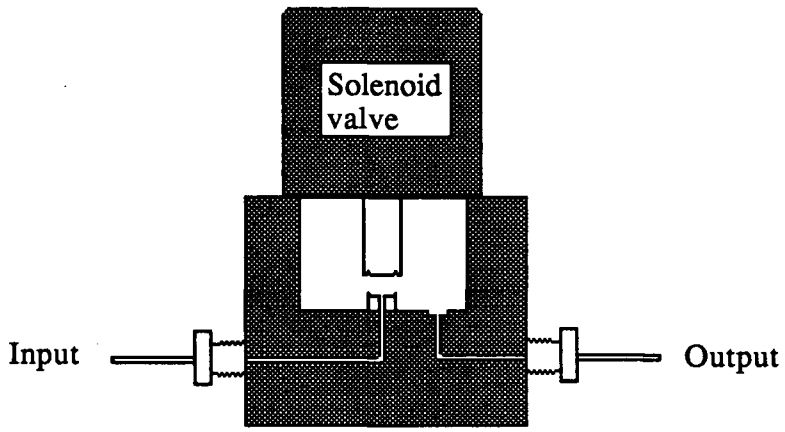

Figure 3.14: Schematic diagram of the solenoid valve used in the interface between the graphite furnace and the ion trap.

3.5 - The Graphite Furnace and its Container:

The graphite furnace is contained in a stainless steel can built by UBC Chemistry department's mechanical engineering shop. Figure 3.15 gives a schematic diagram of the graphite furnace in its container. The container has a diameter of 15.5 cm and a height of 11 cm. There are eight openings around the can: one opening for the interface with the ion trap, one for a vacuum gauge, an opening for bleeding background gas (helium) into the container, one opening to a vacuum pump, two for electrical feed-throughs for the graphite furnace, and two for cooling water lines for the graphite furnace. The graphite furnace assembly is positioned on a sliding base at the bottom of the container, allowing for the displacement of the graphite tube closer to or farther from the sampling tube. The graphite furnace used is a standard Varian Techtron model 63 Carbon Rod Atomizer. Only the base of the atomizer was modified to be attached to the sliding piece of metal at the bottom of the graphite furnace container. The pressure inside the container is monitored using a Balzers model PKG 020 Pirani-

Cold cathode gauge control pressure meter equiped with a Balzers model number TPR 010 thermocouple vacuum gauge.

Both standard graphite tubes and cups obtained from Varian were used to atomize the sample. No differences were noticed in the results obtained with these two types of graphite furnace.

3.6 - Laser Ablation Set Up:

Some modifications had to be made to the ring electrode of the ion trap to allow for the execution of the laser ablation experiments. The design of the experiment called for the ability to push the sample, through the ring electrode, until it just reaches the internal surface of the cavity. The laser beam would come from the opposite direction, through the ring, hitting the sample and producing a laser induced plasma inside the cavity of the ion trap. Thus one entrance (through the ring electrode) for the sample and one entrance for the laser beam were needed. Two 1.5 mm diameter holes were drilled at 180^{o} from each other in the centre of the ring electrode. Figure 3.16 illustrates the modifications which had to be made to the ring electrode. These holes were put in position so as to align with the optical port of the ion trap container when the ion trap is in place. The sample can be pushed into position until it has just reached the surface of the ring electrode, almost becoming part of it. The laser used for these experiments was a 1 J ruby laser (model number 104A) manufactured by TRG Data System Corporation. Figure 3.17 shows the set up used to hold the laser in position and to align it on the target.

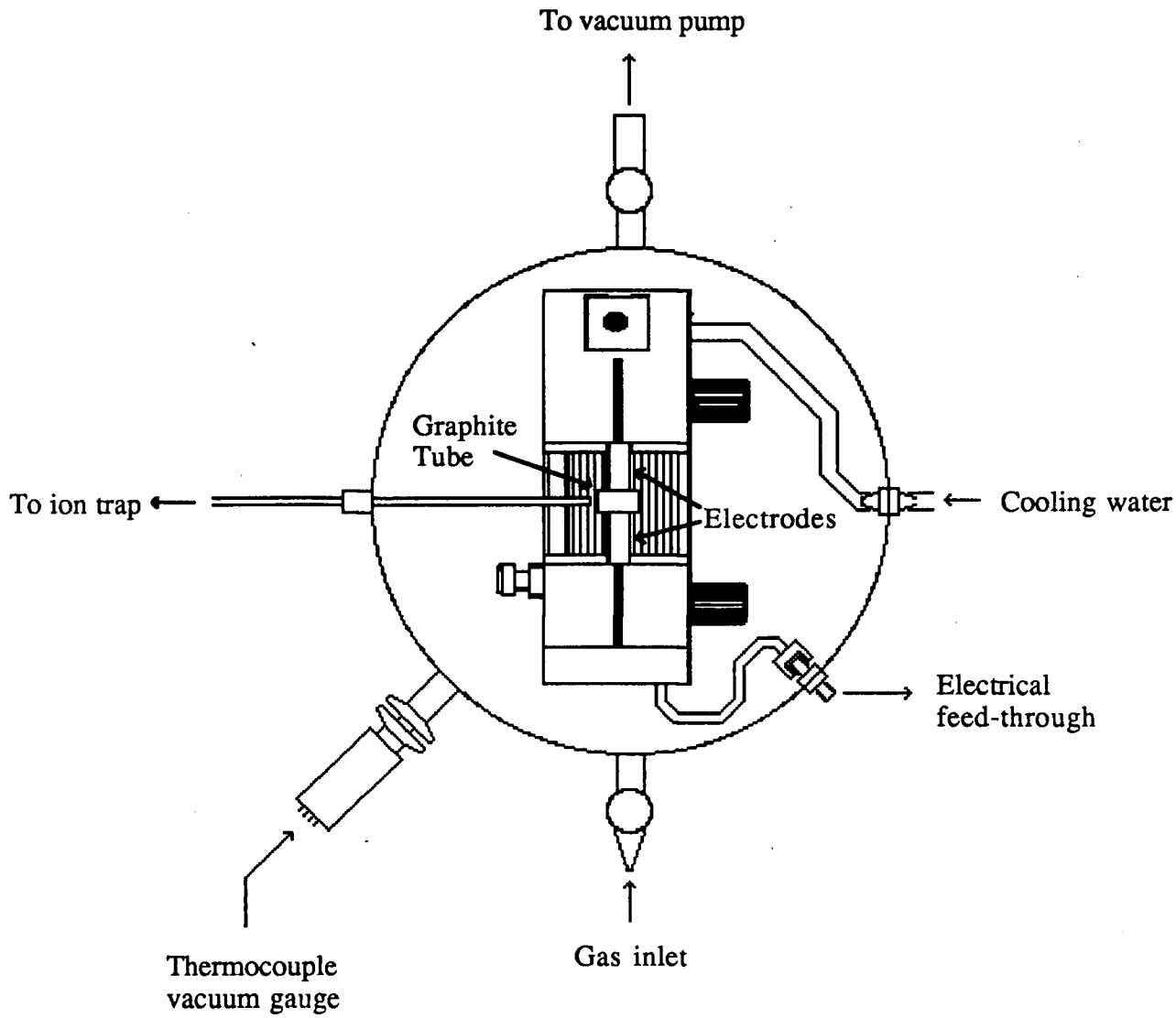

Figure 3.15: Graphite furnace and container. The graphite furnace was enclosed in a stainless steel container to control the pressure and the atmosphere surrounding it. Figure 1.2 presents a side view of the graphite furnace, please refer to it for further details.

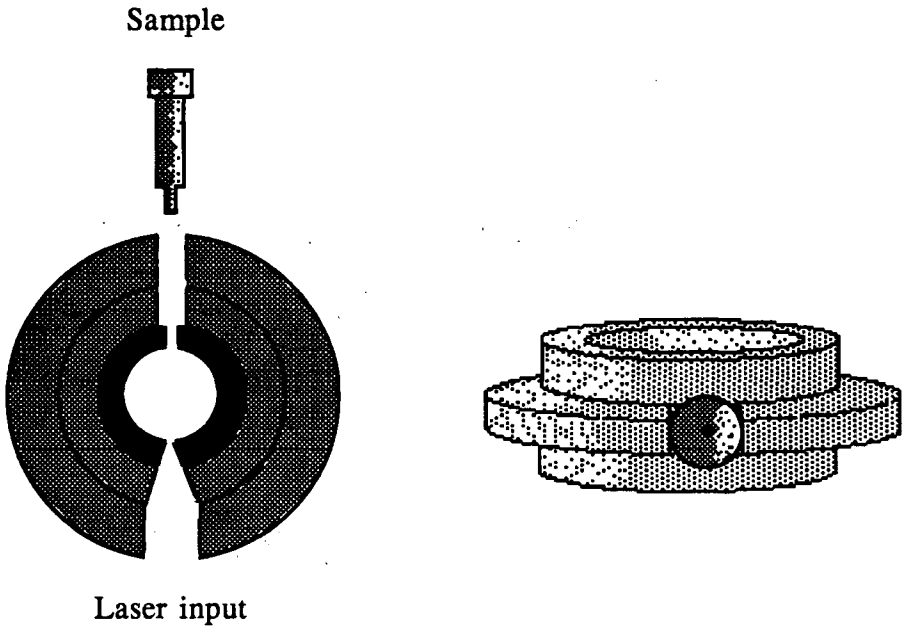

Figure 3.16: Modifications made to the ring electrode for the laser ablation experiments.

The laser set up consists of a metal plate, equiped with three kinematic mounts, to which the ruby laser is tightly attached. The kinematic mounts sit on a larger metal plate which is clamped to the table holding the ion trap set up. Behind the ruby laser is an helium/neon alignment laser which can be shone through the ruby laser. The two lasers can be tuned to fire at exactly the same point in space. The He-Ne laser can thus be used to align the ruby laser exactly on the target. To focus the ruby laser on the sample, a 30 cm focal length quartz lens was used.

To align the laser on the target, a phototransistor placed in a teflon holder was positioned in place of the sample. The phototransistor is used in a circuit whereby the voltage output is proportional to the amount of light which falls on the transistor, in fact the phototransistor is used (in the circuit) as a photodiode. The first step is to align the He-Ne laser with the phototransistor, the quartz lens is then put in front of the ruby laser, and its position is optimized to obtain the maximum potential output

from the phototransistor circuit. Once the alignment was completed the laser system was clamped into position. It could be left in place for several days without showing signs of being displaced. After the completion of the alignment the phototransistor was replaced with the sample of interest and the vacuum was established in the ion trap container. Different pressures of helium were used during these experiments for damping the motion of the ions produced inside the trap.

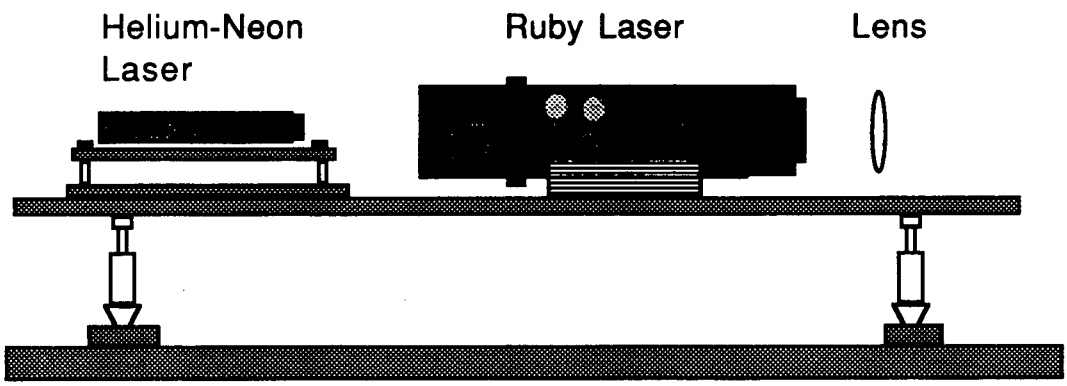

Figure 3.17: Schematic diagram of the laser ablation experimental set up.

It should be noted that the power supply to the ruby laser had to be triggered by grounding its trigger input line with a special computer-triggered relay because of a 175 V potential present on this line (which can seriously damage the computer if connected to it). This made the timing of the experiment somewhat more complex since the reaction time of the relay/laser system had to be determined and taken into account in the experiment and since this reaction time would vary from one experiment to the next.

3.7 - Electronics and Controls:

Most of the electronics used to run the instrument were assembled in our labs with the help of the Chemistry Department's Electronic shop. Figure 3.18 gives a schematic diagram of the electronics and the controls required to run the ion trap. The electronics can be divided into four parts: the radio-frequency quadrupole power supply, the supplies for the electron gun, the data acquisition system, and the computer hardware used to control the experiments and acquire the data. Each of these parts will be described in the following sections.

3.7.1- The Radio-Frequency Power Supply:

The first thing which should be pointed out about the operation of the ion trap is the fact that the end cap electrodes were always kept at ground potential. No DC potential was ever used between the ring electrode and the end cap electrodes.

The radio-frequency power supply used to create the confining electric field was a modified Extranuclear Laboratories Inc. (Pittsburgh, PA) quadrupole power supply model number 011-1. The modifications made to the power supply were needed in order to operate at the lower frequencies required by the quadrupole ion trap. These modifications consisted essentially in changing some tuning coils and capacitors in the radio-frequency power source. After these modifications the power supply could provide 3500 V at frequencies ranging from 595 KHz to 3.3 MHz. All the data presented in this thesis were acquired at a frequency of operation of the trap of 1.05 MHz. The High-Q head, which assured capacitance matching between the power supply and the ion trap, is an Extranuclear Laboratories Inc. High-Q Head model number 012-16. It is designed to work at the frequency required for the ion trap. The matching of the impedance of the two output channels of the quadrupole

power supply was done by using different lengths of RG-8A/U coaxial cable for the output connector to the ion trap and the output connector which is kept floating.

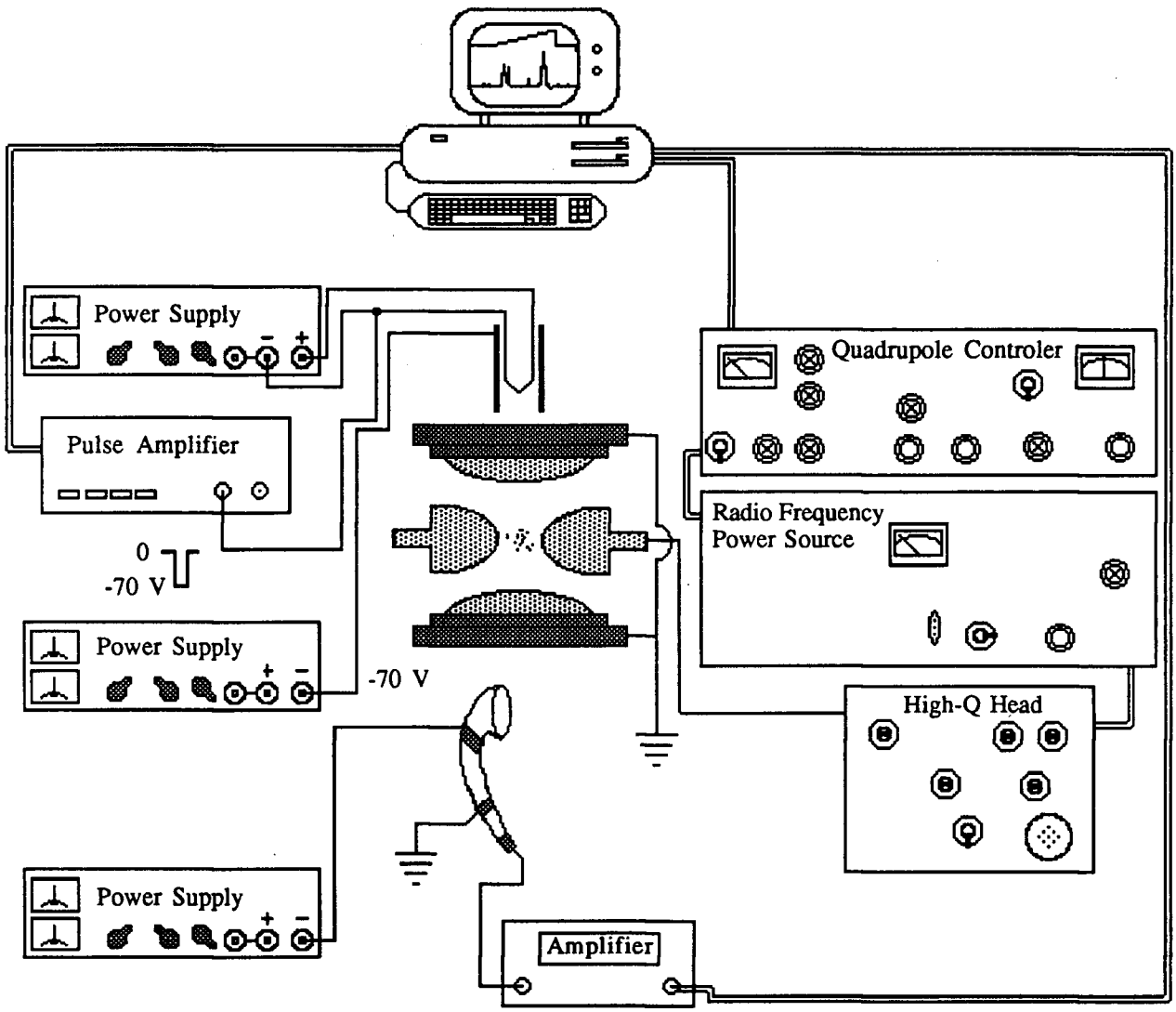

Figure 3.18: Diagram of the electronic set up for the ion trap.

3.7.2- Electron Guns:

As described in section 3.2.2 two different electron gun designs were used. Figures 3.19 and 3.20 present the two schematic diagrams for the electronics of the electron guns set ups. The first set up, presented in figure 3.9, had a fairly complex set of electronics (shown in figure 3.19). The filament and the ring surrounding it were biased at -70 V and the extraction plate of the gun was biased at -80 V, so that no electrons could escape the electron gun. To turn on the electron gun an 80 V pulse was applied to the extraction plate to bring the voltage of the plate to zero. Under these conditions the electron beam passes through the 1.0 mm hole in the extraction plate and, hopefully, enters the trap with an energy of around 70 eV. The pulse amplifier used to gate the electron gun was built in the electronics shop of the department of Chemistry at UBC. This pulse amplifier required a TTL pulse for triggering, and could output square pulses of voltage ranging from 0 to 120 V with pulse durations ranging from 0.1 μs to 10 ms.

The electron beam pulse shape coming out of this electron gun was very poor due to the presence of the two large capacitors in the system (see figure 3.19). A simulation of the electron trajectories under the conditions where the electron gun is on is presented in figure 3.20. This simulation was done using a program called MacSimmion™ developed by D. C. McGilvery and R. J. S. Morrison at Monash University, in Victoria, Australia. This simulation shows that with this design for the electron gun and the conditions used, only the electrons produced at the tip of the filament can reach the cavity of the ion trap. To obtain an acceptable electron beam current the filament has to be operated at a much higher temperature imposing extra stress on it and on the components of the system positioned close to it. The model also shows that the energy of the electrons when passing the centre of the trap range from 20 eV to 40 eV, which is much lower than the standard 70 eV used in most

instruments. The results of this simulation show that this design for the electron gun was inappropriate for the ion trap.

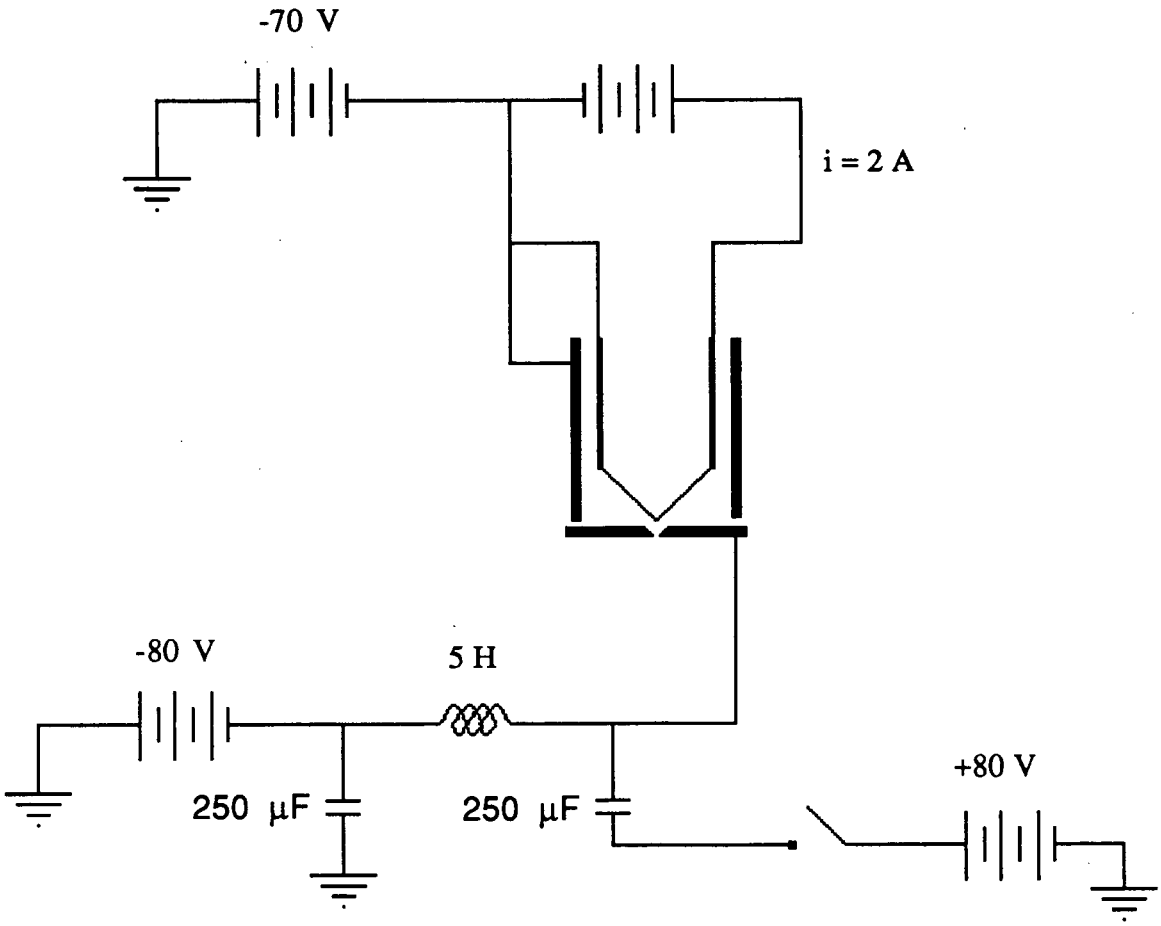

Figure 3.19: Diagram of the electronic set up of the first electron gun used.

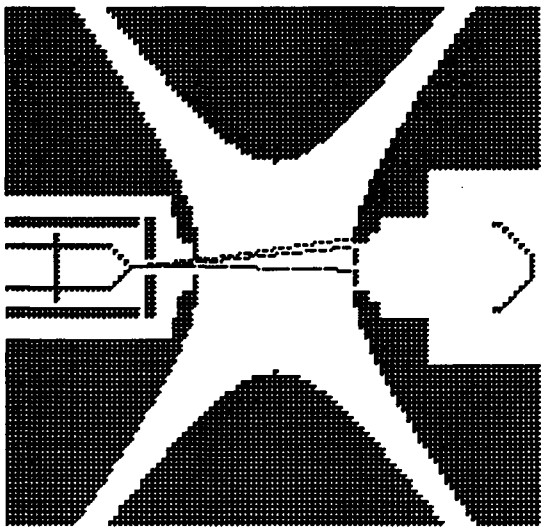

Figure 3.20: Simulation of the operation of the first electron gun used.

The second design, presented in figure 3.10, performed much better. Figure 3.21 shows a schematic diagram of the electronics of this electron gun set up. With this system the filament is kept at 0 V. The gate for the electron beam is the focussing ring, biased at a constant -70 V, surrounding the filament. Under these conditions no electrons enter the trap. The electron beam is sent into the trap by pulsing the voltage applied to the filament to -70 V. The performance of this electron gun is much better both in terms of electron beam current and in terms of pulse shape. The improvement is achieved through the use of a new pulse amplifier; the base output of this amplifier can be varied from -150 to +150 V. The voltage pulse can be varied from 0 to ±150 V and the pulse duration can be varied from 0.1 μs to 10 ms. This pulse amplifier was also built in the electronics shop of the Chemistry department of the University of British Columbia.

A MacSimmion™ simulation of the performance of this electron gun set up under the "gun on" conditions is presented in figure 3.22. This simulation shows that electrons created anywhere on the "V" shaped filament will enter the cavity of the ion trap. For the same filament temperature this electron gun will produce a much more

intense electron beam than the first electron gun used. The simulation also shows that the energy of the electrons, when they pass through the centre of the cavity, is around 65 eV (under the conditions used) and their energy distribution is much narrower that what was found with the first electron gun set up.

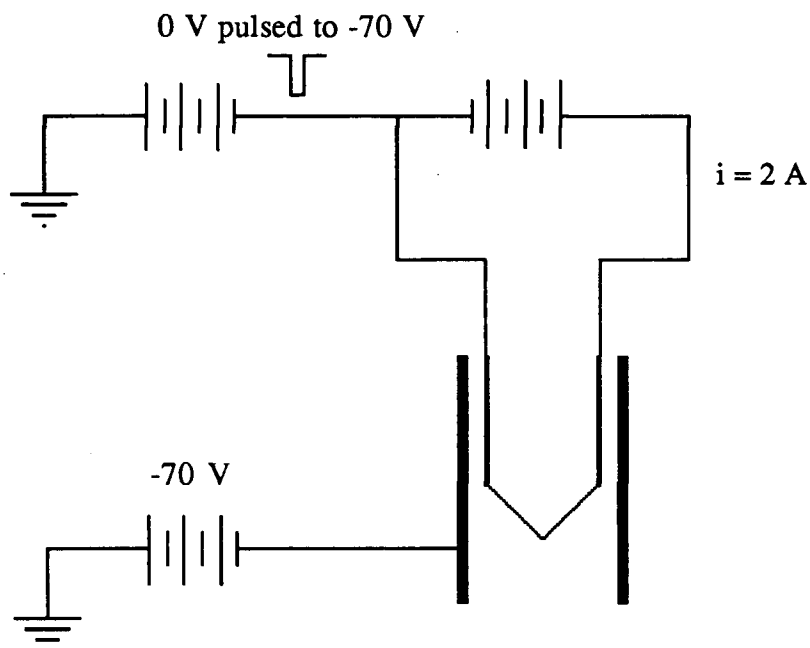

Figure 3.21: Schematic diagram of the second electron gun used with the ion trap.

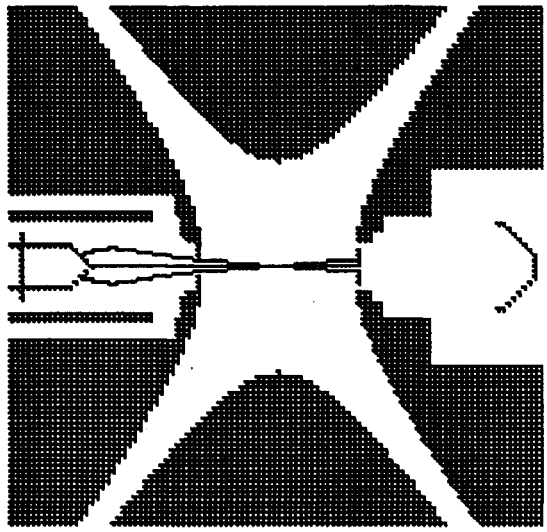

Figure 3.22: Simulation of the operation of the second electron gun used.

3.7.3- The Detection System:

The channeltron electron multiplier (Galileo Electro-Optics (Sturbridge, MA) model 4870) used to detect the ions coming out of the trap was operated in the analog mode. The voltage applied to the channeltron ranged from -1700 to -2000 V. For most of the experiments reported in this document the voltage was set at -1800 V. The output of the detector was fed into a Keithley (Cleaveland, OH) model 427 current amplifier using a gain of 10^7 or 10^8. The voltage output from the current amplifier was fed to the computer for digitization and data handling.

3.7.4- Computer Hardware:

The experiments are controlled by a Zenith Data System Computer (IBM AT compatible) equiped with a QuaTech (Akron, OH) PXB-721 parallel expansion board,

a model DM12-10 12 bit digital to analog converter and an RC Electronics (Santa Barbara, CA) model ISC-16 analog to digital data acquisition system.

The PXB-721 parallel expansion board is a plug in expansion board manufactured to be used in IBM PC and compatible computers. It is equipped with three Intel 8255 programable peripheral interface chips giving the user access to 72 Input/Output lines. The DM12-10 is a module which plugs into the PXB-721 and has two independent output channels. One was used to control the voltage coming out of the RF supply, while the other was used to trigger the laser in the ablation experiments. Other output ports on the PXB-721 were used to trigger the pulse amplifier for the electron gun and the data acquisition system.

The ISC-16 is a 16 channel analog-to-digital converter plug-in interface, designed for IBM AT compatible computers, which comes with a BNC terminator box. It is capable of digitizing 16 analog input channels at a sampling rate of up to 1 MHz (when a single channel is sampled). The analog to digital conversion is done with 12 bits precision. The voltage range covered by the converter can be hardware selected; for all our data acquisition it was set to cover values ranging from -10 to 10 V. A 64 K sample memory buffer on the interface captures the input signal. This buffer is divided into two 32 K buffers, limiting the maximum number of data points that can be collected by the channels. The buffer size used by each channel and the sampling rate can be software selected.

The Zenith Data System Computer is an IBM AT compatible computer equipped with a 20 Mb hard disk and a single floppy disk drive. The central processing unit of this computer is an Intel 80286 chip. The computer is equiped with an Intel 80287 math coprocessor. The computer had 512 K of memory and its operating system was DOS 3.10.

3.7.5-Software for the Data Acquisition:

The computer program used to control the ion trap and acquire the data was initially written in Turbo Pascal by Dr. R. Browne in our laboratory for a photodiode array system. It was subsequently modified to suit the requirements of the ion trap system. The program is written in such a way that after the data acquisition board (ISC-16) has been triggered it acquires and digitizes 4096 points sampled from the data line. The rate at which the data is acquired are set by the operator.

The program starts with the Main Menu offering 10 choices of operations to the user:

1- Scan New Spectrum
2- Calculations and Corrections
3- Display Spectrum
4- Plot Spectrum
5- Dump Array to Printer/Screen
6- Save the Spectrum to Disk
7- Load Spectrum from Disk
8- Set Clock Time
9- Set Scanning Sequence
0- Exit this Program

The "Scan New Spectrum" option allows the user to perform the data acquisition. At this stage the number of spectra to be acquired and averaged must be set by the operator. However, the user must set the clock time (item 8) and set the scanning sequence (item 9) before starting the data acquisition. Setting the clock time controls the rate at which the data are acquired. In our entire set of experiments, the clock time used ranged from 30 to 35 ms. Setting the scanning sequence involves chosing the amplitude of the trapping voltage applied to the ring electrode, chosing the final voltage amplitude of the scan, chosing the storage time, and the initial delay

before starting the data acquisition (this last variable is used only for the graphite furnace experiments).

The calculations and correction section of the Main Menu allows for the subtraction of a background spectrum from the data obtained previously. This option was used to subtract the bias voltage (from the Keithley current amplifier) from the data. No peaks were ever eliminated from the spectra with this feature of the program.

Once the data has been acquired and corrected as required, the operator has the choice of displaying it on the screen, plotting it on a Hewlett Packard model number 7475A plotter (option 4 on the "Main Menu") or displaying the data on the screen or on a print out. The data can also be saved to disk. Data can also be read from the disk to be examined and plotted later.

The most important part of the program is the data acquisition subroutine. It starts by setting up the ISC-16 data acquisition board, and then the data acquisition part of the subroutine starts. The objective of this second part of the subroutine is to obtain an average spectrum; it starts by setting up the Qua Tech expansion board and the DM12-10 digital to analog converter. The array that will contain the data is then initialized to zero. The program waits for the delay requested by the operator before starting the data acquisition. The next step is the acquisition of the data, which involves the setting of the ISC-16 board for receiving the trigger pulse, setting the initial RF voltage amplitude, triggering the electron gun (or the laser), triggering the data acquisition system, ramping up the RF voltage amplitude and accumulating the data. After all the scans have been completed the data are averaged. This completes the work done by the data acquisition subroutine and control is then passed to the "Main Menu" subroutine. This subroutine is presented in appendix II.

3.8 - Detection of the Ions and Timing of the Experiments:

The timing sequence for the operation of the ion trap is essentially the same for the three types of experiments reported in this study. The mass spectra are obtained using the "mass selective instability" mode of operation first described by Stafford et al. [22]. This method of obtaining the mass spectrum from the ions trapped is described in the following paragraphs, as are the modifications which must be done on the basic timing sequence to accommodate the different experiments performed.

The radio-frequency quadrupole ion trap used in the total pressure mode (along the $a = 0$ line of the stability diagram) will trap and accumulate ions of all mass to charge ratios with a limit, imposed by the amplitude of the RF voltage, on the low mass end of the spectrum. The lowest mass-to-charge that can be trapped at a given voltage amplitude "V" is defined by:

$$m_{min} = \frac{e\,V}{q_{ejt.}\,r_o^{\,2}\,\Omega^2} \qquad (5)$$

where "m_{min}" is the lowest mass that can be trapped and "$q_{ejt.}$" is the value of "q" (from Mathieu's equation) at which ions are ejected from the trap (this value is around $q_{ejt.} = 0.91$).

Once the ions are trapped in the cavity of the device they have to be identified according to their mass-to-charge ratio, and their different relative amounts must be established. This can be done by either leaving the ions inside the trap and selectively identifying and quantifing each type of ion present, or by selectively extracting them from the trap to be detected with an electron multiplier. The "mass selective instability" mode of operation of the trap (which is the method used to obtain mass spectra from our instrument) involves external detection of the ions.

3.8.1- The "Mass Selective Instability" Mode of Operation of the Ion Trap:

In the "mass selective instability" mode of operation, the spectrum of the ions trapped at the centre of the device is obtained by rapidly ramping up the amplitude of the RF voltage applied to the ring electrode of the ion trap. Equation 28 (chapter 2) allows us to understand how this technique works. First, when the voltage has been set to its trapping value, ions of a wide range of mass-to-charge ratio are trapped (starting with ions having the minimum trapable mass-to-charge ratio). But, as the RF voltage on the electrode is increased, the "q_z" value of a given ion increases. At one point (if the voltage is increased to a high enough value) the ion will attain the "q_z" value of ejection ($q_z \approx 0.91$). This causes the trajectory of the ion to sharply increase in space. When the "q_z" value of this ion has reached the extraction value, its "q_r" value is still well into the stability diagram (when $q_z = 0.91$, $q_r = 0.455$, see equation 28, chapter 2). So the trajectory of the ion in the "r" direction is still bounded while along the "z" axis it is not. The detection of the ions is accomplished by placing an electron multiplier outside one of the end caps to capture the ions ejected.

The timing of the acquisition of a spectrum with this method of operation of the trap is presented in figure 3.23. The experiment starts by setting the trapping voltage. Once the trapping voltage has been set, the electron gun is turned on for a short period of time (around 1 ms) and a period of stabilization of the ions (called the storage time) starts. The storage time may be varied according to the requirement of the experiment. Once the storage time has passed, the data acquisition is triggered and the RF voltage amplitude is rapidly increased. When the maximum RF voltage amplitude has been reached the data acquisition system stops, the RF voltage amplitude is dropped to zero and a certain time is given to the ions that may have

been left in the trap to escape. The entire process can be repeated a number of times to obtain an average spectrum.

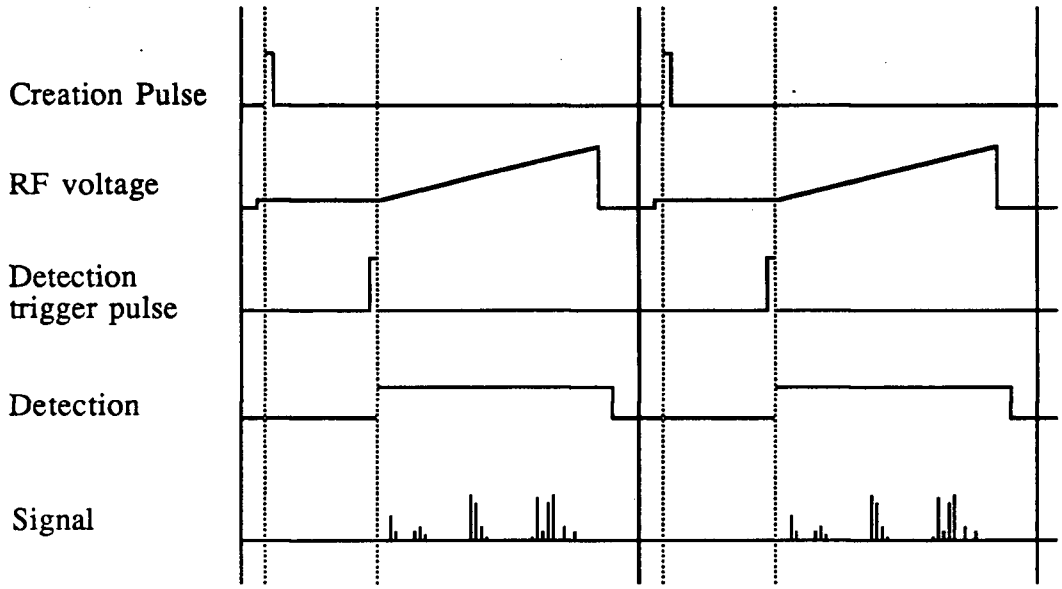

Figure 3.23: Timing of the "Mass selective instability" mode of operation of the ion trap.

3.8.2 - Timing for the Graphite Furnace Experiments:

In the series of experiment done with the graphite furnace, the timing on the ion trap operation was exactly the same as presented in the previous section but, since there is a certain delay between the time the graphite furnace is fired and the time the analyte reaches the ion trap, the timing of the experiments must take this delay into account. When the graphite furnace starts its atomisation cycle the computer keeps track of the time that passes. After this initial delay the ion trap data acquisition cycle starts. The delay between the firing of the graphite furnace and the firing of the data acquisition cycle can be varied as required by the operator.

3.8.3 - Timing of the Laser Ablation Experiments:

Many attempts at using different timing sequences to improve the results of the laser ablation experiments were made. The most successful timing sequence for the laser ablation experiments is presented in figure 3.24. The main difference between this mode of operation and the one presented in section 3.7.1 is the fact that the electron beam pulse has been totally replaced by the laser pulse. As the results will show, the laser ablation process creates, in most cases, too many ions to be handled by the ion trap and the detection system; there is really no need to use the electron gun to increase the number of ions in the trap.

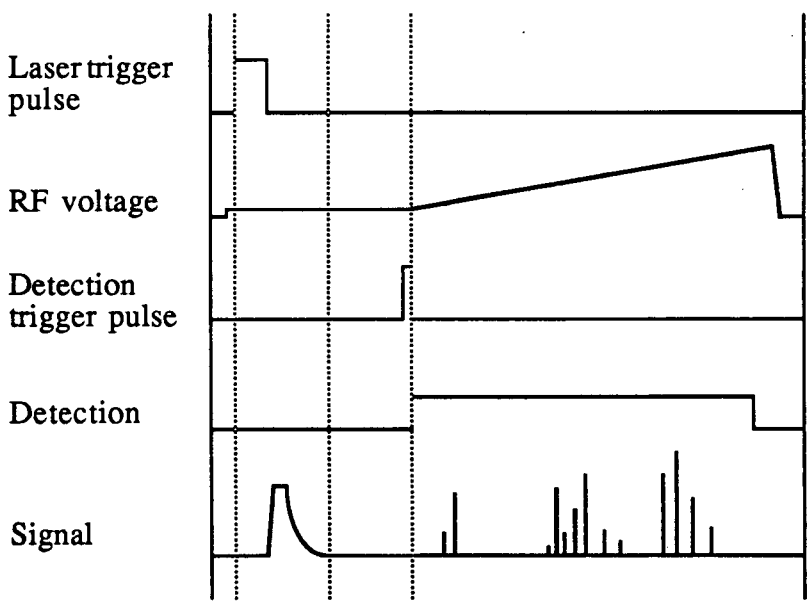

Figure 3.24: Timing sequence for the laser ablation experiments.

A time delay has to be introduced between the firing of the laser and the triggering of the data acquisition system because the laser flash creates a large

disturbance for the channeltron electron multiplier. This time delay is also part of the storage time for the ions. The minimum time used between the triggering of the laser and the start of the data acquisition was 40 ms. It should be noted that the system relay/laser trigger will not respond unless the signal from the computer to the relay is kept high for a minimum of 20 ms.

Summary:

The instrument designed and built in our laboratory to perform elemental mass spectrometric analysis on small volume samples or solid samples is based on a radio-frequency quadrupole ion trap mass spectrometer. To vaporize and atomize the small sample a graphite furnace was enclosed in a container and interfaced to the ion trap. For the study of solid samples, the ring electrode of the ion trap was modified to allow the passage of the sample to the cavity of the trap and to allow for the entrance of a laser beam inside the tap. The graphite furnace used was a standard carbon rod atomiser, marginally modified to be placed in the container, allowing the control of the atmosphere surrounding it. The laser used for the ablation experiments was a 1 J ruby laser; the laser ablation was performed directly inside the cavity of the ion trap.

CHAPTER IV

OPERATION OF THE ION TRAP

4.1 - Introduction:

As described in the previous sections the ability of the ion trap to store ions for extended periods of time has prompted much interest in a number of fields. It has been used as a mass spectrometer [25, 42, 77], as a pressure meter, as an ion reservoir for spectroscopic studies [14, 18, 51, 78-80], as a reaction chamber [43, 44, 81, 82] and as an ion source for classical mass spectrometers [83, 84]. Since the appearance of the commercially available ITD™ and ITMS™ most of the work has been performed using these instruments; certainly the recent analytical applications in the field of ion trapping are using them. The use of the ion trap in the field of analytical chemistry has been mostly as a detector for gas chromatography. However there is some interesting work being done with the instrument which broadens its scope of application: work has been presented demonstrating the capability of the ion trap to perform MS^n analysis on an analyte [12], chemical ionization has been used to produce the ions for analysis [41] and more recently a paper published in Analytical Chemistry presented spectra of a sucrose sample, a leucine-enkephalin sample and an hexadecyltrimethylammonium bromide sample obtained by laser desorption directly in an ion trap mass spectrometer [24]. These are signs that research in the field of new applications of the ion trap is starting in earnest; the work done during the last three years in our laboratory on the quadrupole ion trap is evidence of the continuing evolution and diversification of this research.

The ability of the ion trap to confine ions to a well defined space for long periods of time could prove to be of great benefit to the field of analytical chemistry if the development of ion trap based instruments can take advantage of two consequences of this particular attribute of the ion trap. Firstly this capability can be used to accumulate the analyte before performing the analysis, in essence preconcentrating the analyte before attempting to detect it. This may lead to the

development of instrumentation capable of detecting lower concentrations of analyte in smaller volumes of samples. Secondly, the long residence time of the analyte in the cavity of the trap may also lead to much higher signal-to-noise ratios. The proof of this can be seen from Neuhauser's observation of a single ion confined at the centre of a trap [18, 50]. An applicable method of detection that comes immediately to mind to take advantage of those features is optical spectroscopy. The use of the ion trap as a mass spectrometer can also take advantage of these two features: accumulate the analyte before performing the mass spectrometric analysis and, when using chemical ionization, let trapped ionizing agents react with the analyte for long periods of time. The ion trap also offers the possibility of performing a complete mass spectrometric analysis on the trapped ions.

The long term plans for the development of an analytical methodology using ion trapping, undertaken in our laboratory, are aimed at applying these two features of the ion trap to inorganic analysis. The development of a methodology capable of taking a small volume of sample, transfering it quantitatively to the cavity of the ion trap and performing an ultratrace analysis is well worth pursuing. The first step in the development of such an instrument is the production of an ion trap suitable to the needs of the research to be undertaken and the investigation of the possible means by which a sample could be transported to the ion trap cavity, followed by the characterization of the device. The possibility of using a graphite furnace atomiser to vaporise a liquid sample that would then be transfered to the trap was investigated. We have also explored the possibility of vaporising a solid sample directly inside the cavity of the quadrupole ion trap by laser ablation. The latter methodology has the advantage of being able to use a solid sample directly with minimum handling. Furthermore, this technique would eliminate the need to transfer the analyte from an outside source to the cavity of the trap, eliminating the problems related to the loss of analyte during the transfer.

As a mass spectrometer the radio-frequency quadrupole ion trap is usually used in the total pressure mode (along the $a = 0$ line of the stability diagram), which is a low resolution mode of operation. The instrument used in this work was also operated in the total pressure mode. The use of the ion trap in a higher resolution mode (at the apex of the stability diagram) has seldom been reported in the literature describing analytical applications of the trap. The conditions under which the ion trap is run are very important to the signal obtained. The use of background gas, its pressure, the trapping conditions and the voltage range scanned will all influence the signal intensity and/or the resolution of the instrument. In the first part of this chapter the operation of the ion trap including the resolution of the instrument, the identification of the peaks, the errors associated with assigning the mass-to-charge value of peaks, the error associated with the measurement of the signal intensity, the effect of the analyte pressure in the ion trap container, the effect that the trapping voltage has on the signal intensity of a peak and the effect of the storage time will be described. The influence of helium (when used as a background gas) on the signal obtained from the ion trap will also be described. To complete this chapter some chemical reactions in the ion trap and their possible use in analytical methodologies will be discussed.

4.2 - The Operation of the Ion Trap:

The development of the ion trap mass spectrometer involved a number of steps and before any data could be obtained from the system all the different components of the instrument had to be ready: the trap, the vacuum system, the electronics, the computer hardware and software. The first attempts at using a storage oscilloscope to acquire the data were not very successful (because of the low resolution obtained with the oscilloscope), but the use of the ISC-16 data acquisition board greatly

enhanced our ability to obtain reliable data. The first series of experiments was done with the Zenith computer controlling the experiments while the data acquisition was carried out using another computer (because the data acquisition board had to be shared by many different experimental set ups in our laboratory). This problem was solved when a second data acquisition board was obtained and installed in the Zenith computer.

The timing of the operation of the ion trap was presented in section 3.7 of this thesis. During each step of this operation the detector will respond to the positively charged particles escaping the ion trap along the "z" axis or to those created in the volume between the ion trap and the detector. The signal at the detector during a typical scan of the RF voltage applied to the ring electrode of the ion trap is presented in figure 4.1. The detector will first experience a burst of ions coming to it during the creation process; these are the ions created in the path of the electron beam which are not trapped due to their initial energy, initial position, or because their mass-to-charge ratio is too low. These ions will be lost from the trap along the "z" axis.

After the initial pulse of ions is detected, there will be a slow leakage of ions from the trap during the storage time. This leakage can be attributed to two main causes: firstly, the initial trapping conditions for those ions may have been such that after a certain number of RF cycles their trajectory has increased so much in space that they escape the trap (quasi-stable initial trapping conditions). The second cause is the mechanical imperfections that can exist in the trap; the field defects caused by these imperfections would affect the ions at each cycle of the the RF voltage they experience. Therefore ions which would normally be trapped if the device were built perfectly are lost because the defects in the trapping field causes them to be ejected after a finite number of RF cycles.

When the RF ramp starts, the detector will respond to ions being selectively ejected from the trap by the increasing voltage. In figure 4.1 the data presented covers

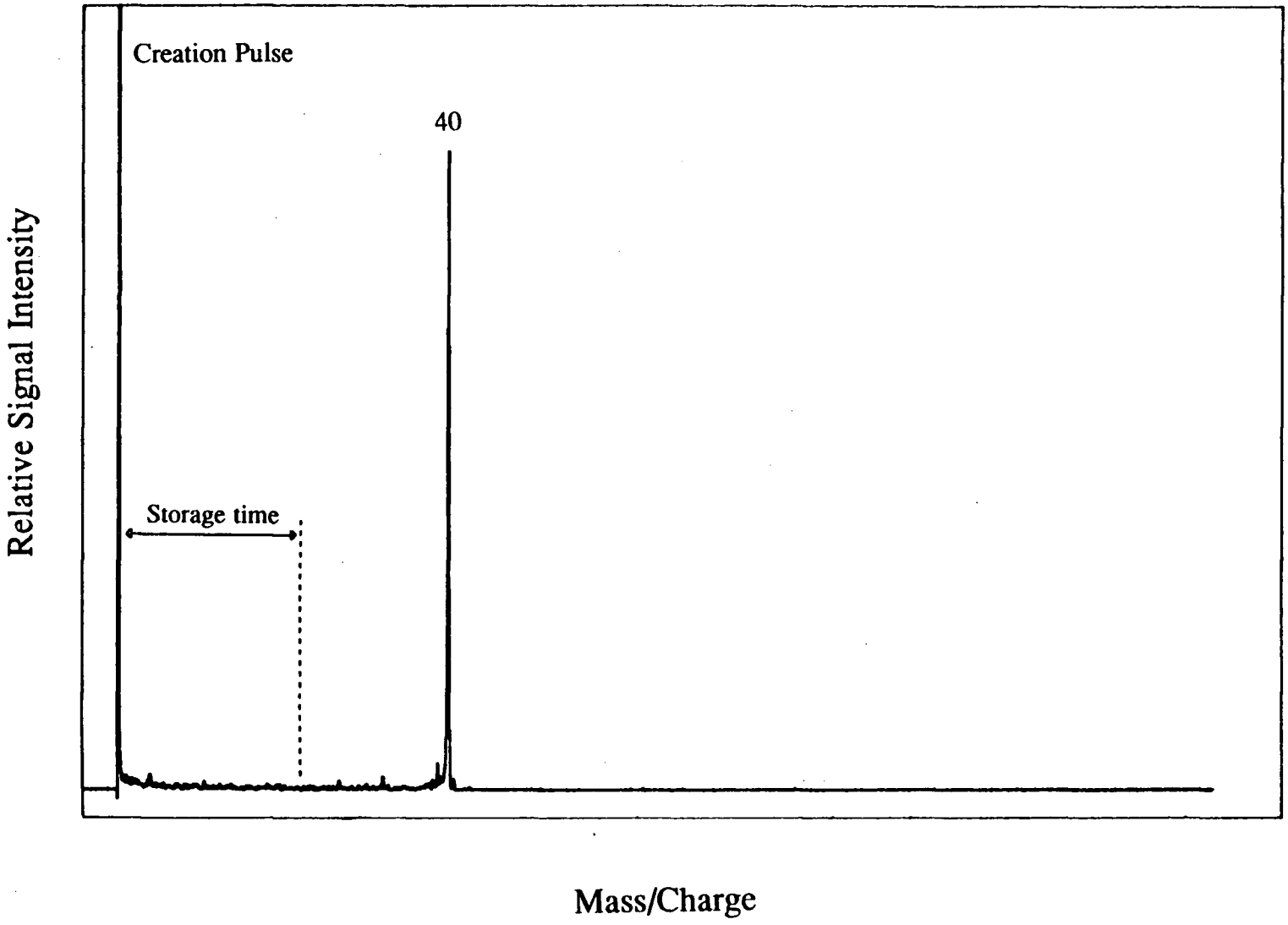

Figure 4.1: Signal detected by the channeltron as the operations of the ion trap are performed (Ar^+ appearing at m/e = 40).

the entire experiment from the creation pulse to the end of the mass range scanned. In all the other spectra presented in this thesis the data was acquired only during the period in which the actual mass spectrometric analysis is performed (during the RF ramping). The creation pulse and storage period are not included in the data acquired.

4.2.1 - Identification of the Peaks:

To identify the value of the m/e ratio of the various peaks appearing on a given mass spectrum their position in the data array is compared with the position of known peaks. The m/e axis is linear so the calculation for the m/e ratio of an unknown peak is very simple. Three standards were used to establish the m/e axis: the four peaks corresponding to the CCl_3^+ ions from carbon tetrachloride (m/e ratio 117, 119, 121 and 123, see figure 4.2), the six most abundant isotopes of xenon (m/e ratio ranging from 129 to 136, see figure 4.3) and the four peaks corresponding to $SbCl_2^+$ in the antimony trichloride spectra (m/e ratio 191, 193, 195 and 197, see figure 4.4). Once the standard spectrum has been taken, there is no need to keep the standard gas in the trap container since the position of the peaks from one spectrum to the next does not change by more than ±4 parts in 4096. This remains true as long as the initial RF voltage setting and the RF voltage range setting are not changed on the RF power supply.

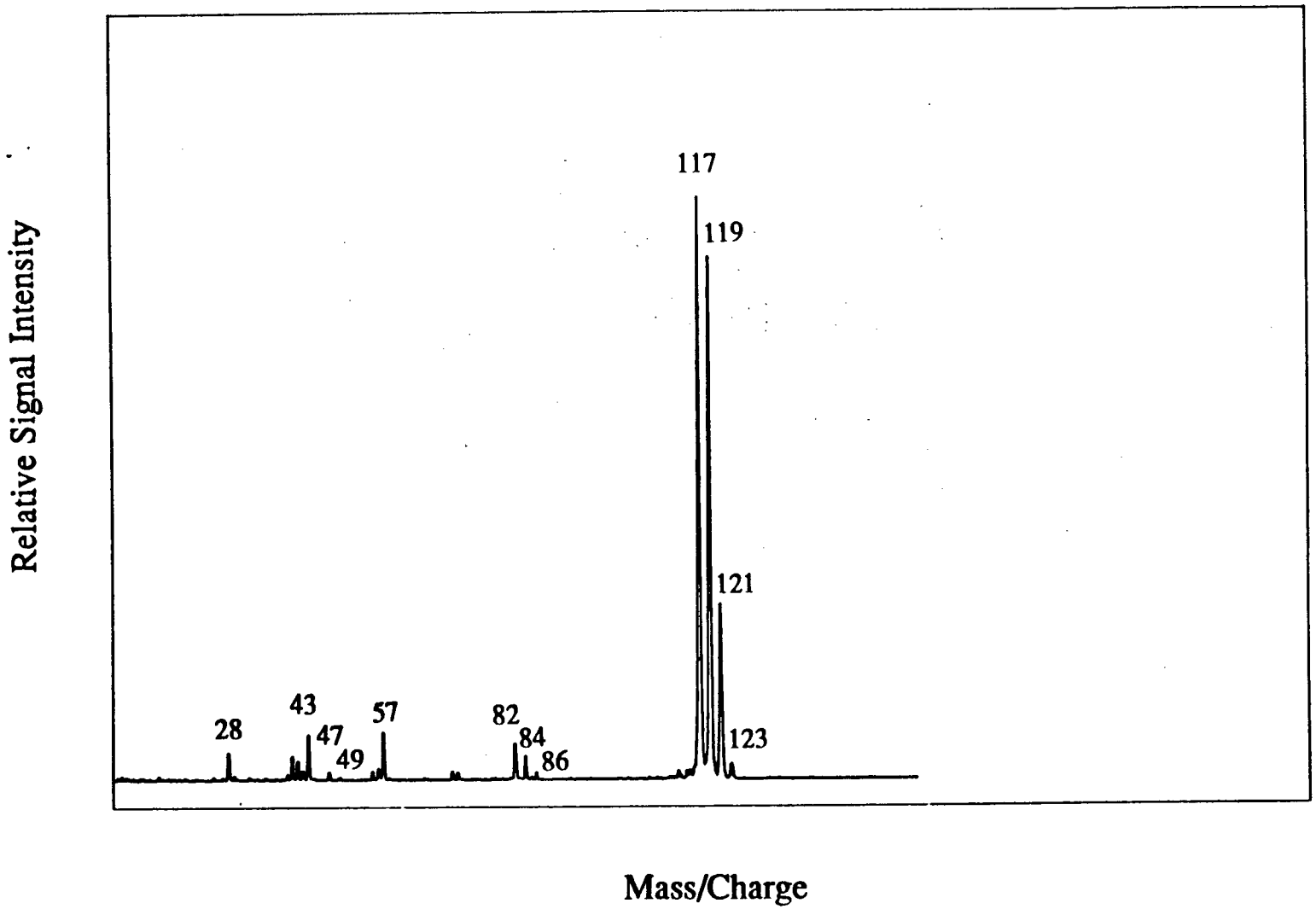

Figure 4.2: Ion trap mass spectrum of carbon tetrachloride.

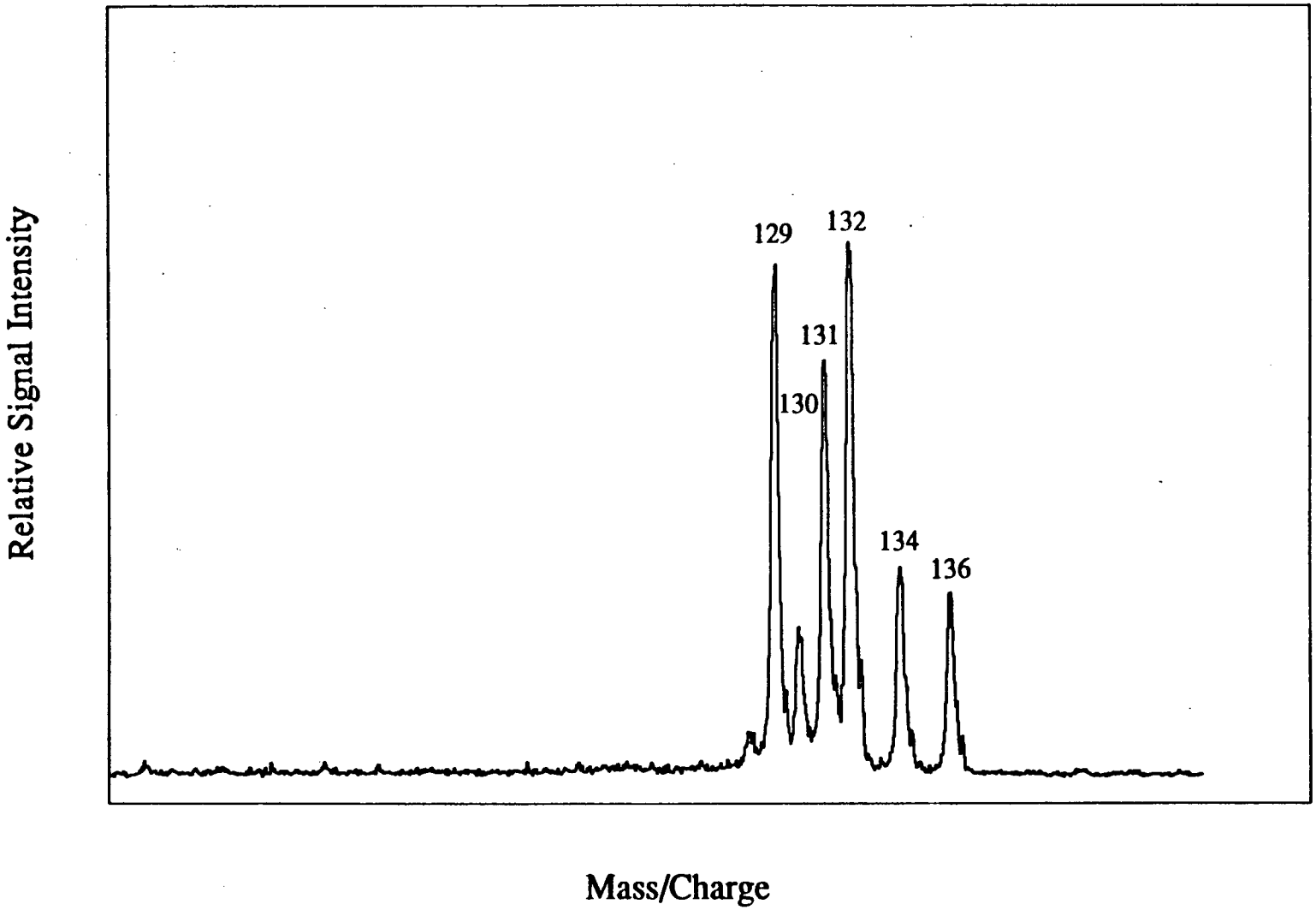

Figure 4.3: Ion trap mass spectrum of xenon.

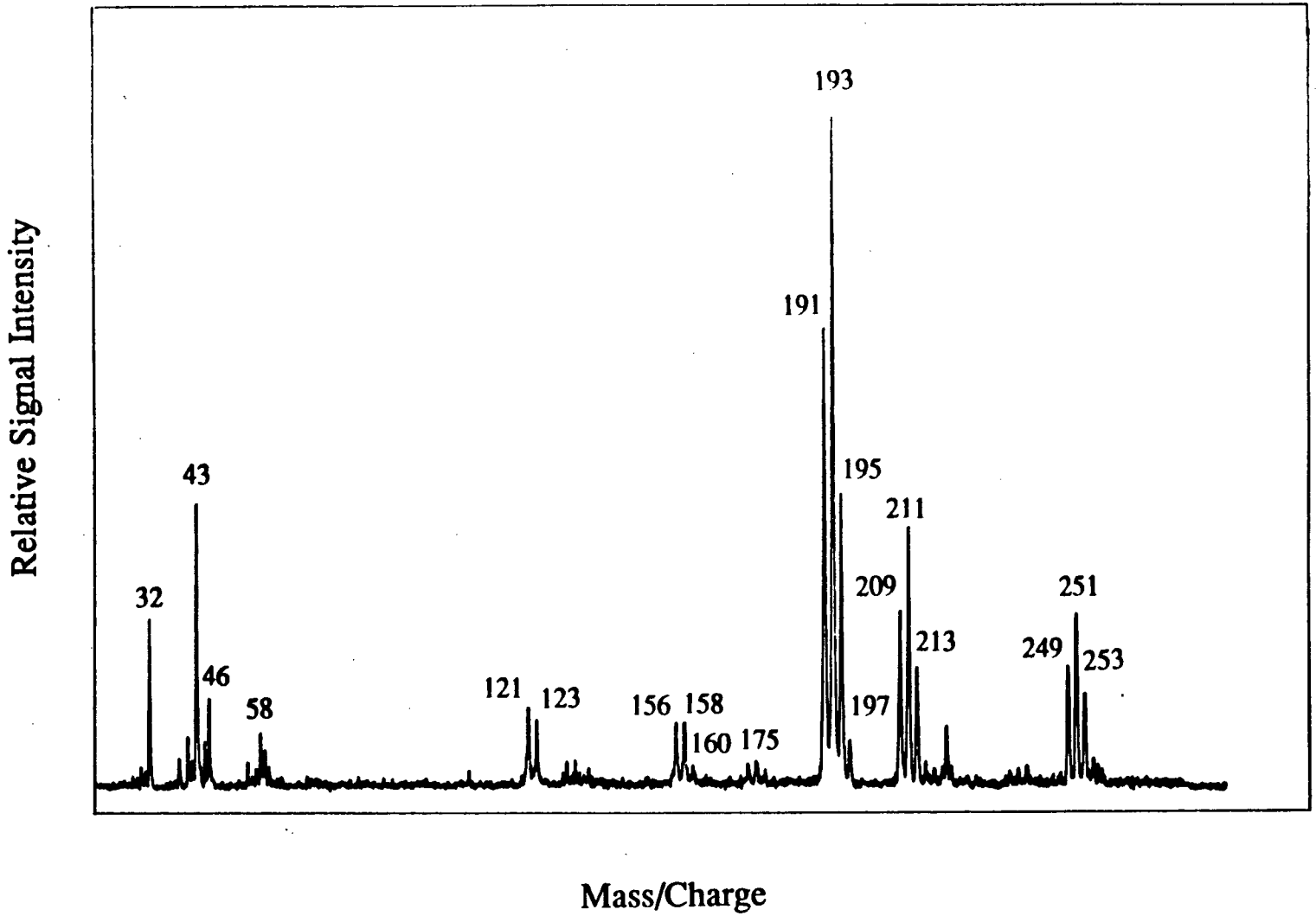

Figure 4.4: Ion trap mass spectrum of antimony trichloride.

4.2.2 - Errors Involved in Assigning the Mass-to-Charge Values of the Peaks:

Although the position of a peak may change by 4 parts in 4096 from one spectrum to the next, the relative position difference between two peaks from one spectrum to an other is never greater than 1 part. So if, for example, peaks 191 and 195 of antimony chloride are used to standardize a full range mass spectrum the error in the assignment of a peak would be in the order of 2 % (the distance between these two peaks is about 50 data points, in most of the experiments reported, so 1 in 50 is 2 %). If the peak to be identified is located fairly close to one of the standard peaks this error does not generally cause any problems but, if the peaks to be identified are located far away from one of the standard peaks this error has to be taken into account when assigning the mass-to-charge value of the peaks; if the unknown peak is located 50 amu away from the nearest standard peak the assignment of the m/e value of the peak can be up to 1 amu away from the true value. On a given spectrum this error remains the same across the m/e range so it can be systematically taken into account.

4.2.3 - Errors Associated with the Signal Intensity Measurement:

To find the errors associated with the measurement of the signal intensity of peaks a series of 30 spectra of argon were taken. Each of the 30 spectra was obtained by averaging 50 scans. The average of the signal intensity for the argon peak was computed as was the standard deviation of the data. The percentage relative standard deviation ($\frac{\text{standard deviation}}{\text{average}} * 100\ \%$) was found to be 7.9 %; This gives an estimate of the repeatability of the results for a given, constant, set of operating conditions.

The value obtained indicates that from one scan to the other the difference in signal intensity for an ion is quite large. However, another way to assess the reliability of the results is to determine the reproducibility of the isotopic ratios of different isotopes of the same ion, and compare them with the natural abundances presented in the literature. To obtain this information, the peak intensities of the detectable isotopes of xenon were measured on 30 spectra obtained over the entire time the experiments on the ion trap were performed. The conditions under which these spectra were obtained almost covered the entire range of conditions under which the ion trap has been operated. As the results presented in Table 1 indicate, the values found for the isotopic distribution of xenon show that for peaks corresponding to relatively abundant isotopes the ratios are close to those reported in the literature (the difference for peaks 129, 131, 132 and 134 is lower than 5%, and the percentage relative standard deviation for these peaks is also reasonable, below 7% for all of them). However, the situation for the peaks corresponding to less abundant isotopes of xenon (mass-to-charge ratios of 128 and 130) is very different. The isotopic ratios found for these peaks are quite differrent from the ones presented in the literature (their relative standard deviation is also very high). There is a trend that should be noted in these results: the isotopic ratios found for isotopes of higher abundance are always underestimated while the isotopic ratios for the isotopes of lower abundance are overestimated. The reason why the small peaks have such a large variation in their signal intensity and are overestimated comes from the fact that they are positioned very close to larger ones. Most of the spectra used to compile this information were taken with large amounts of xenon present in the trap and as will be shown in the next section of this chapter, the resolution of the instrument decreases when the pressure of the analyte increases past a certain value (presumably due to space charge effects) and the large peaks overlap on the small ones introducing a large error in the measurement of the height of the small peaks.

The results from these two studies on the reliability of the signal intensity indicate that the error associated with the measurement of the signal intensity for peaks of high abundance is in the order of 10%, while for the lower intensity peaks the error is much larger especially if these small peaks are close to high intensity peaks.

Isotopic ratios for xenon

Mass-to-charge value	128	129	130	131	132	134	136
Average found	3.6	24.8	7.7	20.0	26.0	10.2	7.9
Standard deviation	1.1	1.6	1.7	1.2	1.6	0.5	0.9
% RSD	30.5	6.5	22.8	5.9	6.0	5.1	11.0
Reported isotopic ratio	1.9	26.4	4.1	21.2	26.9	10.4	8.9

Table I: Isotopic ratios found with the ion trap for the measurable isotopes of xenon. The reported isotopic ratios are taken from the CRC Handbook of Chemistry and Physics, 1979.

4.3 - Effect of the Pressure of the Analyte in the Ion Trap on Signal Intensity and Peak Shape:

As with any other instrument one would expect the radio-frequency quadrupole ion trap to respond to increases in the number of analyte molecules (or atoms) present by giving an increase in signal intensity. Instruments generally suffer from two limitations in their ability to respond to changes in concentration of an analyte. Firstly, they all have a concentration limit below which the signal becomes indistinguishable from the background noise (their limit of detection). Secondly, when the concentration of the analyte becomes too high, the instrument saturates and loses

linearity in its response. The ion trap system built will also have a limit of detection. In the case of the ion trap the second limitation will correspond to the maximum number of ions which can be confined by the trap under a given set of conditions. Figure 4.5 (and Table II) presents the response of the ion trap to an increase in pressure (the increase in pressure is produced by increasing the intake rate of the helium/xenon mixture into the ion trap container). The response seems to be relatively linear up to a certain point (around $2 * 10^{-6}$ torr) beyond which the increase stops and the signal levels off. This point corresponds to the maximum number of ions that can be contained and extracted efficiently from the trap.

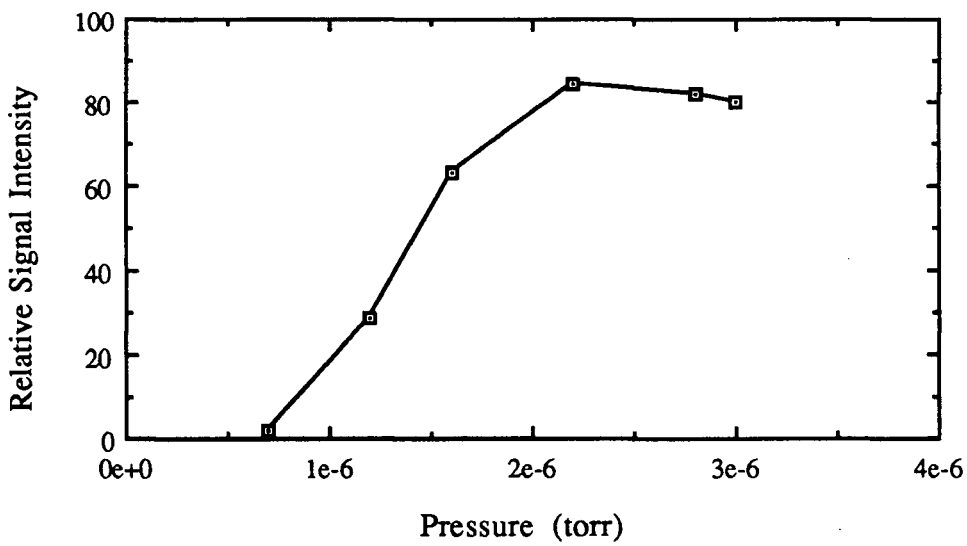

Figure 4.5: Signal intensity for mass/charge 132 of xenon as a function of the total pressure of the helium and xenon mixture in the ion trap container.

The data plotted in figure 4.5 comes from the set of xenon spectra presented in figure 4.6. As can be seen, the increase in analyte pressure not only affects the signal intensity, but also the peak shape. As the pressure of xenon is increased inside the trap the leading edge of the important peaks deteriorates. The baseline of the spectra

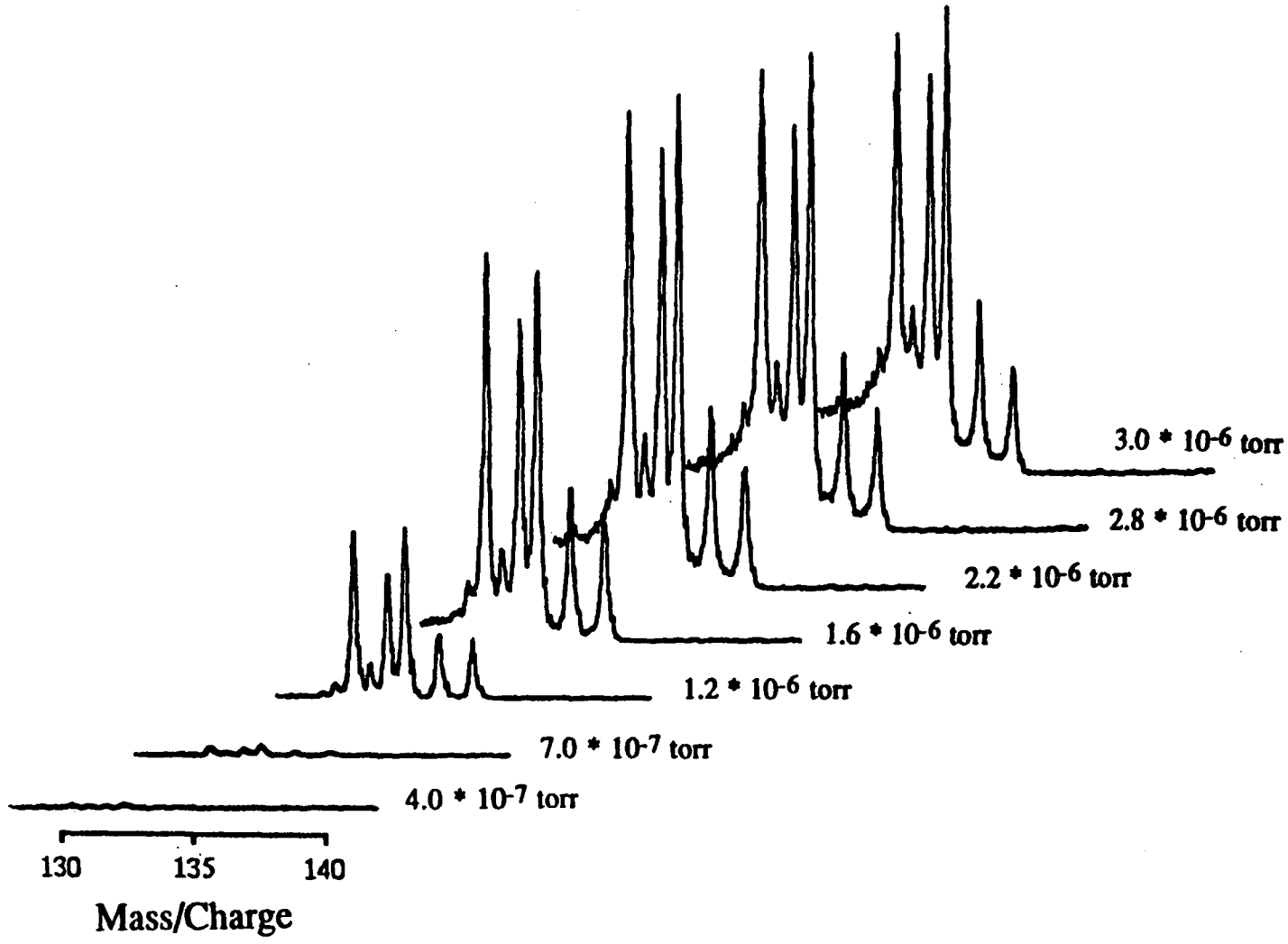

Figure 4.6: Xenon signal intensity as a function of pressure in the ion trap container.

Table II

Pressure (Torr)	Relative Signal Intensity
0.7e-7	2
1.2e-6	34
1.6e-6	71
2.2e-6	92
2.8e-6	88
3.0e-6	86

Table II:Signal intensity for mass/charge 132 of xenon as a function of the total pressure of the helium and xenon mixture in the ion trap container.

also change; the spectra acquired at relatively high pressures of xenon show a constant leaking of ions as the RF voltage amplitude is scanned - as each important peak passes, the leakage becomes smaller and smaller and the baseline falls closer and closer to the baseline corresponding to the detector noise.

4.4 - Signal Intensity as a Function of the "q" Value for a Given Ion:

It has been shown in the literature that the choice of the trapping value for the parameters "*a*" and "*q*" of the Mathieu equation will influence the trapping efficiency of the device. Figure 4.7 shows the spectra of xenon obtained using different trapping voltages which can be converted to the "*q*" value of particular ions. Figure 4.8 presents a plot of the intensity of peak 129 as a function of its "*q*" value. Table III presents the data appearing in figure 4.8. The behaviour observed with the peak at mass-to-charge ratio 129 was similarly observed with all other isotopes of xenon. As can be seen the maximum signal intensity is obtained when low values of "*q*" are used

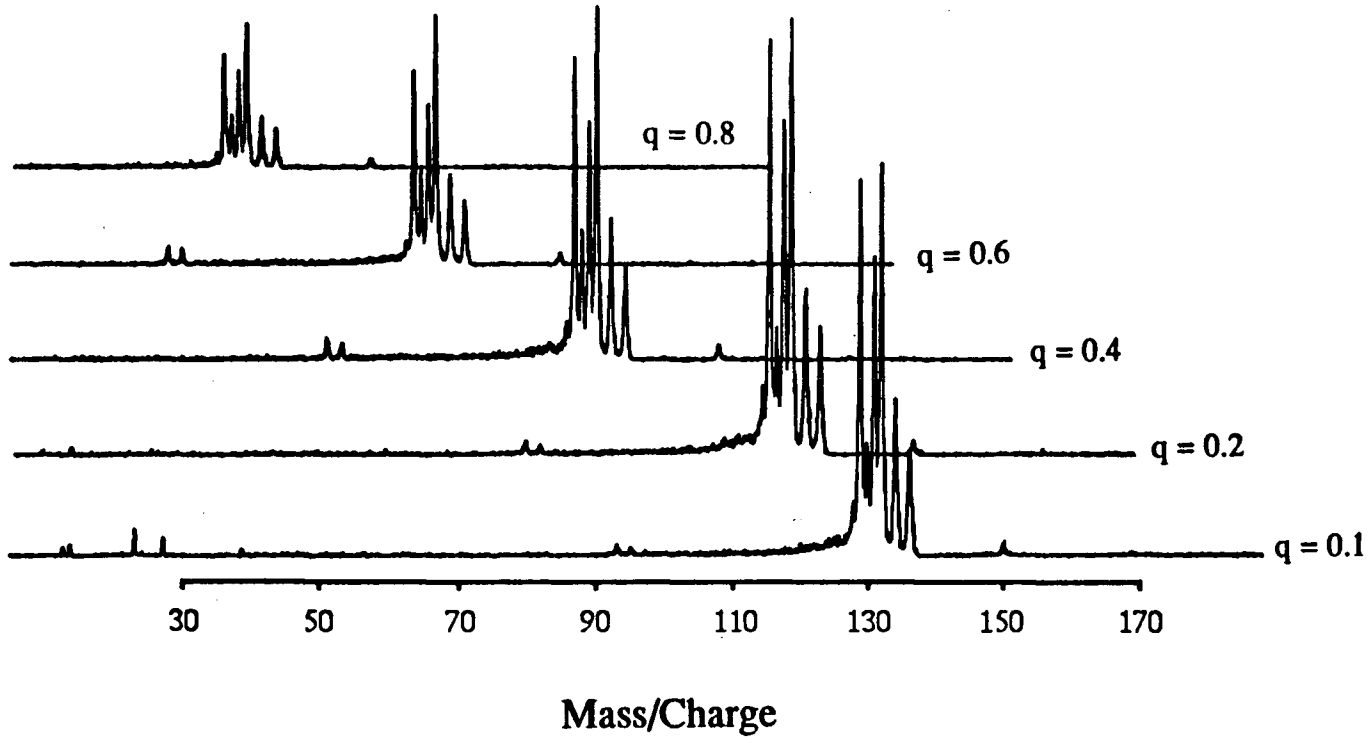

Figure 4.7: Spectra of xenon obtained as a function of the "*q*" value corresponding to the trapping voltage.

for trapping the ions; as the value of "q" is increased the signal intensity, and thus the number of ions in the trap, decreases. This indicates that the ion trap detector, under a given set of conditions, will trap ions with high mass-to-charge values more efficiently than to those with low mass-to-charge values. It also means that if the operator is interested in a particular ion, the trapping voltage should be chosen so that the "q" value for the isotope of interest is low regardless of what it is for the other ions. The plot of figure 4.8 shows that the optimum value for xenon in our system is around 0.2.

These results differ significantly from those of Iffländer and Werth [56] and Baril and Septier [85]. Using fluorescence measurements Iffländer and Werth found that the maximum number of ions will be trapped when their "q" value is about 0.5. Their experiment was done by measuring the fluorescence of barium ions trapped at different values of "q" and "a". Baril and Septier obtained similar results to the ones obtained by Iffländer and Werth, but their study was a theoretical one. However, the results from these two groups do not take into account the extracting efficiency of the "mass selective instability" mode of operation of the ion trap. The results presented in figure 4.8 were verified by performing the same experiment using argon ions. The results presented in figure 4.9 confirm the previous findings. To our knowledge no other study has established the optimum operating conditions (as far as "q" values are concerned) when operating the ion trap under the "mass selective instability" mode of operation.

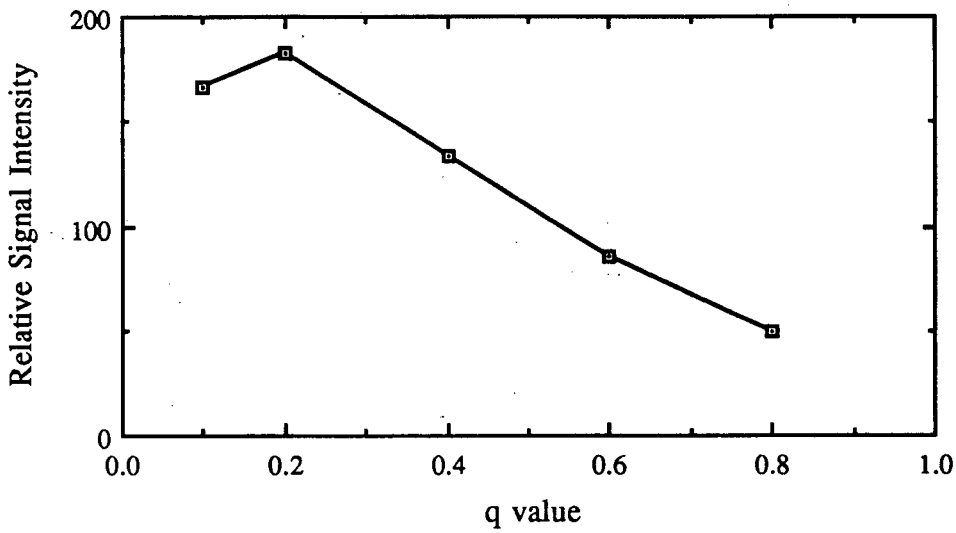

Figure 4.8: Relative signal intensity for xenon ions with mass-to-charge ratio of 129 as a function of the "*q*" value corresponding to the trapping voltage used.

Table III

"*q*" value	Relative signal intensity
0.1	166
0.2	183
0.4	134
0.6	86
0.8	50

Table III: Relative signal intensity for xenon ions with mass-to-charge ratio of 129 as a function of the "*q*" value corresponding to the trapping voltage used.

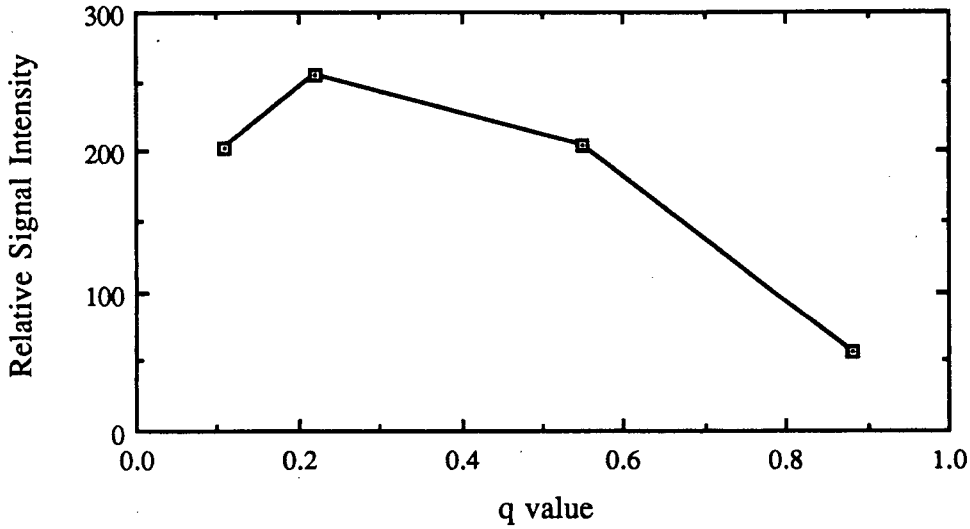

Figure 4.9: Relative signal intensity for argon ions with mass-to-charge ratio of 40 as a function of the "*q*" value corresponding to the trapping voltage used.

Table IV

"*q*" value	Relative signal intensity
0.11	203
0.22	255
0.55	205
0.88	57

Table IV: Relative signal intensity for argon ions with mass-to-charge ratio of 40 as a function of the "*q*" value corresponding to the trapping voltage used.

4.5 - Storage Time Obtainable with the Ion Trap:

One of the most interesting features of the ion trap is its ability to confine ions for very long periods of time and the length of time an ion trap can hold the ions is a reflection of the quality of fabrication of the instrument; a trap which is improperly constructed will not be able to confine ions for long times. The storage times reported in the literature are generally more a reflection of the time required to perform the different experiments undertaken, however Neuhauser et al. in 1980 [18] presented pictures of ion clouds trapped in a RF quadrupole ion trap (the pictures were taken using time exposures of 10 minutes). Nagourney et al. [51] reported experiments using storage times of 45 minutes. In the same paper they reported keeping ions in their trap overnight, showing the capability of the ion trap to confine the ions for very long periods of time. On the other hand, most researchers report experiments performed over much shorter storage times (in the order of ms).

The longest storage time at which experiments were performed with the system built for this project is 5 minutes. A spectrum of toluene obtained after a storage time of 5 minutes is presented in figure 4.10. As can be seen from this spectrum a large number of ions remain in the trap after this time. In fact, during this series of experiments, the total number of ions found in the ion trap did not change significantly between a storage time of 1 minute and one of 5 minutes.

4.6 - Resolution of the Ion Trap:

Very little work, dealing with the resolution of the quadrupole radio-frequency ion trap instrument, has been presented in the literature. Furthermore, most of the publications on this subject deal with the resolution of these instruments under the mass selective storage mode of operation of the ion trap, which differs substantially

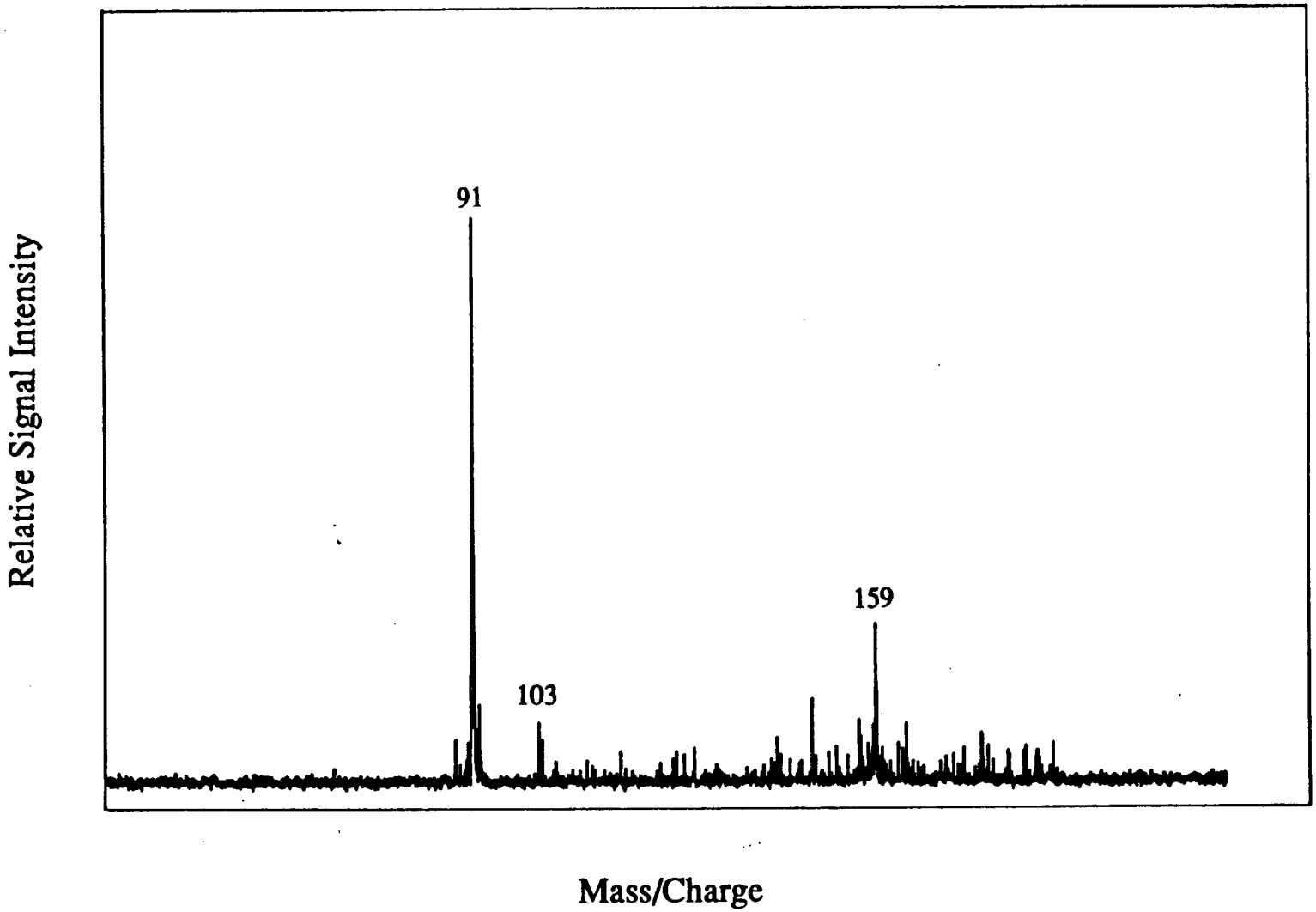

Figure 4.10: Spectrum of toluene obtained after a storage time of 5 minutes.

from the situation encountered when using the ion trap under the "mass selective instability" mode of operation. The only publication in which the resolution of the radio-frequency quadrupole ion trap was examined using the mass selective instability mode of operation for different experimental conditions is a paper by Stafford et al. [22], in which a discussion was presented on the effect that the presence of helium as a background gas has on the resolution of the instrument. The conclusion that can be drawn from the results presented in this paper is that an increase in the pressure of helium has very little effect on the resolution for low mass ions, while for higher mass ions the increase in resolution can be very important when the pressure of helium is increased from 10^{-5} torr to 10^{-3} torr.

Ultimately, in the "mass selective instability" mode of operation the limiting factor on the resolution will be the "fuzziness" of the boundary of the stability diagram of the ions present in the trap. In theory the boundary of the stability diagram should be very sharp but, in practice, experimental conditions may be such that ions will be withdrawn from the trap even if they have not reached their stability boundaries, while other ions may stay, for similar reasons, inside the trap although their stablility boundaries have been passed. In papers presented in 1978 [86] and 1981 [87] Todd presented results which clearly showed that experimental stability diagrams differ appreciably from theoretically derived ones. Todd speculated that this effect arises from the influence of the initial thermal velocity of the ions at the moment of creation, space charge effects and geometrical imperfections in the trapping device. Fulford et al. [27] showed, by establishing the stability diagram of different ions in three different cylindrical traps and in a QUISTOR, that the geometry of the device as well as the trapping conditions will influence the geometry of the stability diagram. In 1980 [88] Todd et al. linked the changes in the stability diagrams to variables such as storage time, RF voltage phase at the time of the extraction of the ions, mass-to-charge ratio and the initial density of ions. In all these studies the extraction of the ions present in

the trap was done by applying a voltage pulse on one of the end cap of the device. The results of these experiments indicated only the presence or the absence of ions in the trap under a given set of conditions. There has been no work done on the behaviour of the ions as the RF voltage on the ring electrode is ramped up. But, the publications presented above suggest that the boundaries of the stability diagram will significantly change with the particular conditions under which an ion has been created. This, along with the position at which each ion has been created in the trap and the amount of material being trapped during the experiment could explain the peak width observed with this instrument.

If a wide distribution of kinetic energy of the ions is a cause for the lowering of the resolution of the ion trap, experimental conditions leading to similar kinetic energy for all the ions would likely improve the resolution. Uniformity in the kinetic energy of the ions would limit the volume in which the ions travel, and render the trajectories more similar from one ion to the other. In their 1984 paper [22] Stafford et al. proposed the use of helium as a background gas in their system to improve the resolution of the instrument; they found that the resolution was improved. They concluded that helium was damping the motion of the ions at the centre of the trap restricting the kinetic energy distribution between ions. They observed a significant improvement in the resolution for ions of large mass-to-charge ratios, but the difference in resolution was less noticeable for ions with lower mass-to-charge ratios. They also observed an increase in signal intensity as they increased the pressure of helium and concluded that the restriction of the kinetic energy distribution produced the collapse of the ion cloud toward the centre of the ion trap, putting the ions in a better position for being efficiently extracted from the trap. This improvement of resolution by using larger amounts of helium was not observed in our system. It should be noted that our study was not conducted under as wide a pressure range as that of Stafford et al.

The resolution of the commercial instrument sold by Finnigan MAT is of the order of one mass unit resolution across the entire mass range. The resolution of our instrument is a function of the mass range covered. As the mass range covered passes from its maximum (around 300 amu) to a lower value the resolution improves to the point where we obtain unit mass resolution over a mass range of around 150 amu. Figure 4.11 presents two spectra of heptane. The first covers the entire mass range (300 amu) while the other covers 150 amu. Using a mass range smaller than 150 amu did not improve the resolution; the improvement in resolution between the 300 amu range and the 150 amu range is most probably due to the fact that the RF ramp covers a lower range while the DAC that controls it still outputs 4096 points to control the ramp. The voltage resolution is better: 1500V/4096 points is twice as good as 3000V/4096 points. The other factor is that the 4096 points acquired by the data acquisition system also cover a smaller mass range; the resolution there should also improve. On the higher resolution heptane spectrum the resolution for peak 71 is calculated to be 215 (the resolution is here calculated as $\frac{m}{\Delta m} = \frac{71}{0.33} = 215$ where Δm is the peak width at half intensity).

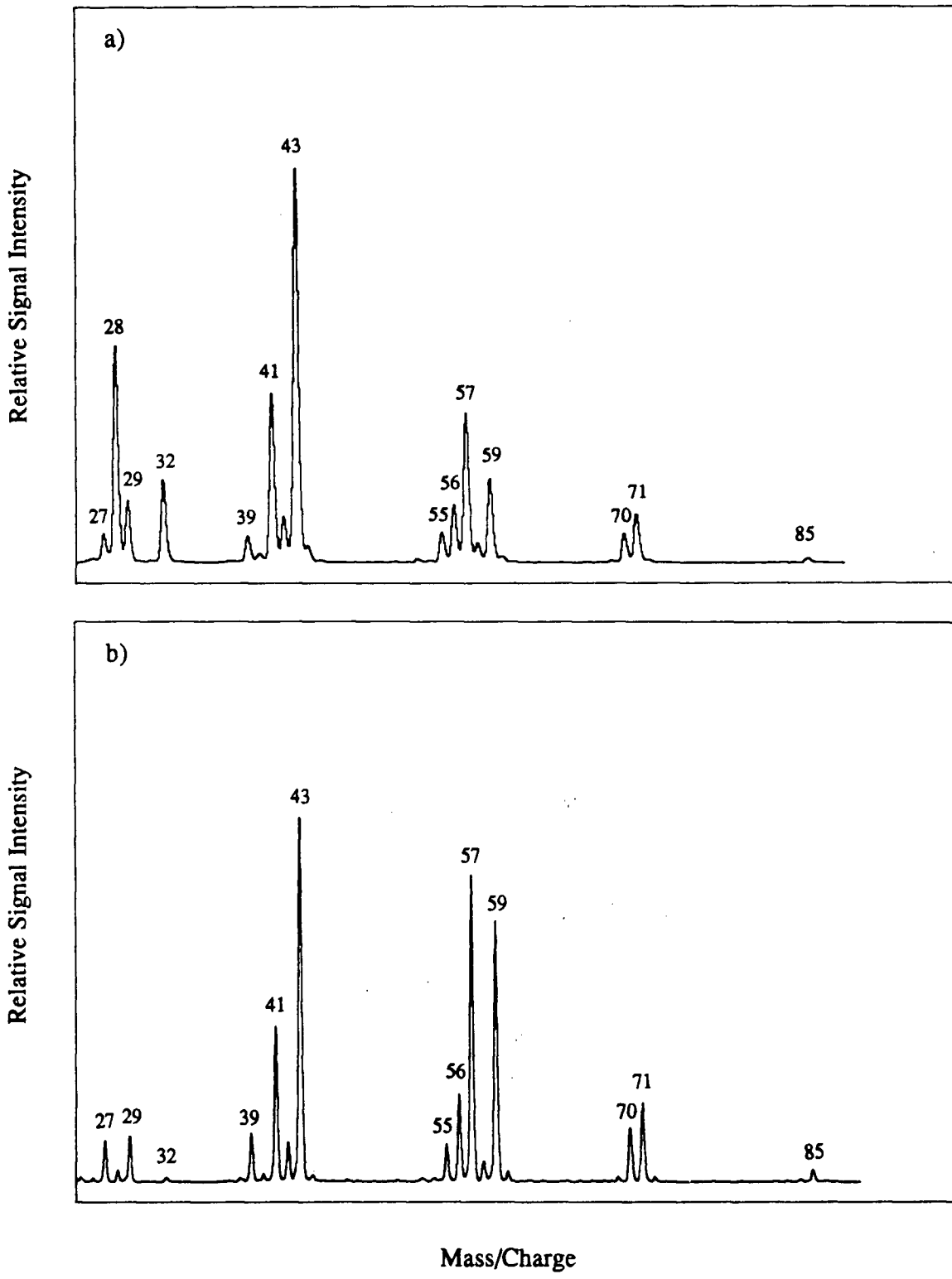

Figure 4.11 - Spectra of heptane taken at two resolution using differents mass ranges: a) the mass range covered on this spectrum was 300 amu, b) the mass range covered on this spectrum was 150 amu.

4.7 - Storage Time Effects:

In the absence of ion/neutral and ion/ion interactions, one would imagine that the signal intensity of the trapped ion would be at its maximum when the storage time is at its minimum, and in a perfect trap the signal intensity should remain constant as the storage time is increased, but imperfections in the field caused by imperfections in the trapping device will provoke a steady loss of ions. Therefore, as the storage time is increased, the signal intensity will decrease. Now since the ions will likely react if they collide with other particles, it becomes very difficult to observe the behaviour of ions of a given mass-to-charge ratio in the trap with only the storage time as an experimental variable, but it is possible to get an idea of the behaviour of the ions in the trap as storage time passes by looking at the total number of ions inside the trap. When these plots are made, one observes that initially the total number of ions increases as the storage time is increased; the signal intensity reaches a maximum and then drops slowly. Figure 4.12 shows this behavior. Table V presents the data used to produce figure 4.12. The initial increase in signal intensity will be explained in detail in a subsequent section. To explain the decay of the total number of ions, the processes of ion loss have to be examined. There are a number of processes that will induce the loss of ions from the trap [12, 34]. One of the causes of ion loss is the field imperfection that may exist due to mechanical imperfections in the ion trap assembly. An ion travelling in the cavity will experience this field imperfection at every cycle of its motion. This may modify its trajectory and make it escape the trapping field after a limited number of cycles inside the trap. Another process for ion loss from the trap is ion-neutral reactions: if a neutral atom or molecule collides with one of the trapped ions, and if this neutral particle has an ionization potential smaller or equal to the ionization potential of the trapped ion, there is a probability that a reaction will occur turning the previously trapped ion into a neutral (thus untrapped) particle. The ion

created by this reaction may or may not be trapped depending on its mass-to-charge ratio and the initial trapping conditions for this ion. In some cases one can imagine ions with a large mass-to-charge ratio being created through chemical ionization and trapped but not detected because of the fact that the RF supply used cannot output a high enough RF voltage amplitude. A third path for ion loss is ion-ion scattering; ions having similar polarity, which come to close to each other can have their trajectories rendered unstable by the encounter. The ions could then be lost.

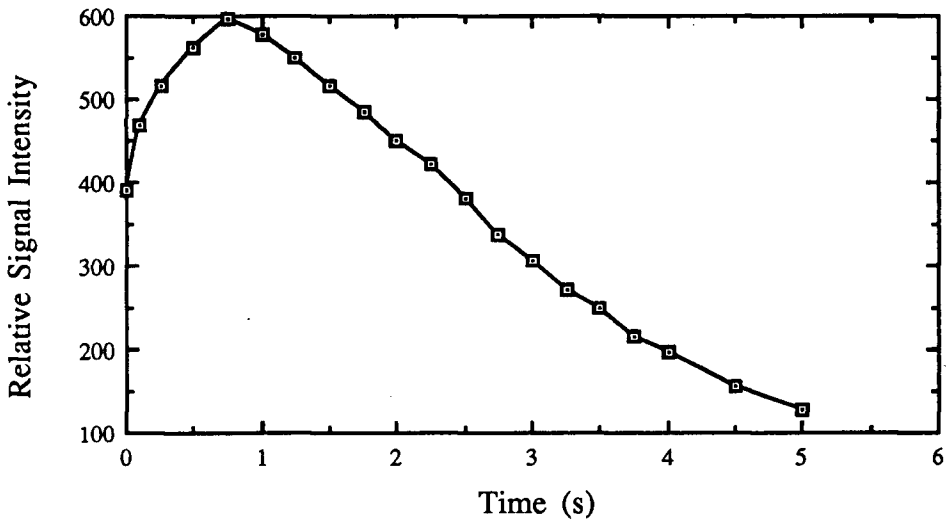

Figure 4.12: Effect of the storage time on total signal intensity. The intensity of all the major peaks of the spectra obtained were added to produce a number representing the total number of ions on the spectrum for all spectra.

Table V

Storage time (s)	Relative signal intensity
.005	392
.10	470
.25	517
.50	562
.75	597
1.00	579
1.25	552
1.50	516
1.75	486
2.00	449
2.25	422
2.50	381
2.75	339
3.00	305
3.25	273
3.50	249
3.75	215
4.00	197
4.50	155
5.00	130

Table V: Effect of the storage time on total signal intensity. The intensity of all the major peaks of the spectra obtained were added to produce a number representing the total number of ions on the spectrum for all spectra.

4.8 - Effect of the Presence of Helium on the Signal Intensity Obtained:

In their 1984 publication Stafford et al. [22] investigated the benefits of using high background pressures of helium in the ion trap container. They claimed that the presence of helium inside the trap improves the resolution and increases the signal intensity. The helium pressures used in their study ranged from 10^{-5} to 10^{-3} torr. Since this publication the usual operating conditions of the ion trap mass spectrometer include the use of a high pressure (around 10^{-3} torr) of helium background gas. However, there is no other publication, to our knowledge, dealing with the effect of the presence of helium in the ion trap cavity. We have thus carried out some experiments in an attempt to assess and understand the effect of the presence of helium on our ion trap system. The pressures used in the experiments reported here were much lower than the pressures used in Stafford's study; we have not only studied the effect of the helium pressure, but we have also linked the effects observed to the storage times used.

The data acquired indicates that an increase in the pressure of helium does not increase the maximum signal intensity obtainable from the system, but that helium does have a definitive effect on the storage time required to attain the maximum signal intensity from an ion. In their paper Stafford et al did not observe that because they worked at a constant storage time, they simply observed an increase in signal intensity as a function of the pressure of helium inside the container. Figure 4.13 is a plot of the time at which the maximum signal intensity for mass-to-charge 119 of CCl_3^+ is obtained as a function of the total pressure in the trap, and figure 4.14 presents the signal intensity of peak 119 of CCl_3^+ as a function of the storage time for different pressures of helium. Table VI presents the data used to create figure 4.13 and Table VII presents the data used to create figure 4.14.

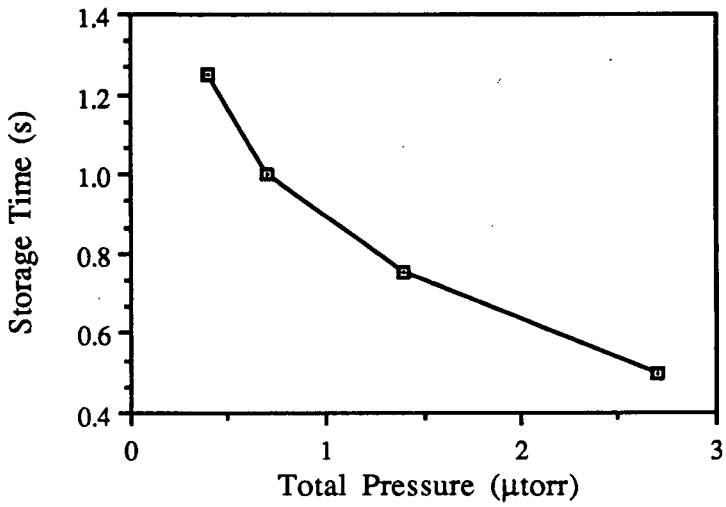

Figure 4.13 : Storage time at which the maximum signal intensity is obtained as a function of the total pressure inside the ion trap container. The increase in pressure from one point to the next was achieved by introducing helium inside the ion trap container.

Table VI

Total Pressure (μTorr)	Storage time (s)
0.4	1.25
0.7	1.00
1.4	0.75
2.7	0.50

Table VI: Storage time at which the maximum signal intensity is obtained as a function of the total pressure inside the ion trap container.

Stafford et al.[22] have stated that the presence of helium in the trap had a cooling and damping effect on the motion of the ions, thus provoking a collapse of the

ion cloud to the centre of the cavity of the trap (where the ions would be in a better position for being efficiently withdrawn from the trap and detected). Figure 4.14 indicates that (at a given pressure of helium) as the storage time increases, the signal intensity increases. An increase in helium pressure will decrease the time required to obtain the necessary number of collisions that will dampen the motion of the ions. When a high pressure of helium is used (of the order of 10^{-4} torr) the storage time required to obtain the maximum signal intensity would be very short. But, the same effect can be observed at lower pressures using longer storage times.

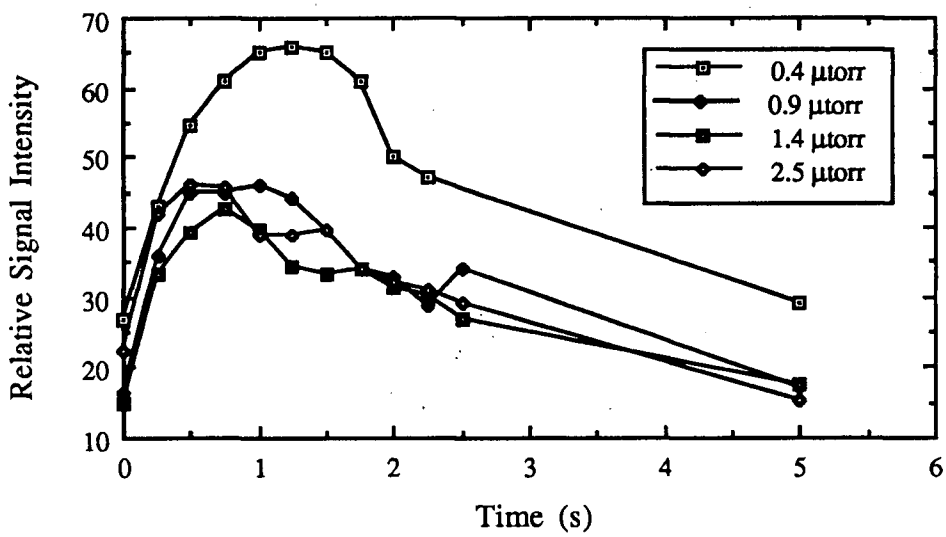

Figure 4.14: Signal intensity of mass 119 of CCl_3^+ as a function of storage time for four different pressures inside the ion trap container.

Table VII

Storage time (s)	Total Pressure (μTorr)			
	0.4 μtorr	0.9 μtorr	1.4 μtorr	2.5 μtorr
0.005	27	16.5	15	22.3
0.25	43	36	33.3	42
0.50	54.7	45	39.2	46
0.75	61	44.8	42.5	45.6
1.00	65	46	39.5	39
1.25	66	44	34.3	38.8
1.50	65	39.8	33.3	39.6
1.75	61	34	34	34
2.00	50	33	31.3	32.2
2.25	47.2	28.8	30.3	31
2.5	- - -	34	27	29
5.00	29	17	17.5	15.3

Table VII: Signal intensity of mass 119 of CCl_3^+ as a function of storage time for four different pressures inside the ion trap container.

4.9 - Effect of the Presence of Helium on the Resolution:

The data acquired at different pressures do not support the conclusion that an increase in helium pressure improves the resolution. Figures 4.15 and 4.16 present two spectra of CCl_4 taken with different pressures of helium and show no noticeable improvement in peak resolution or peak shape. It should be noted that the helium pressures used in this study were much lower than those used by Stafford et al. [22].

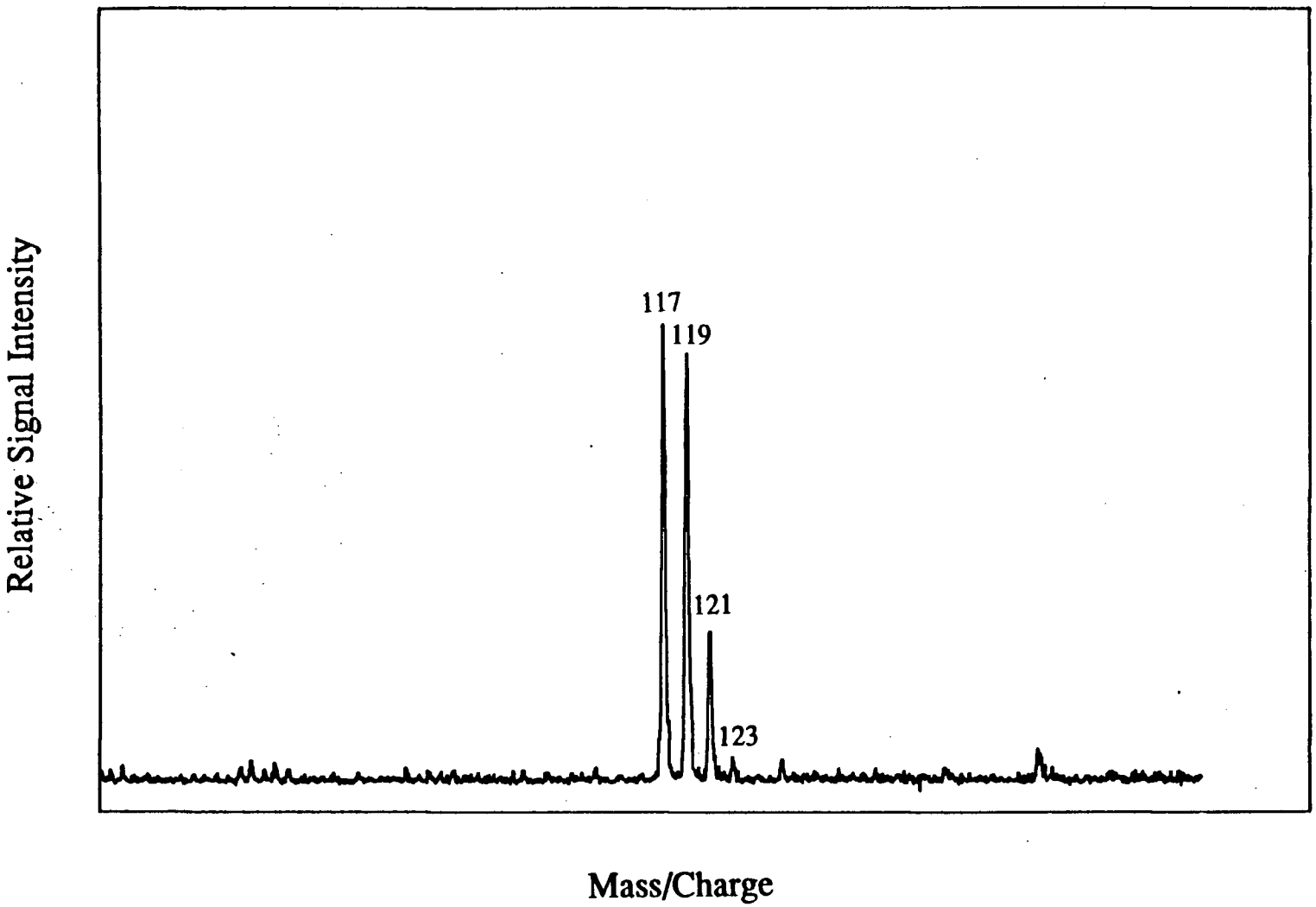

Figure 4.15: CCl_4 spectrum obtained with a total pressure in the ion trap container of $4.0 * 10^{-7}$ torr.

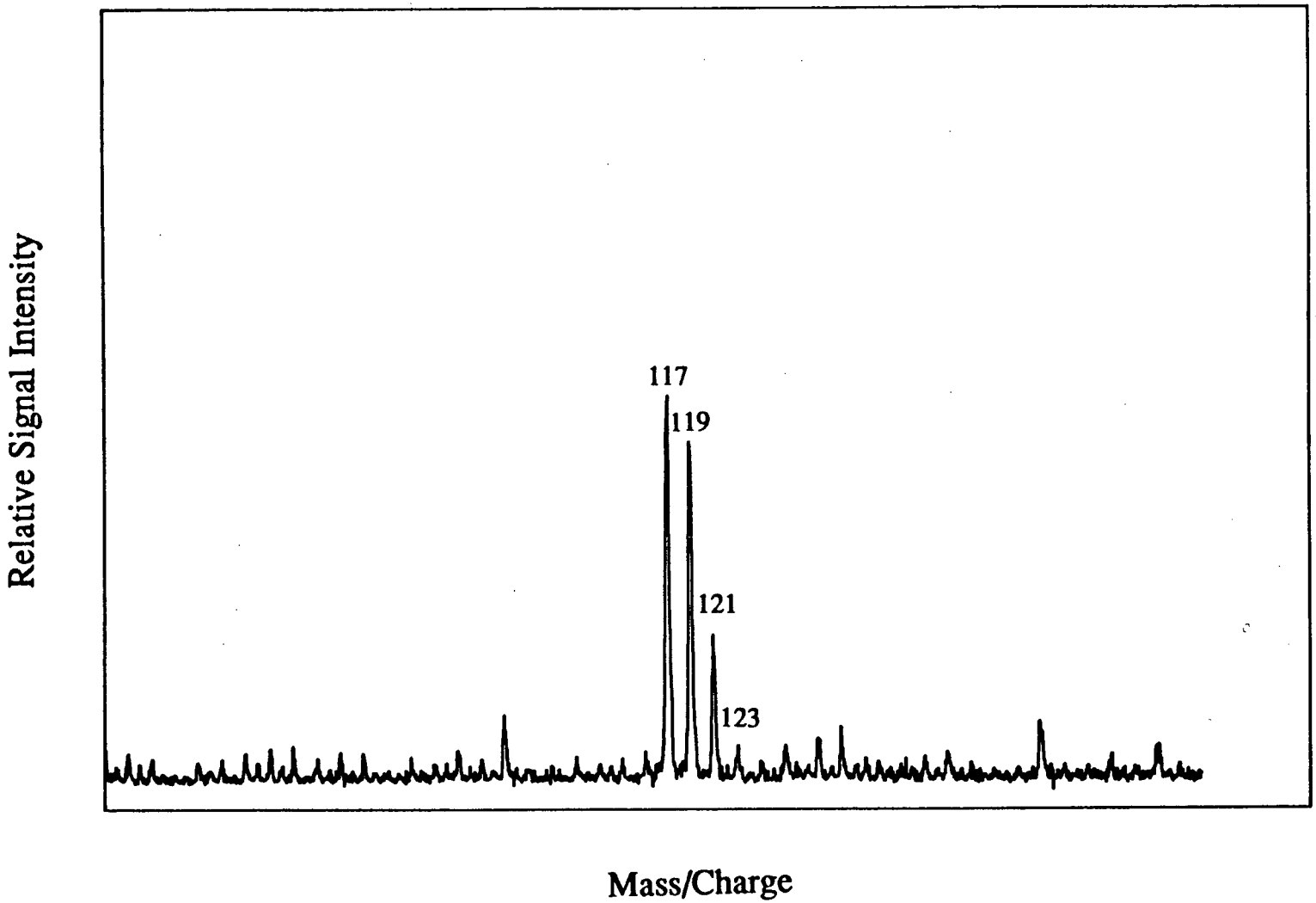

Figure 4.16: CCl_4 spectrum obtained with a total pressure in the ion trap container of $2.7 * 10^{-6}$ torr.

4.10 - Chemical Reactions in the Ion Trap:

The first signs of chemical ionization noticed in the ion trap system studied were observed during experiments aimed at establishing the behaviour of the xenon signal intensity as a function of the storage time used. These results are presented in figures 4.17 and 4.18. As can be seen from these figures, at short storage times the isotopic distribution found for xenon is very close to the natural isotopic distribution presented in the literature (Handbook of Chemistry and Physics, CRC Press, 1979). But, as the storage time is increased the isotopic ratio starts changing progressively, and when storage times longer than 5 seconds are used only three peaks remain in this area of the spectrum (peaks 130, 132 and 134). These peaks do not appear in an electron impact spectrum, when xenon is not present in the trap. It appears that trichloro-ethylene, which was used to clean the ion trap container and the ion trap assembly before going to high vacuum, was still present in the ion trap container. Although the concentration of trichloroethylene left in the container was too low in the residual gas for these peaks to appear on an electron impact spectrum, chemical ionization between xenon and trichloro-ethylene, over a long period of time, was concentrating the trichloro-ethylene ions at the centre of the trap before the analysis, making their detection possible. In this case we are in a situation where using standard electron impact ionization the number of ions produced is too small to be detected, but where the use of chemical ionization over long periods of time will give signal intensities that are much higher. This reveals the potential of time integrated chemical ionization in the ion trap for analytical purposes.

The ability of the ion trap to confine the chemical ionization agent for long periods of time and to trap the charged products of the reaction, renders possible the substitution of the high pressures used in conventional chemical ionization sources (0.1 - 1 torr) and the short residence time of the analyte in the reaction cell for longer

residence times of the reactive species and lower analyte pressures in the ion trap. As pointed out by McIver et al.[89] and Hunter and McIver [90] the use of low pressure chemical ionization performed over long periods of time could prove to be very useful in situations where the analyte has a very low vapour pressure. In fact, since the residence time of the analyte in the reaction zone of the instrument can be 10^6 times longer in the case of a trapping device [90], analytes with vapour pressures 10^6 times lower than those which the conventional chemical ionization sources can analyse could be analysed with the ion trap. Working under low pressures also eliminates the problem of the clustering of polar reagents (H_2O and NH_3) around the sample [91]. This technique can also be used to obtain signal for analyte present in the sample at concentrations below its detection limit for electron impact ionization or below the detection limit of conventional chemical ionization instruments.

Although chemical ionization is used in the commercial model of the ion trap, the pressures at which these reactions are conducted are quite high given the fact that this instrument uses a high helium background pressure therefore, the instrument cannot take advantage of its ability to analyse low vapour pressure analytes. To obtain an idea of the potential of this technique to produce higher signal intensities, chemical ionization studies of carbon tetrachloride and toluene with xenon were conducted at low pressures inside the ion trap container.

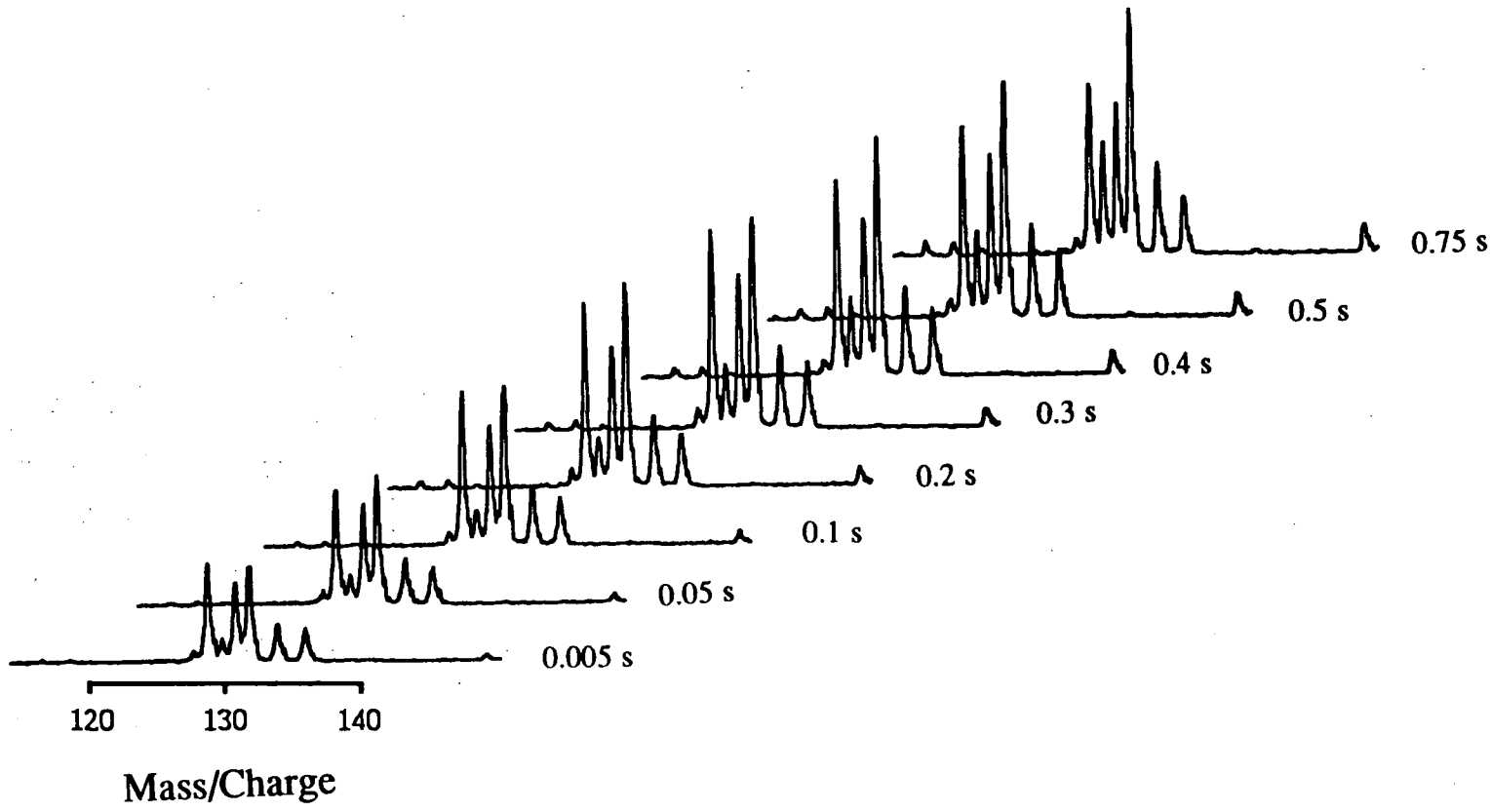

Figure 4.17: Signal intensity of xenon as a function of time (0.005s to 0.75s).

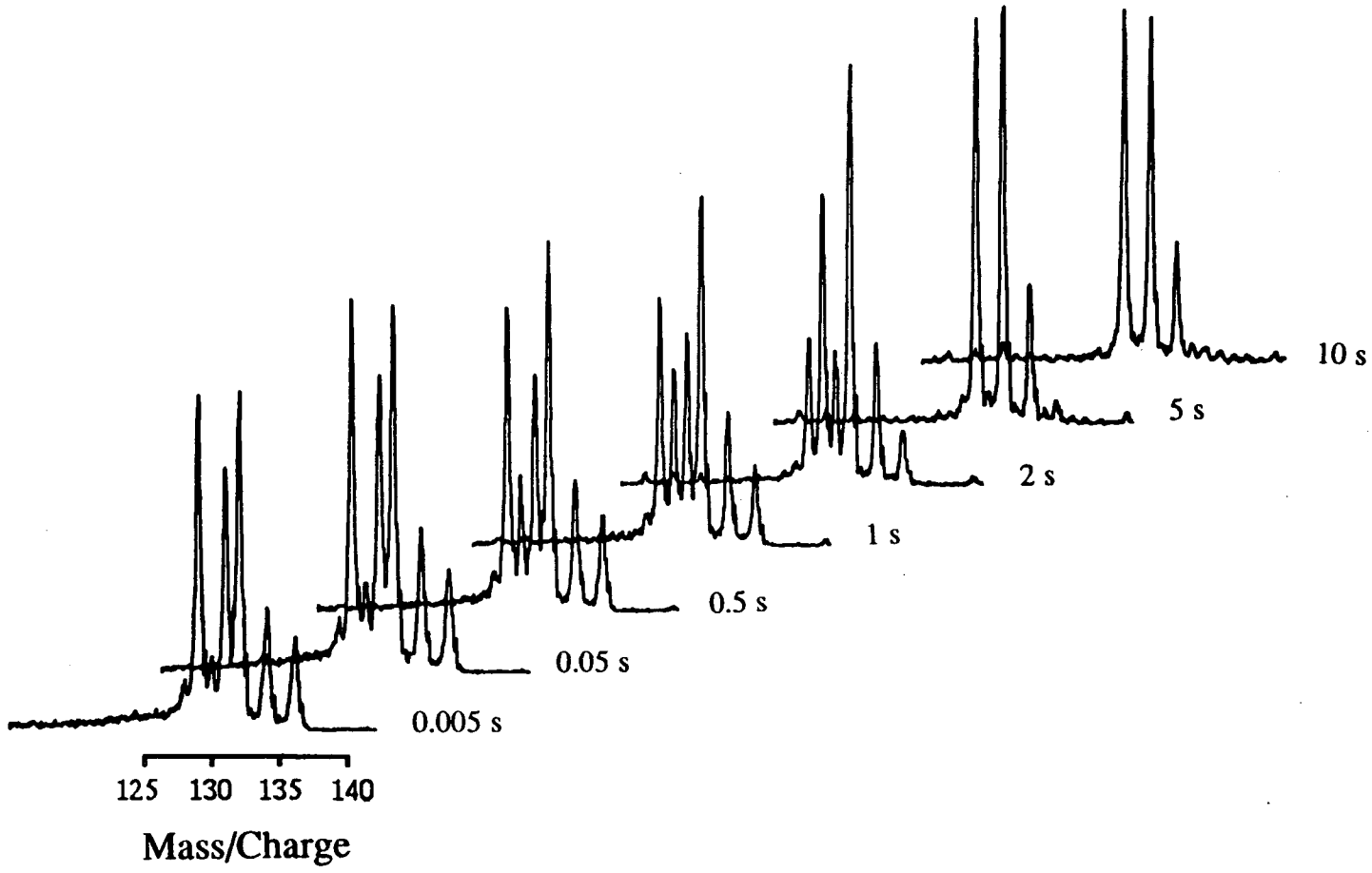

Figure 4.18: Signal intensity for xenon as a function of time (0.005s to 10s).

4.11 - Xenon Chemical Ionization of Carbon Tetrachloride:

In this experiment a small amount of carbon tetrachloride was bled into the cavity of the ion trap. A mixture of 10% xenon in helium was used as the background gas in the ion trap container. The experimental set-up used to introduce the analyte has been presented in section 3.3.1 of this document; electron impact ionization was used to produce the xenon ions used as the chemical ionization agent. Spectra of the ions present in the cavity of the trap were taken at different storage times.

The spectra obtained for the chemical ionization of carbon tetrachloride by xenon are presented in figures 4.19 and 4.20. A plot of the intensity of a xenon peak (m/e = 129 amu) and a carbon tetrachloride peak (m/e = 119 amu) as a function of reaction time is presented in figure 4.21. Table VIII presents the data used to produce figure 4.21. The increase in signal intensity for the CCl_3^+ peak at its maximum is of the order of 5 times its initial intensity.

The five fold increase in signal intensity seen in figure 4.21 is not only the result of chemical ionization between xenon and carbon tetrachloride: as shown in section 4.9 the presence of helium as a background gas in the ion trap mass spectrometer enhances the signal obtained for a given ion by a factor of sometimes up to two. But, the use of chemical ionization to increase the signal intensity of carbon tetrachloride would definitely lower the limit of detection for this analyte.

The reaction between xenon and carbon tetrachloride is believed to be:

$$CCl_4 + Xe^+ \rightarrow CCl_3^+ + XeCl$$

Attempts to observe the presence of XeCl were not successful. The attempts were made by letting the chemical ionization process progress during the time required to obtain the maximum amount of CCl_3^+ in the container, which implies having the maximum amount of XeCl produced. At that point the electron beam of the instrument

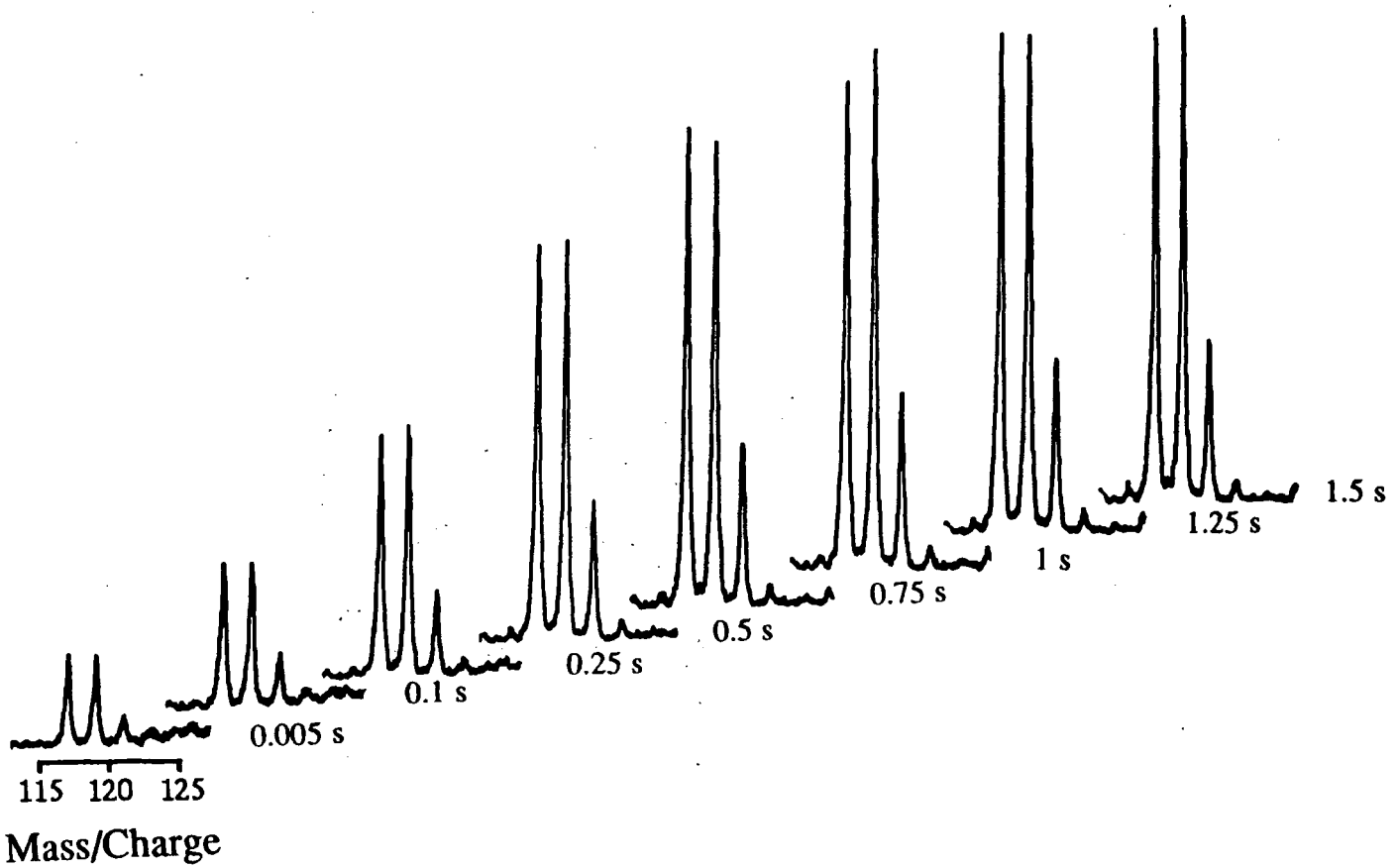

Figure 4.19 - Chemical ionization spectra of carbon tetrachloride by xenon (0.005s to 1.5s).

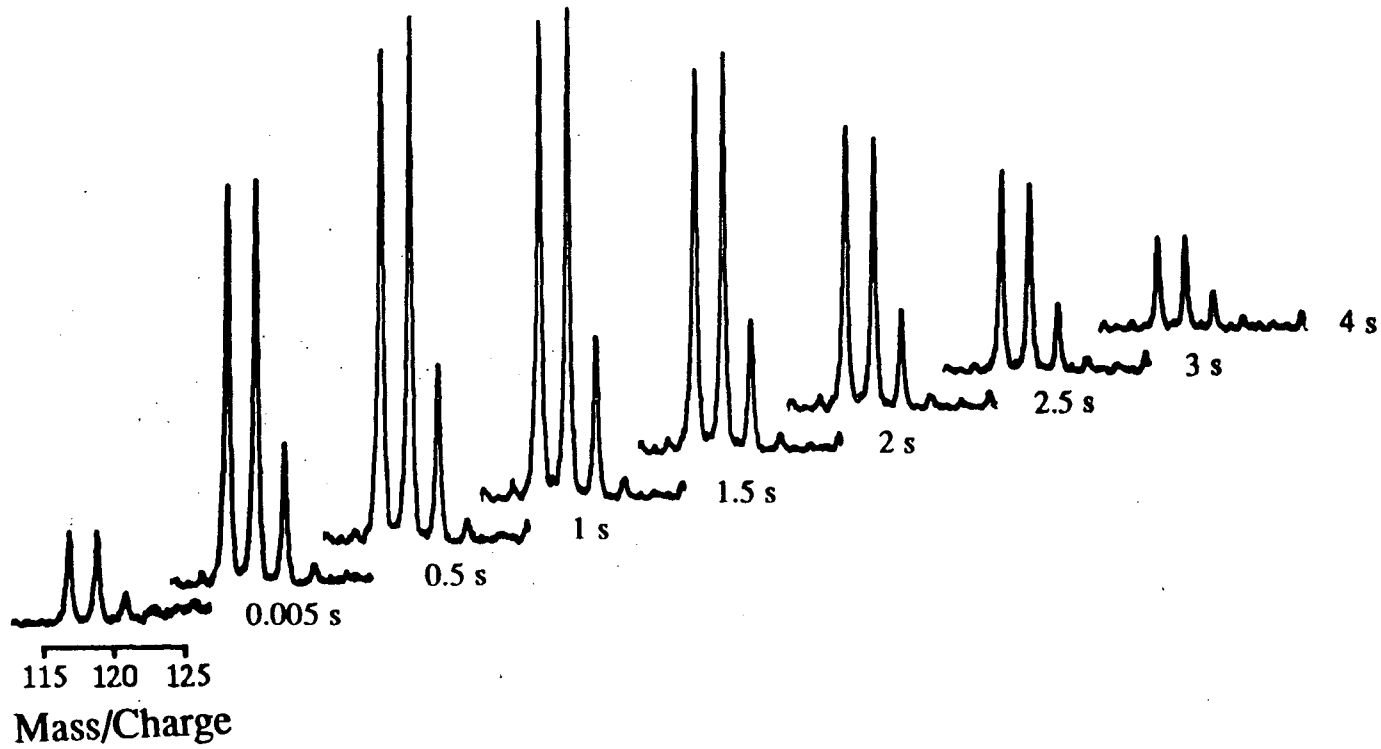

Figure 4.20 - Chemical ionization spectra of carbon tetrachloride by xenon (0.005s to 4s).

was turned on and a mass spectrum of the ions present in the trap was taken. The only peaks seen on these mass spectra were the peaks observed in an electron impact spectrum of a mixture of CCl_4 and xenon.

The chemical ionization of carbon tetrachloride does not change the distribution of the ions in the mass spectrum obtained with this method compared to the spectrum obtained by electron impact ionization of carbon tetrachloride.

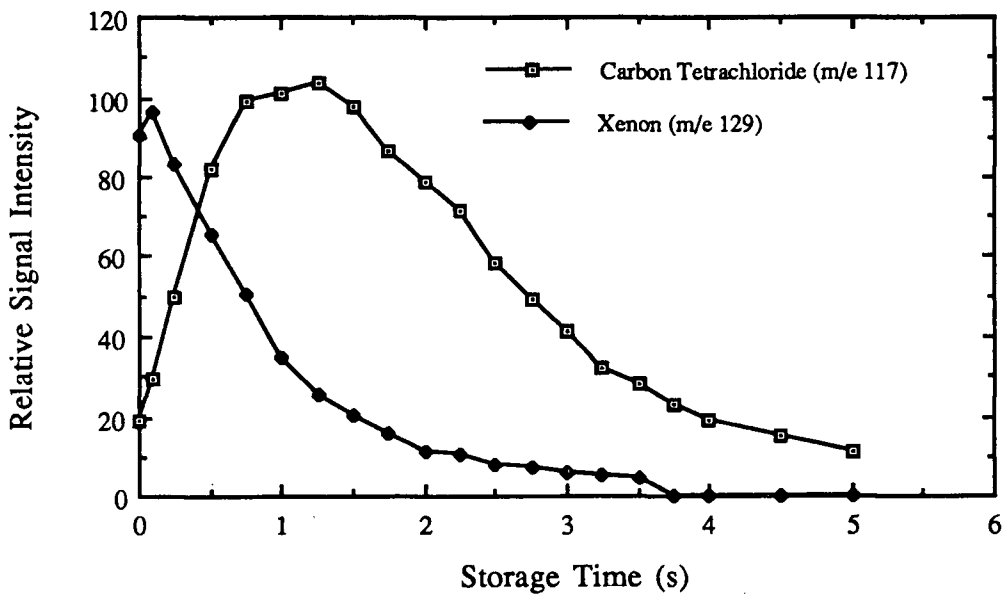

Figure 4.21: Signal intensity of isotope 129 of xenon and isotope 117 of CCl_3^+ as a function of storage time.

Table VIII

Storage time (s)	Relative signal intensity	
	Carbon tetrachloride	Xenon
0.005	19.2	90.7
0.10	29.8	96.3
0.25	49.8	83.3
0.50	82	65.9
0.75	99.2	50.2
1.00	101	34.5
1.25	103.4	25.3
1.5	98	20.1
1.75	86.5	16
2.00	78.8	11.1
2.25	71.2	10.8
2.50	58.5	8
2.75	49.2	7
3.00	41.1	6
3.25	32.2	5
3.50	28.1	4.8
3.75	23	
4.00	19.2	
4.50	14.8	
5.00	11.3	

Table VIII: Signal intensity of isotope 129 of xenon and isotope 117 of CCl_3^+ as a function of storage time.

4.12 - Chemical Ionization of Toluene by Xenon:

The results obtained from chemical ionization of toluene (methyl benzene) by xenon are even more interesting than the results obtained with CCl_4. The toluene and xenon signal intensities as a function of storage time are presented in figure 4.22. The signal intensity of toluene after 1.5 s of storage time has increased by a factor of more than 16 compared to what it was at a storage time of 5 ms. Again, in this case the increase in not only due to the effect of chemical ionization but also to the presence of helium in the ion trap container. But, a sixteen fold increase definitely shows the potential of chemical ionization for improving limits of detection and also for giving the ability to analyse samples containing small amounts of analyte by allowing for a preconcentration stage in the analysis. This could be applied to the analysis of trace elements in small volume samples.

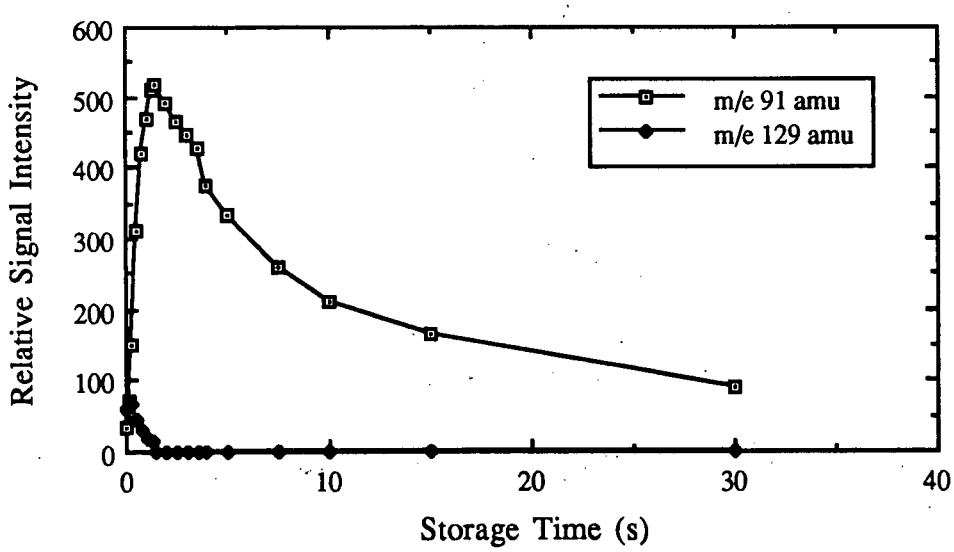

Figure 4.22: Toluene (m/e 91) and xenon (m/e 129) signal intensity as a function of storage time.

Table IX

Storage time (s)	Relative signal intensity	
	m/e 91	m/e 129
0.005	32	59
0.10	72.9	67.5
0.25	150	68.1
0.50	312.5	45
0.75	418.5	30
1.00	467.5	20
1.25	510	14
1.50	519	0
2.00	492	
2.50	464.6	
3.00	447	
3.50	426	
4.00	375	
5.00	335.4	
7.50	258	
10.00	208.8	
15.00	166.8	
30.00	89.9	

Table IX: Toluene (m/e 91) and xenon (m/e 129) signal intensity as a function of storage time.

There are two reactions between xenon and toluene which produce ions of mass-to-charge ratios of 91 and 92. At low storage times these two peaks are the most important on the spectra (see figure 4.23). In the chemical ionization spectra the peak appearing at a mass-to-charge ratio of 92 is the result of charge exchange reaction between xenon and toluene [92]:

$$C_7H_8 + Xe^{+\cdot} \rightarrow C_7H_8^{+\cdot} + Xe \qquad (1)$$

In this reaction an electron is transfered from toluene to xenon [92].

The peak present at a mass-to-charge of 91 could be the result of two different processes. The first possibility is a fragmentation of $C_7H_8^{+\cdot}$ to $C_7H_7^{+}$ through the following reaction:

$$C_7H_8^{+\cdot} \rightarrow C_7H_7^{+} + H^{\cdot} \qquad (2)$$

The second reaction involves a negative ion transfer from toluene to xenon [92]:

$$C_7H_8 + Xe^{+\cdot} \rightarrow C_7H_7^{+} + XeH \qquad (3)$$

Attempts to verify the production of XeH from reaction (3) were made by turning on the electron gun after the optimal storage time, however these attempts were unsuccessful. Most probably, both of these two possible reactions are responsible for producing the ions observed in the chemical ionization experiments.

When longer storage times are used, other ions begin to appear on the mass spectra in significant amounts at mass-to-charge ratios of 105 and 106 (see figure 4.24). These two ions are likely the result of reactions between the toluene ions

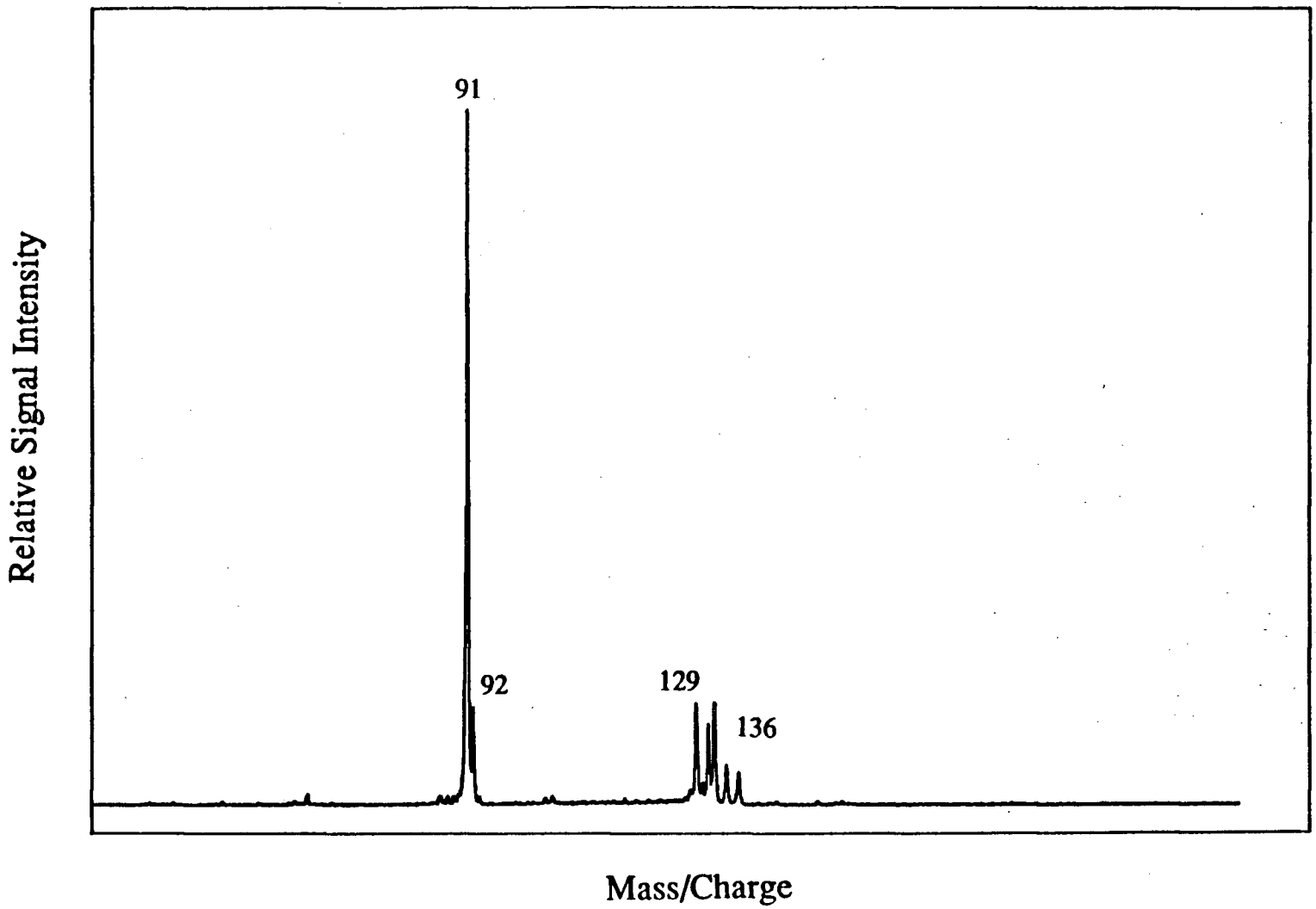

Figure 4.23: Chemical ionization spectrum of toluene. The chemical ionization agent for this experiment is xenon. The storage time used to obtain this spectrum was 5 ms.

trapped in the cavity and neutral toluene molecules flowing into the cavity of the ion trap.

The reactions can be writen as:

$$C_7H_7^+ + C_7H_8 \rightarrow C_8H_9^+ + C_6H_6 \qquad (4)$$

and

$$C_7H_8^{+\cdot} + C_7H_8 \rightarrow C_8H_{10}^+ + C_6H_6 \qquad (5)$$

Attempts to obtain proof of the production of the C_6H_6 product from the two reactions were unsuccessful.

The spectra of toluene obtained using chemical ionization differ significantly from those obtained with electron impact ionization. At short storage times the electron impact ionization spectrum mainly shows the presence of two ions positioned at mass-to-charge values of 91 and 92 (see figure 4.25). The reaction producing ions at mass-to-charge of 92 is:

$$C_7H_8 + e \rightarrow C_7H_8^{+\cdot} + 2e \qquad (6)$$

The further fragmentation of this radical ion produces the main product appearing on the mass spectrum at mass-to-charge 91 from the reaction [92]:

$$C_7H_8^{+\cdot} \rightarrow C_7H_7^+ + H \qquad (7)$$

It is well known that ions are more stable than radical ions which tend to fragment and lose a neutral molecule to form another ion, rather than losing a radical and forming another radical ion [93]. As time passes, a peak appears at a mass-to-

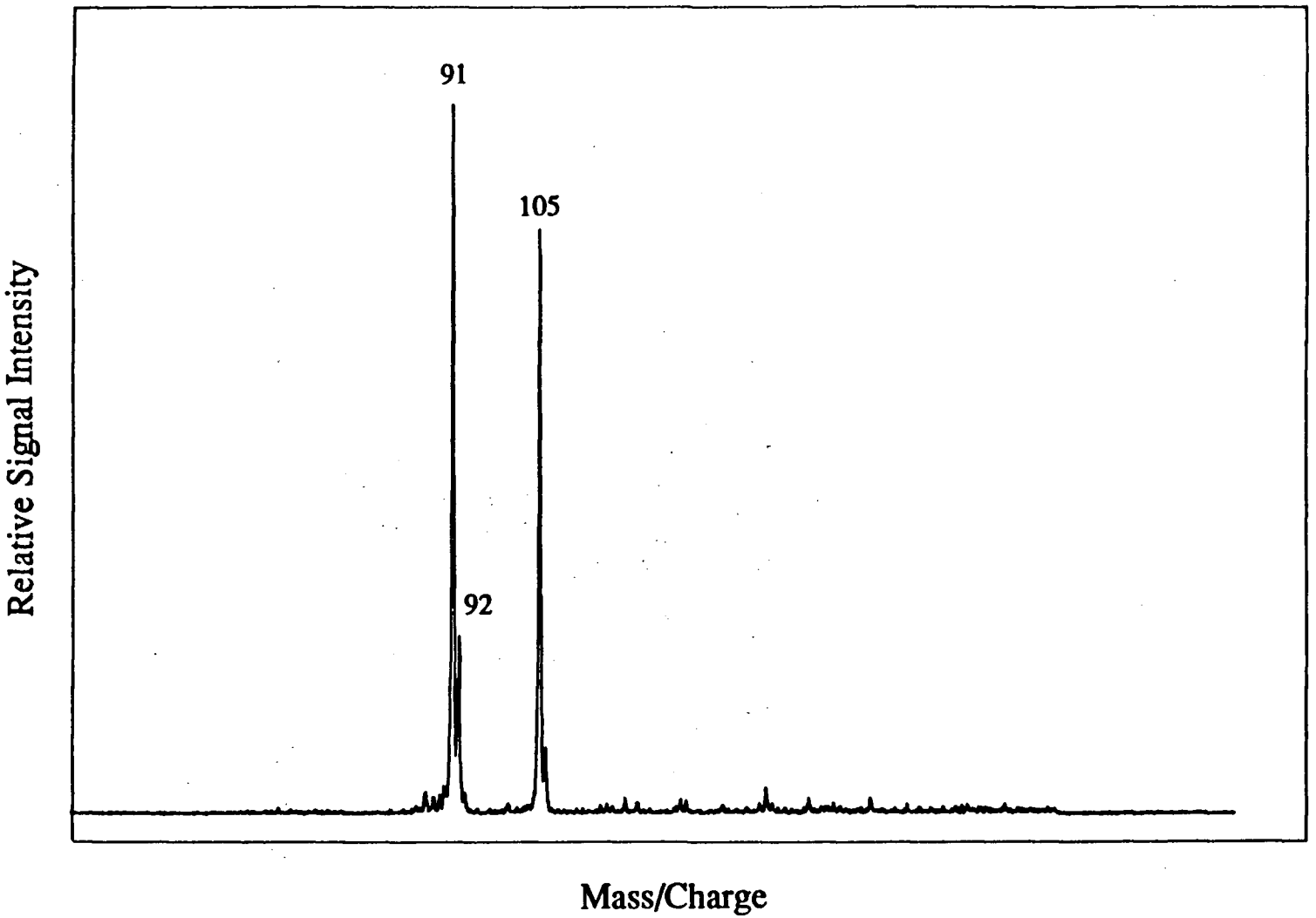

Figure 4.24: Chemical ionization spectrum of toluene. The chemical ionization agent for this experiment is xenon. The storage time used to obtain this spectrum was 10 s.

charge ratio of 105 and keeps growing until it becomes the most abundant ion present in the spectrum (see figure 4.26). The reaction postulated to produce that ion is the same as reaction (4):

$$C_7H_7^+ + C_7H_8 \rightarrow C_8H_9^+ + C_6H_6$$

and for the small peak present at mass-to-charge value of 106 the reaction postulated is the same as reaction (5):

$$C_7H_8^{+\cdot} + C_7H_8 \rightarrow C_8H_{10}^+ + C_6H_6$$

Attempts to observe the presence of C_6H_6 in the trap using electron impact ionization after a given reaction time were unsuccessful. The formation of $C_6H_6^+$ or $C_6H_5^+$ appears to be absent from this system. The absence of these ions at mass-to-charge ratios of 78 and 77 indicates that the reactions

$$C_7H_8^{+\cdot} + C_7H_8 \rightarrow C_8H_{10} + C_6H_6^{+\cdot} \qquad (8)$$

and

$$C_7H_7^+ + C_7H_8 \rightarrow C_8H_{10} + C_6H_5^{+\cdot} \qquad (9)$$

are not happening in the system.

When longer storage times are used, a number of peaks other than the main peaks at 105 amu and 106 amu appear on the electron impact ionization spectra of toluene.

These peaks are appearing on the electron impact spectra and not on the chemical ionization spectra because the process by which electron impact produces ionization in a molecule leaves it with more internal energy than the chemical

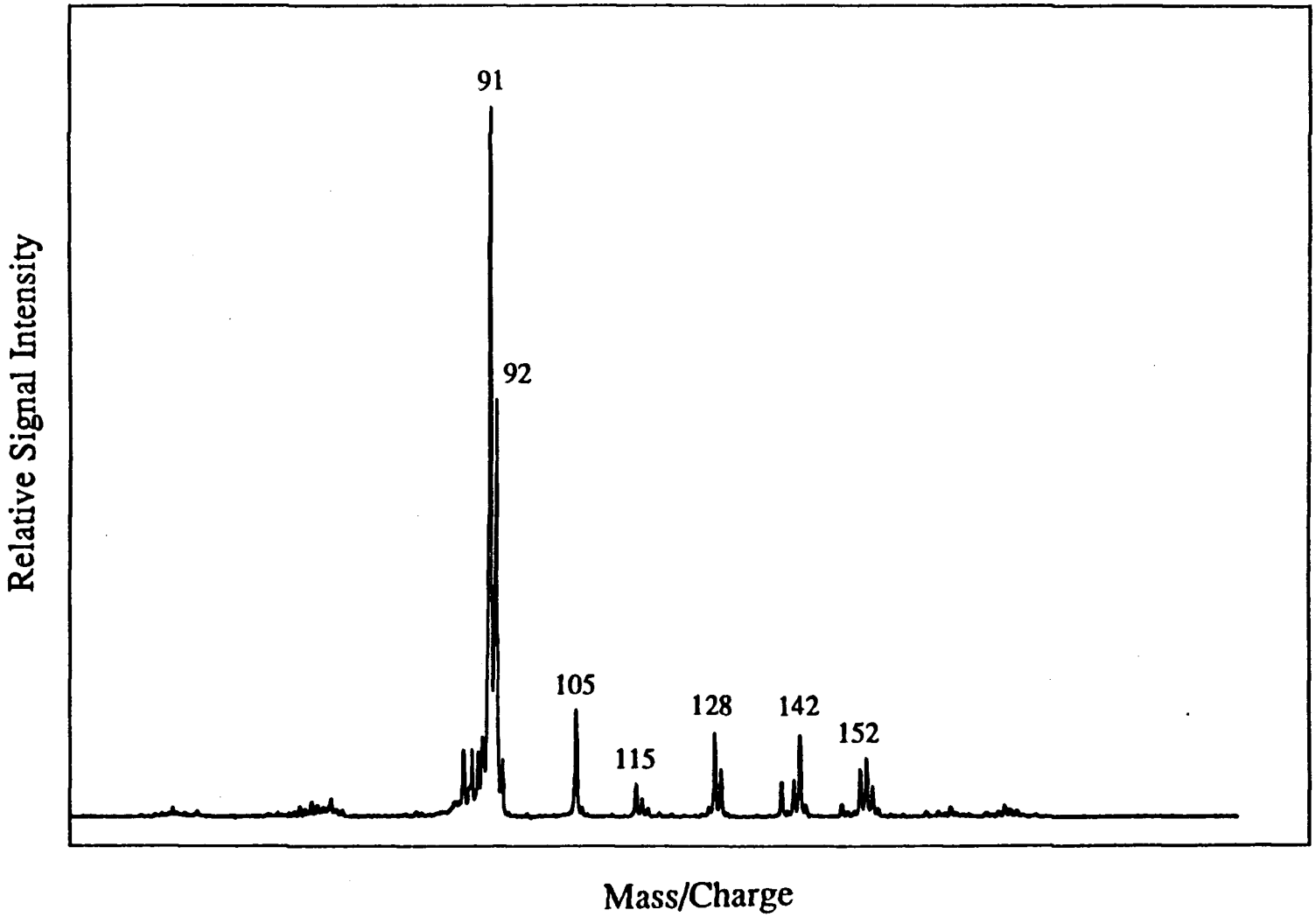

Figure 4.25: Electron impact ionization spectrum of toluene. The storage time used to obtain this spectrum was 5 ms.

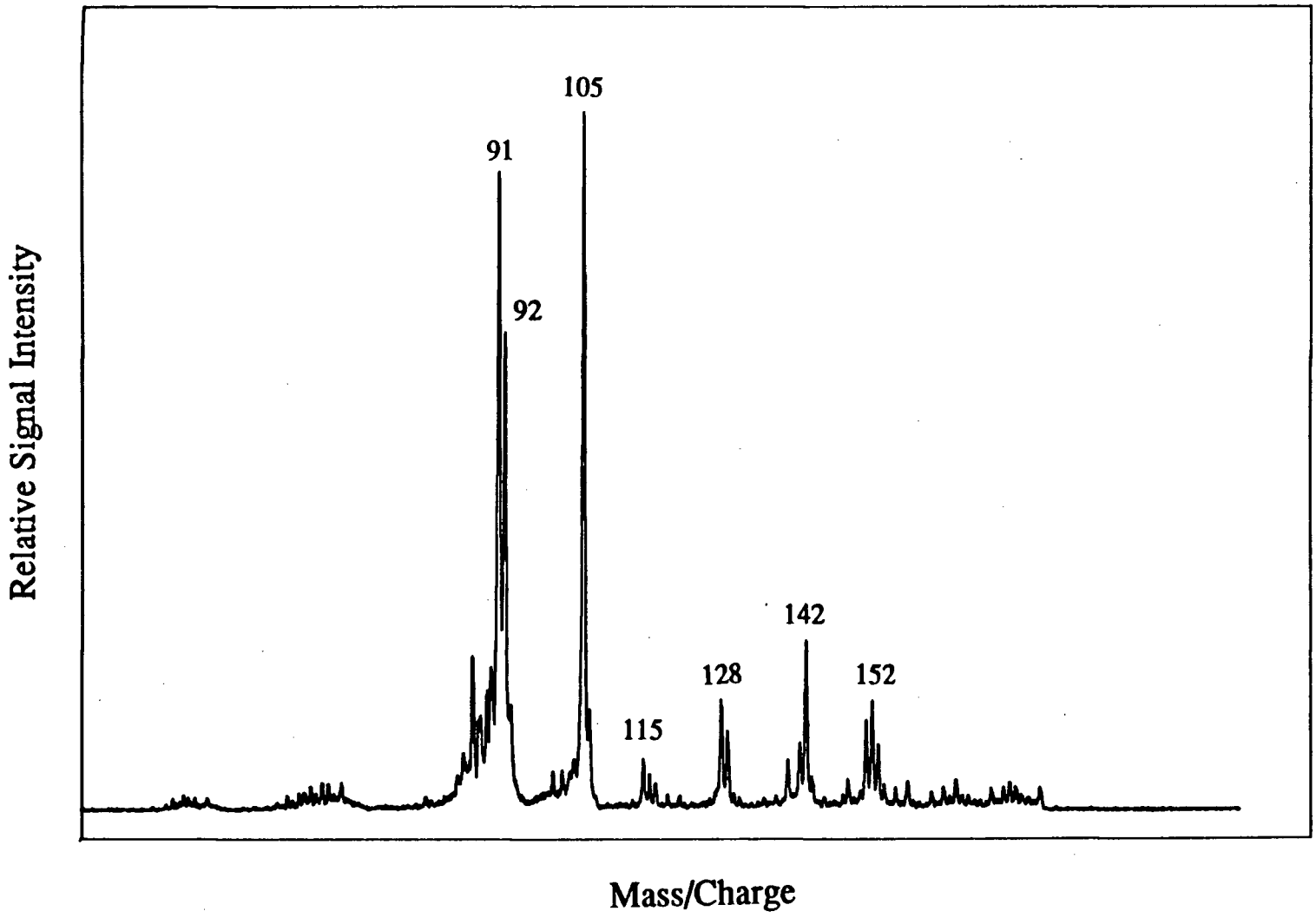

Figure 4.26: Electron impact ionization spectrum of toluene. The storage time used to obtain this spectrum was 1.5 s.

ionization process does. This excess internal energy may be eliminated by dissociation or by an increase in vibrational, rotational or even kinetic energy of the molecule. This excess internal energy can facilitate the progress of a reaction between colliding particles. It should be noted that the relative signal intensity of the ions at 91 amu to the ions at 105 amu as a function of storage time differs significantly from the chemical ionization process to the electron impact process. This can be seen in figure 4.27: this figure shows that the ratio of mass 91 to 105 is always larger in the case of chemical ionization than electron impact ionization, indicating that the reaction rate is lower in the case of ions produced through chemical ionization. The data used to create figure 4.27 is presented in Table X. In the spectra obtained using electron impact ionization this ratio falls below 1 when the storage time is longer than 1.5 s, the reaction products appearing in larger quantities than their precursors.

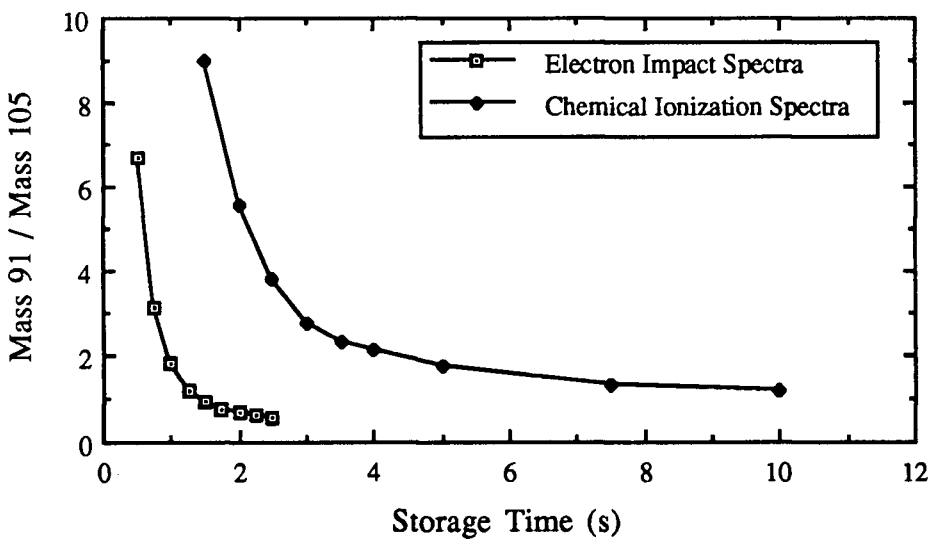

Figure 4.27: Ratio of intensity of peaks positioned at 91 amu and 105 amu for electron impact ionization and chemical ionization.

Table X

Storage time (s)	Ratio signal intensity from m/e 91 and m/e 105	
	Electron impact ionization	Chemical ionization
0.005	6.7	
0.75	3.1	
1.00	1.8	
1.25	1.2	
1.50	0.9	9.0
1.75	0.8	
2.00	0.7	5.6
2.25	0.6	
2.50	0.6	3.8
3.00		2.8
3.50		2.3
4.00		2.1
5.00		1.7
7.50		1.3
10.00		1.2

Table X: Ratio of intensity of peaks positioned at 91 amu and 105 amu for electron impact ionization and chemical ionization.

Summary:

This chapter has served to demonstrate how the ion trap mass spectrometer is operated and to show some examples of the quality of the results that can be obtained from it. Some of the important variables influencing the resolution of the signal intensity obtained with the instrument have been investigated. We have also shown the effect that the presence of helium has on the signal intensity and the effect it has on the time behaviour of the signal. Chemical reactions were also investigated and it was shown that the use of chemical ionization performed over long periods of time could be used to improve the limits of detection for low concentration analytes.

CHAPTER V

ATOMIC SPECTROMETRY

5.1 - Graphite Furnace - Ion Trap Mass Spectrometry:

5.1.1 - Introduction:

The development of a graphite furnace ion trap mass spectrometer was prompted by the desire to couple the capabilities of the graphite furnace with those of the ion trap mass spectrometer to solve problems related to the multielemental analysis of very small size liquid samples (a few μL) containing ultra trace levels of the elements of interest. The choice of the graphite furnace to evaporate the sample to be mass spectrometrically analysed with the ion trap mass spectrometer was made on the grounds that it has proven its ability to handle small size samples, its vaporization efficiency is very high, the residence time of the analyte in the furnace is relatively long and the proportion of ionized analyte produced by the furnace is relatively low. The ion trap mass spectrometer was chosen as the detector for this instrument because of its ability to accumulate the analyte ions before the mass spectrometric analysis is performed, its ability to produce an entire spectrum of the trapped ions in a single scan and the possibility of obtaining isotopic ratios offered by mass spectrometry.

As presented in sections 3.3.2 and 3.4, the graphite furnace was placed in its own container to ensure a good control of the composition of the gas surrounding it and to provide the possibility of vaporizing the analyte at a reduced pressure. A transfer line equipped with a shut off valve linked the graphite furnace to the ion trap. During the vaporization process, the valve is open and material can be transfered from the graphite furnace to the ion trap; when the vaporization process is over the valve is closed, allowing access to the graphite furnace without disturbing the vacuum in the ion trap container.

5.1.2 - Initial Results:

The first series of attempts to transfer material from the graphite furnace to the ion trap mass spectrometer were performed using 500 ppm silver and copper solutions, 5 to 10 μL of which were deposited in the graphite furnace, dried and atomized at different temperatures, rates and under different pressures. These experiments were unsuccessful, and even led to the destruction of the channeltron electron multiplier employed during the experiments. Our inability to produce spectra with these solutions made us turn to a much more volatile analyte which was used in large amounts in the furnace: droplets of mercury. Figure 5.1 presents a typical spectrum obtained by placing a 5 μL drop of mercury in the furnace*, vaporizing it and analysing the vapor reaching the ion trap. Table XI gives the identification of the ions appearing on the spectrum presented in figure 5.1; Table XII shows the isotopic ratios found for the isotopes of mercury present on figure 5.1 and also lists values found in the literature for these ratios. These first results proved that it was possible to transfer material from the graphite furnace to the ion trap but they also show that even though a large quantity of material is believed to have been vaporized from the furnace, only a small portion of this vapour is trapped.

After these initial results attempts were made at using antimony chloride crystals to obtain mass spectra. Figure 5.2 presents a typical spectrum obtained by vaporizing a small crystal of antimony chloride with the graphite furnace and analyzing the vapour reaching the ion trap. Identification of the ions observed on this spectrum is given in Table XIII.

---

* The 5 μL of mercury placed in the graphite furnace was not totally evaporated. It appears that a large portion was expelled from the furnace during the heating step. It is believed that only a fraction of the mercury deposited inside the furnace was vaporized.

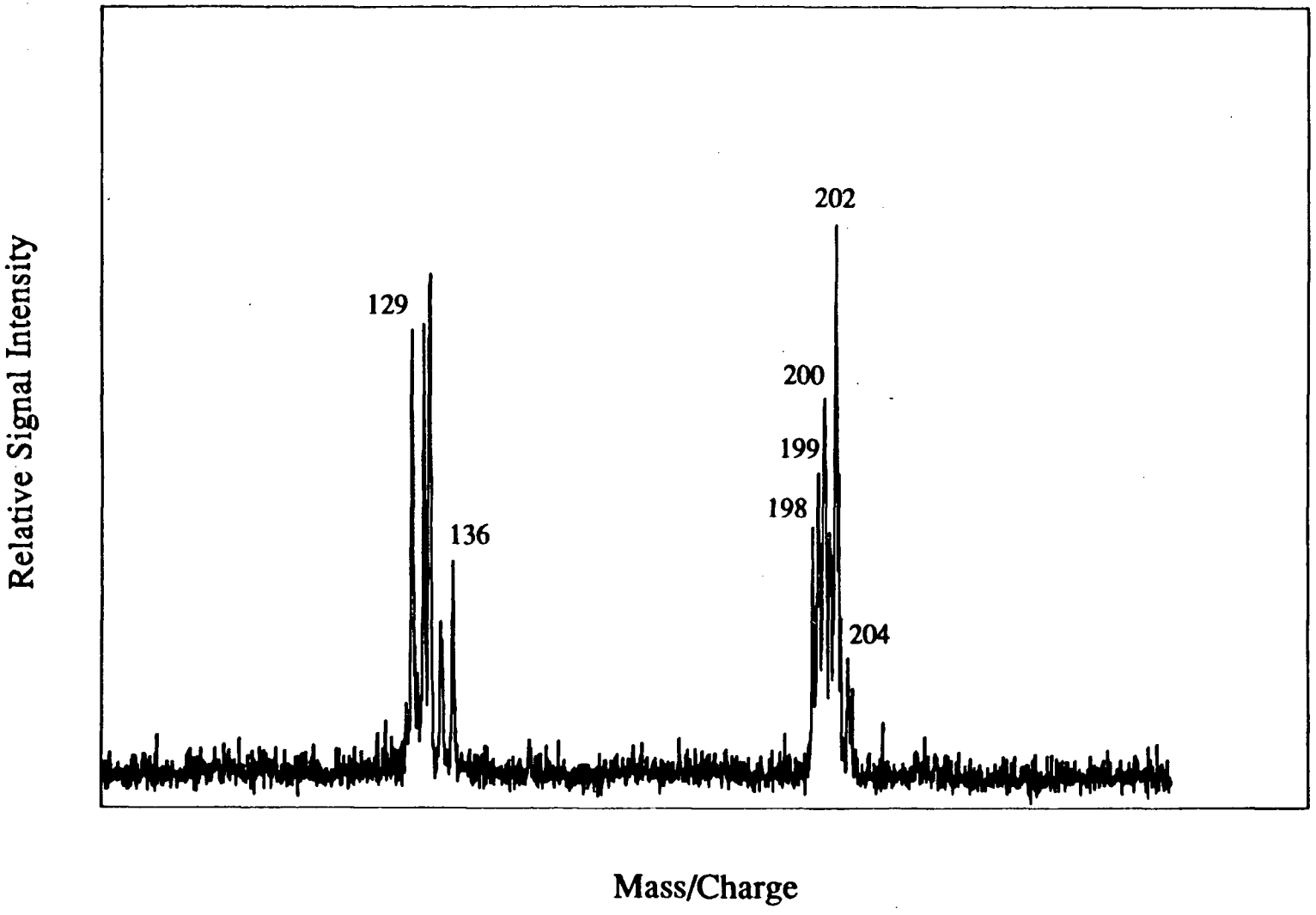

Figure 5.1 - Spectrum of mercury transfered from the graphite furnace to the ion trap. The ions appearing at mass-to-charge ratios of 129 to 136 are isotopes of xenon present in the ion trap container.

Table XI

Mass-to-charge ratio	Identification
198	$_{80}Hg^{198}$
199	$_{80}Hg^{199}$
200	$_{80}Hg^{200}$
201	$_{80}Hg^{201}$
202	$_{80}Hg^{202}$
204	$_{80}Hg^{204}$

Table XI: Identification of the peaks, with mass-to-charge ratio ranging from 198 to 204, appearing on the spectrum presented in figure 5.1.

Table XII

Isotopic ratios for mercury

Isotope	Ratio found	Ratio reported*
$_{80}Hg^{198}$	10.3	10.02
$_{80}Hg^{199}$	17.6	16.84
$_{80}Hg^{200}$	23.4	23.13
$_{80}Hg^{201}$	15.2	13.22
$_{80}Hg^{202}$	27.2	29.80
$_{80}Hg^{204}$	6.2	6.85

Table XII: Isotopic ratios for mercury.

* Values taken from: Handbook of Chemistry and Physics, 59th Edition, 1978-1979.

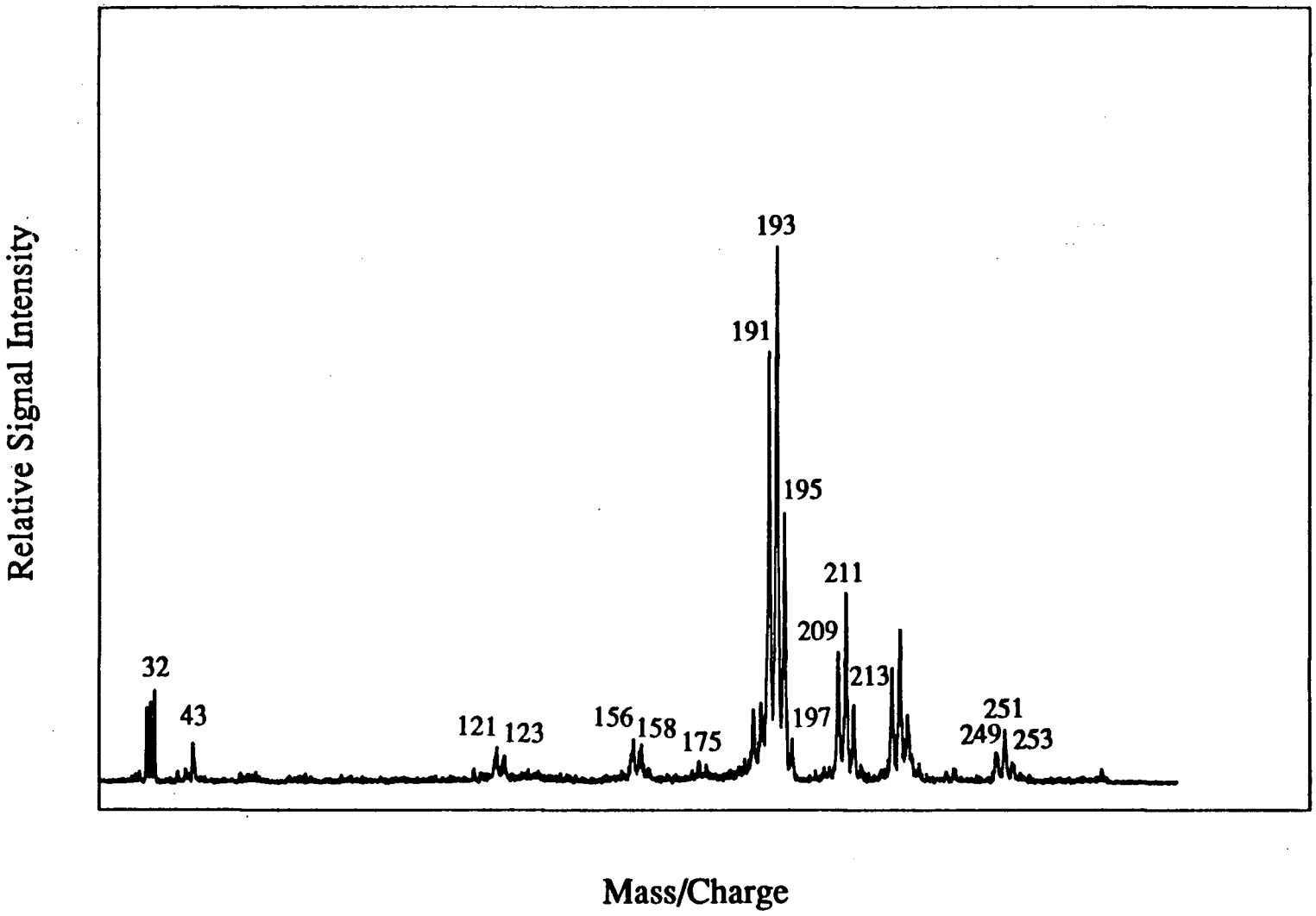

Figure 5.2 - Typical spectrum obtained by vaporizing a small antimony trichloride crystal with the graphite furnace and analysing the vapour reaching the ion trap mass spectrometer.

Table XIII

Mass-to-charge ratio	Identification
121	$_{51}Sb^{121}$
123	$_{51}Sb^{123}$
156	
158	$SbCl^+$
160	
173	
175	$SbClOH^+$
177	
191	
193	$SbCl_2^+$
195	
197	
209	
211	$SbCl_2H_2O^+$
213	
249	
251	Unknown
253	

Table XIII: Identification of the peaks appearing on the antimony trichloride spectrum presented in figure 5.2

Antimony trichloride was also dissolved in a mixture of methanol, water and hydrochloric acid to form a saturated solution. A spectrum obtained with 10 μL of this solution is presented in figure 5.3. It has the same basic features as those appearing on the spectra obtained with crystals of antimony chloride. Attempts were made to obtain spectra of copper, silver, tin and lead (using a lead dichloride solution) but, unfortunately, were unsuccessful.

A 5000 ppm tin chloride solution was prepared, 10 μL of which was placed in the graphite furnace. A spectrum acquired using this solution is presented in figure 5.4. The identification of the ions found in this spectrum is given in table XIV.

This first series of experiments indicates that material vaporized in the graphite furnace could be transfered to the ion trap and analysed. It appears, however, that only analytes with relatively low boiling points were transfered. The presence of atomic antimony on the antimony chloride spectra likely arises from the fragmentation of antimony chloride molecules in the electron beam, and not from the transfer of atomic antimony from the graphite furnace to the ion trap. None of the other spectra show the presence of the atomic species present in the sample evaporated in the graphite furnace. Table XV presents the different analytes used in our attempts to transfer material from the graphite furnace to the ion trap along with their boiling points and a note to indicate if we have been successful in transfering them. The information presented in this table shows that there is a temperature such that analytes with higher boiling points will not be transfered from the graphite furnace to the ion trap.

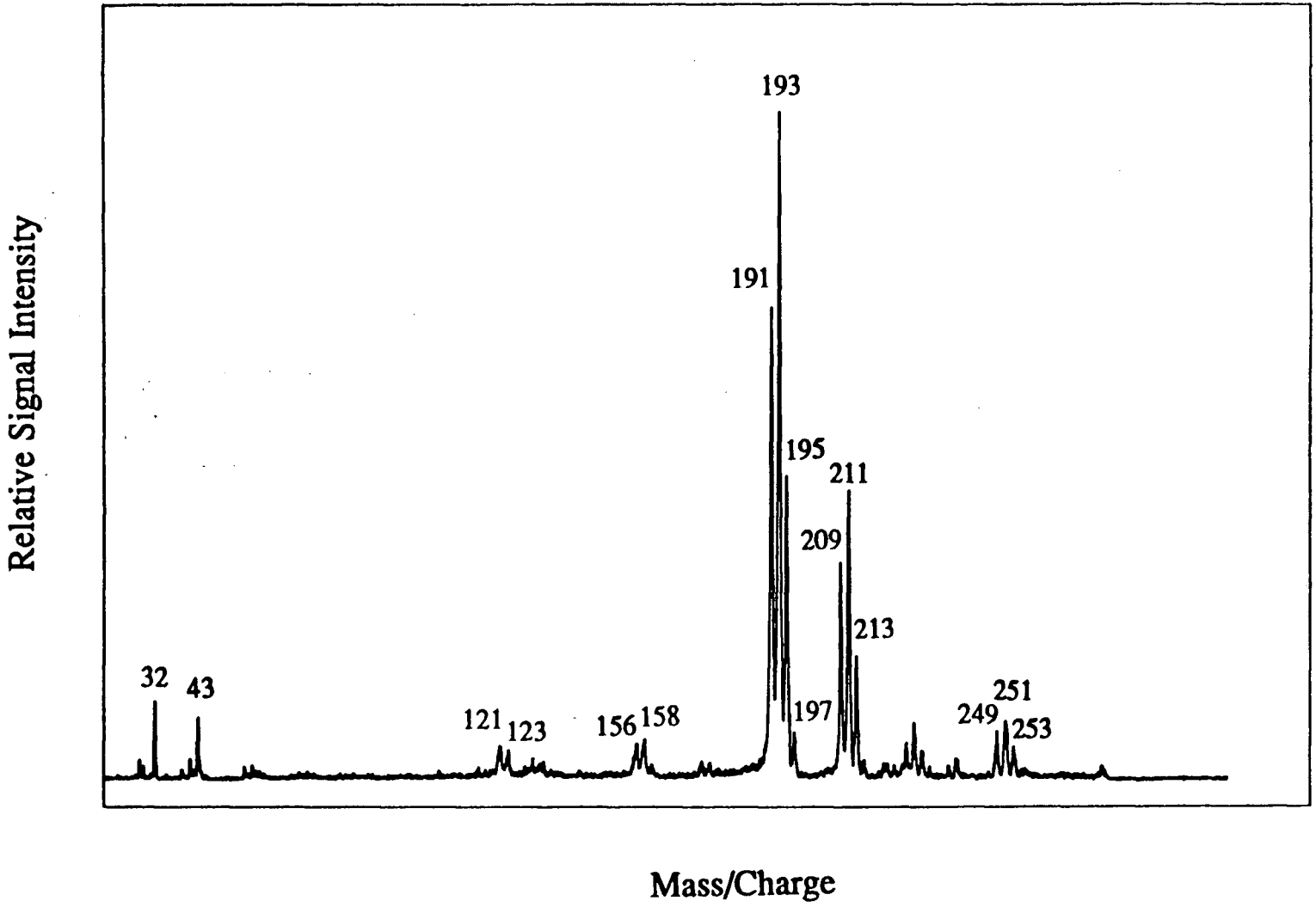

Figure 5.3: Spectrum obtained by placing 10 μL of a saturated solution of antimony trichloride in a mixture of methanol, water and hydrochloric acid.

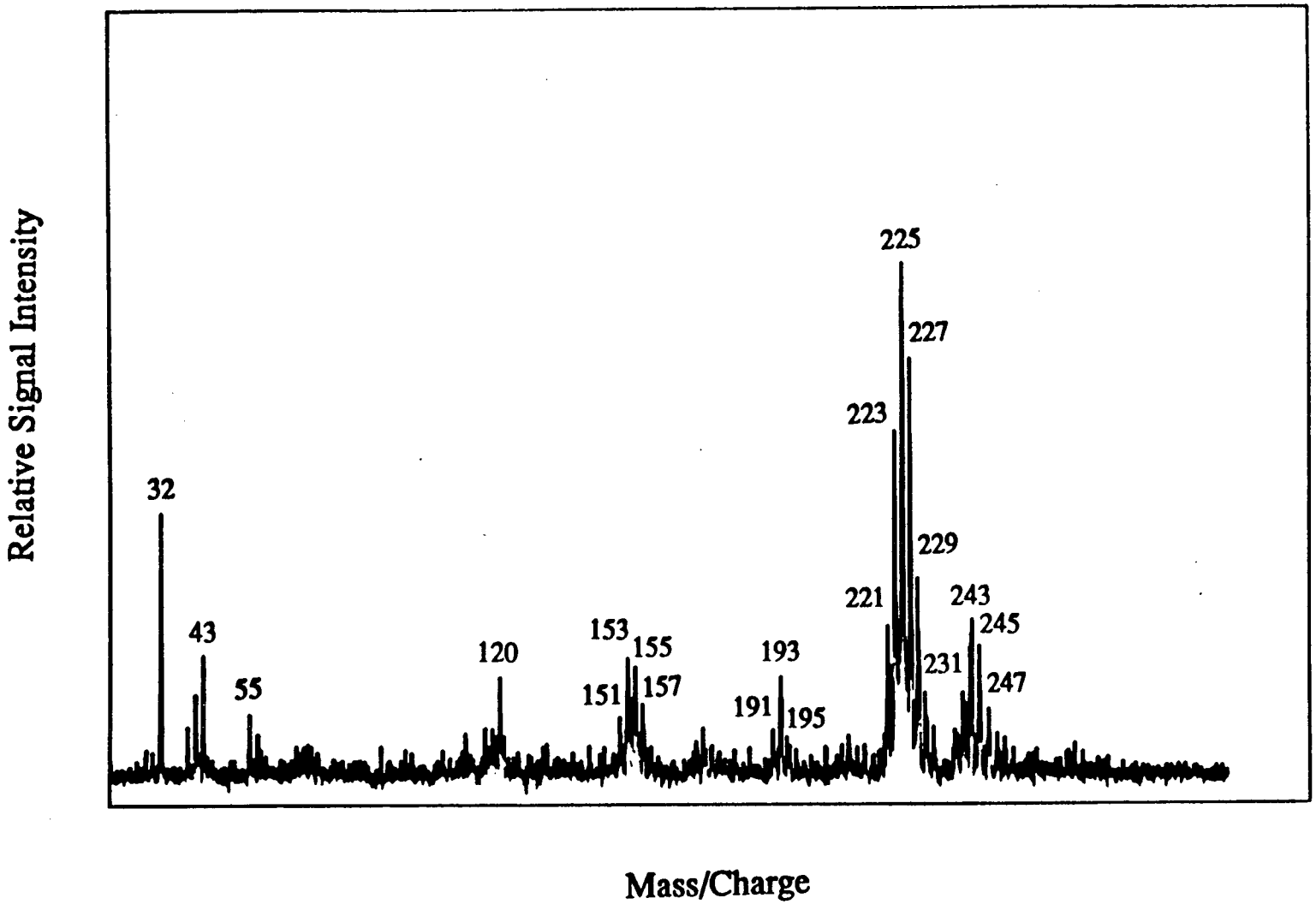

Figure 5.4: Spectrum obtained with 10 µL of a 5000 ppm tin chloride solution.

Table XIV

Mass-to-charge ratio	Identification
151	
153	$SnCl^+$
155	
191	
193	$SbCl_2^{+*}$
195	
221	
223	
225	$SnCl_3^+$
227	
229	
231	
241	
243	
245	Unknown
247	
249	

Table XIV: Identification of the peaks appearing on the tin chloride spectrum presented in figure 5.4.

* Antimony chloride from a previous analysis was still present in the system.

Table XV

Analyte	Boiling point(^{o}C)*	Observed (Y/N)
Cu	2567	N
Ag	2212	N
Sb	1750	N
Pb	1740	N
$PbCl_2$	950	N
Hg	356.6	Y
$SbCl_3$	283	Y

Table XV: List of the analytes used in the graphite furnace/ion trap mass spectrometer along with their boiling temperature and a note indicating their presence on the mass spectra.

5.1.3- Time Behaviour of the Signal Obtained With the Graphite Furnace / Ion Trap System:

Electro-thermal vaporization systems generally use very fast heating rates (2000^{o}C/s [64]) and the signal observed usually lasts only a very short time (a second or so). This method of operation offers some advantages in atomic absorption spectroscopy because the short time taken to vaporize the analyte produces the maximum analyte density possible in the analytical zone; it also reduces some of the interference problems which might otherwise be encountered. However, since our instrument had not been optimized for the trapping of analyte coming into the cavity in such a short time, it was decided to use a slower heating rate for the furnace, so that evaporation of the analyte would take longer, the rate chosen was around 30 ^{o}C/s. An

* Values taken from Handbook of Chemistry and Physics, 59th Edition, 1978-1979.

average heating time for an experiment involving the study of antimony chloride took about 35 s. Even if the ramping rate is slow, the rate at which the analyte vaporizes from the graphite furnace should be relatively quick due to the small amount of material being vaporized. However, the use of a transfer line to the ion trap plus the presence of the solenoïd valve in the transfer line will likely broaden the signal in the time domain.

To assess the behaviour of the instrument in terms of when the signal appears and at what time it reaches its maximum value, a series of eight spectra were acquired; each spectrum is the average of 100 scans. The time required to acquire a spectrum consisting of 100 scans is 36.5 s. Each spectrum was acquired starting at a 36.5 s interval from the previous one (all times are relative to the start of the heating ramp on the graphite furnace). The information obtained is presented in a bar graph format in figure 5.5 and table XVI. The data shows that the period of time where a maximum of analyte reaches the cavity starts after 36 seconds of heating of the graphite furnace*. The data also shows that almost 5 minutes after the beginning of the heating cycle of the graphite furnace some of the analyte is still making its way to the ion trap cavity. The reason for such a broadening of the signal likely comes from a number of factors. The low pressures used in the two containers is probably not very efficient at transfering the analyte quickly from the graphite furnace to the ion trap since the flow of gas between the two is limited. The volume of the cavity inside the solenoïd valve will likely cause a dilution of the analyte coming toward the ion trap, broadening the signal obtained. Because the graphite furnace is being positioned inside a closed container, the analyte that escapes the graphite furnace will diffuse

---

* This value will be a function of the time required by the graphite furnace to reach the temperature at which the analyte will escape the graphite surface (this temperature changes from one analyte to the next) and the analyte travelling time from the graphite furnace to the ion trap.

into the large volume of this container and will be slowly transfered to the trap as the gas flows from the one container to the other.

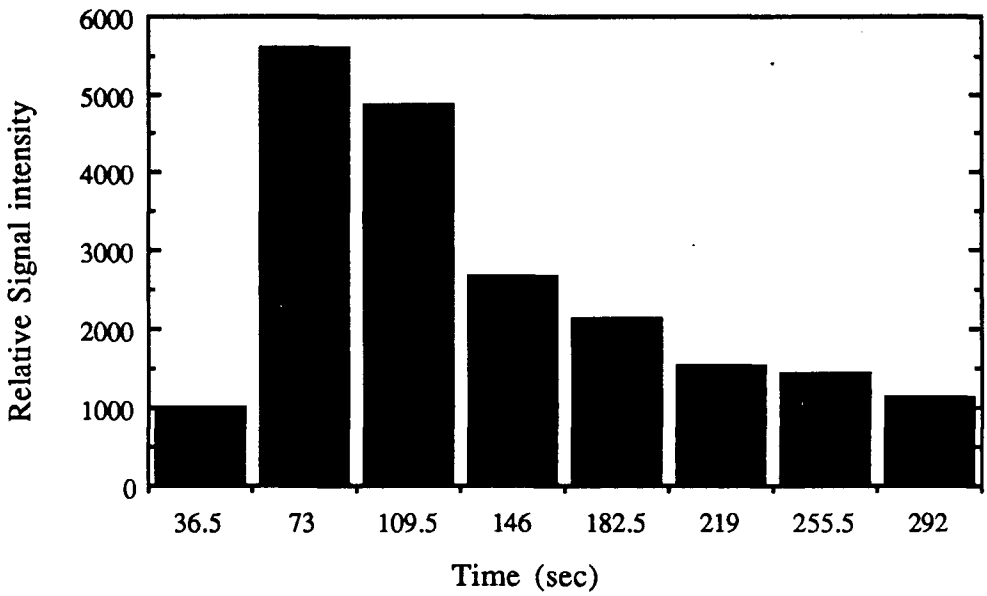

Figure 5.5: Time behaviour of the antimony trichloride signal obtained with the graphite furnace/ion trap mass spectrometer.

The long transfer time required for the analyte to pass from the graphite furnace to the ion trap also causes memory effects. Memory effects arise when the result of the analysis of a sample is influenced by the analysis done on a previous sample. Some of our data shows that even 15 minutes after the vaporization of the sample from the graphite furnace, and even if the graphite furnace had been allowed to reach atmospheric pressure and then evacuated to a lower pressure, a signal corresponding to about 5% of the original signal could still be detected. It is believed that the transfer line was responsible for restricting the flow of analyte to the trap, therefore widening the signal obtained.

Table XVI

Time (s)	Relative signal intensity
36.5	1001
73	5606
109.5	4875
146	2680
182.5	2139
219	1534
255.5	1436
292	1126

Table XVI: Time behavior of the signal obtained with the graphite furnace/ ion trap mass spectrometer.

5.1.4 - Operation of the Graphite Furnace Ion Trap Mass Spectrometer:

The motivation for the development of the instrument was to produce a device capable of the elemental analysis of trace levels of analyte in small volume samples. As indicated in the previous section, the data shows that this particular configuration of the instrument is not appropriate for elemental analysis since it appears impossible to transfer analytes with high boiling points from the graphite furnace to the ion trap. The instrument is able to handle small size samples as the data shows. The question that remains to be answered is: Is this instrument capable of trace analysis? To answer this question, a number of parameters must be optimized to ensure the maximum efficiency in transfering the sample from the graphite furnace to the ion trap and to ensure the highest possible trapping efficiency of the analyte. One of the variables playing an important role on the signal intensity has already been examined

in section 5.1.3; the time at which the acquisition of the spectrum is done is critical so as to obtain the maximum signal intensity from the system studied. The effect of other variables will now be examined

5.1.4.1 - Effect of the Pressure Difference Between the Graphite Furnace Container and the Ion Trap Container:

Since we rely on the pressure difference between the two containers to transfer the vapour produced by the graphite furnace to the ion trap one might expect that the maximum pressure difference would give the maximum signal intensity; however, other factors such as the initial velocity of the ions created in the trap could create a situation in which there is an optimum pressure difference between the two containers.

The choice of helium as the background gas for both containers comes from the need to have it in the ion trap to dampen the motion of the trapped ions (see section 4.8 and 4.9 of this document). Helium also offers other advantages; an inert gas is required to make up the atmosphere surrounding the graphite furnace so that oxidation of the furnace material during the heating sequence is avoided. Due to its high ionization potential it also allows one to operate the channeltron electron multiplier at a much higher total pressure inside the ion trap container than would be possible with any other inert gas.

A series of spectra was acquired using different pressures of helium inside the graphite furnace container. An antimony trichloride solution containing 4000 ppm of antimony was used to perform the study; 10 µL of this solution were vaporized from the graphite furnace and the vapour analysed with the ion trap. Figure 5.6 and table XVII presents the behaviour of the signal intensity of the ions appearing at a mass-

to-charge ratio of 193 amu as a function of the pressure inside the graphite furnace container.

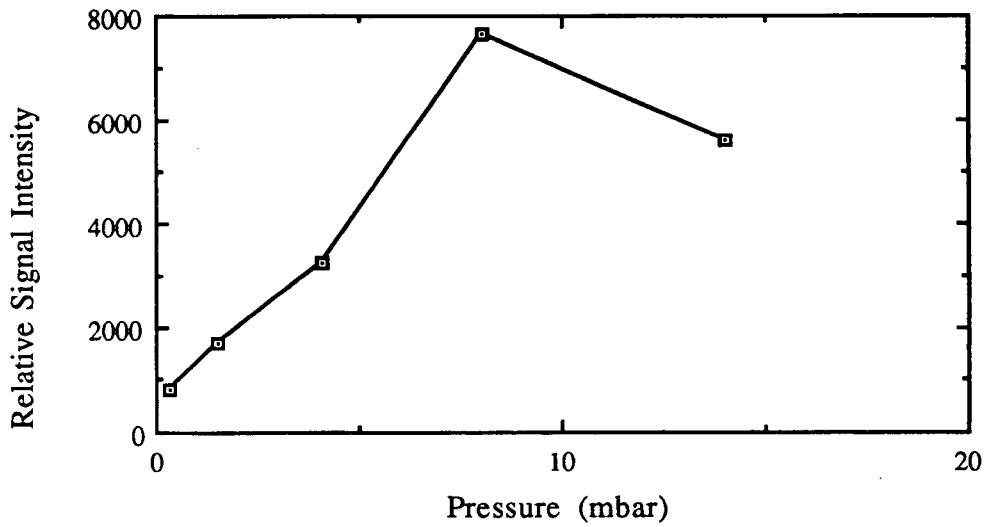

Figure 5.6: Signal intensity of the ions appearing at mass-to-charge ratio 193 as a function of the pressure used in the graphite furnace container.

Table XVII

Pressure (mbar)	Relative signal intensity
14	5612
8	7671
4.1	3239
1.5	1701
0.3	789

Table XVII: Signal intensity of the ions appearing at mass-to-charge ratio 193 as a function of the pressure used in the graphite furnace container.

It is easy to see from this set of data that there exists an optimum pressure difference between the two containers to achieve maximum trapping of the analyte. For the system studied the difference in pressure is around 8 mbar.

The analyte entering the cavity of the ion trap does so through the ring electrode on one side of the trap. It was suspected that this would have an effect on the trapping efficiency because the incoming gas might exercise a constant force, from one side, to the ion cloud through the numerous collisions between the incoming neutral gas species and the trapped ions. It was thought that providing the system with a second jet of gas, entering the cavity through a hole in the ring electrode positioned 180^{o} from the entrance of the analyte might cancel out this force. Therefore, a second inlet for allowing helium to flow into the trap cavity was machined. After many attempts using many different flows of helium it was concluded that there was no beneficial effect to be obtained by adding this second gas inlet through the ring electrode.

5.1.4.2 - Limit of Detection of the System:

As can be seen from the information presented so far, the work done with the graphite furnace ion trap mass spectrometer was carried out with solutions containing very high concentrations of analyte. The operating conditions were studied to optimize the performance of the instrument in order to obtain the lowest possible limit of detection. For reasons that will become evident in the next section, attempts at obtaining standard curves and thus carry out an analysis at low concentrations could not be completed because of instability in the signal from one firing of the furnace to the next. The lowest concentration solution used to obtain a spectrum was a 250 ppm antimony chloride solution from which we obtain the spectrum presented in figure 5.7.

For the larger peak (corresponding to one of the peaks of the antimony dichloride ions) appearing at a mass-to-charge ratio of 193, the signal-to-noise ratio is 157. Assuming that the response of the system is linear, a solution of 5 ppm in antimony chloride would have a signal-to-noise ratio of 3 (which defines the limit of detection of an instrument). This shows that this instrument has the potential for mass spectrometric analysis at the ppm level.

5.1.4.3 - Effect of Repetitive Heating Cycles of the Graphite Furnace on the Signal Intensity:

The problem of aging and deterioration of the graphite tubes used in graphite furnace atomic absorption spectroscopy is known: a graphite furnace can be used only a limited number of times before its performance begins to deteriorate. The deterioration comes from physical damage done to the tube by the repeated heating/cooling cycles (cracking of the tube, evaporation of the pyrolitic coating, damage to the contacts between the furnace and the supporting electrodes, etc.). These problems were observed in our instrument but with a much more pronounced effect. As the number of firings with a given furnace was increased, visual observation of the tube revealed physical damage such as that described above. All these signs of degradation of the instrument appeared very early in the life of the tube. Our data show that the signal obtained under constant operating conditions stays constant for the first few firings, but decreases dramatically as the number of firings is increased: after 10 firings the signal obtained has dropped to a value lower than half the value obtained with a fresh tube. The tubes can be reliably used for only 3 or 4 firings and must then be replaced. The damage done to the contact points between the graphite furnace and the supporting electrodes is important enough to justify tightening the electrodes to the tube after every firing, so as to obtain a reproducible heating of the

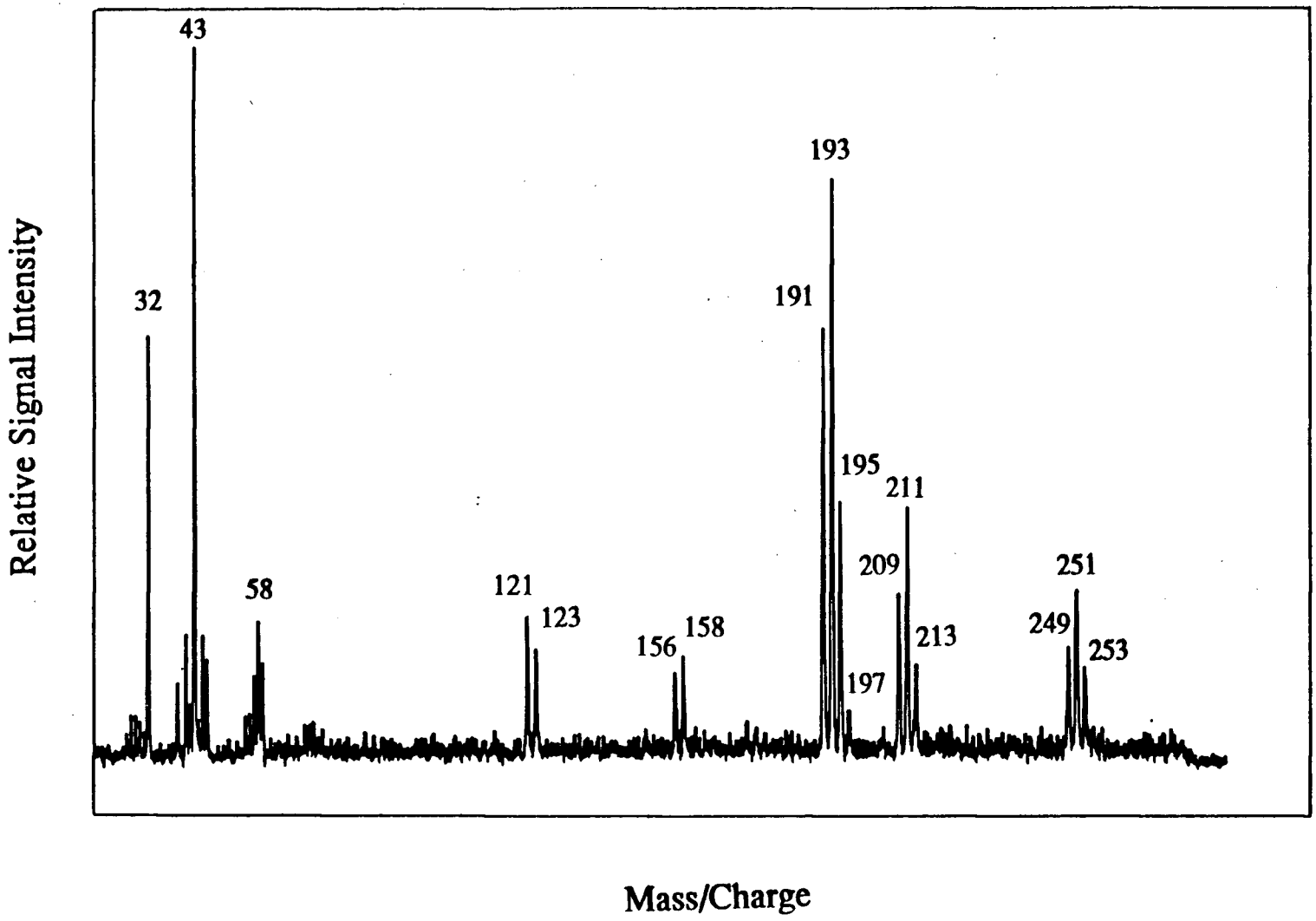

Figure 5.7: Spectrum obtained with a 250 ppm antimony trichloride solution.

tube. The difference in intensities obtained from one tube to the next is large enough that it renders the comparison of data obtained with different tubes very difficult.

The problems observed with the graphite tubes come from the fact that the heating cycle is performed under reduced pressure. There is a very quick loss of the pyrolitic coating of the tube leading to analyte loss on the porous graphite substrate of the tube, and most likely a change in the resistance and heating characteristics of the device. This, along with the interface connecting the graphite furnace to the ion trap, constitute the most important limitations of this instrument.

5.1.5 - Antimony in the Graphite Furnace Ion Trap Mass Spectrometer Instrument:

Most of the experiments performed with the graphite furnace ion trap mass spectrometer were done using antimony as the analyte. Solutions of two compounds were used in the graphite furnace: antimony tartrate dissolved in water and antimony trichloride dissolved in dilute hydrochloric acid. Results obtained with the antimony trichloride solution have already been presented (figures 5.3, 5.7). Attempts at obtaining atomic antimony spectra with an antimony tartrate solution were not successful. However, a slight addition of hydrochloric acid to the antimony tartrate solution made the spectrum of the antimony molecular species appear, indicating how much of an interference chloride can be for the determination of antimony by atomic absorption spectroscopy.

The problem of the interference of chloride on the analysis of antimony seems to be diminished if a fast heating rate of the graphite tube is used. Figures 5.8 and 5.9 respectively present data obtained using a slow rate of temperature increase and a step atomization (when the temperature is ramped at a very fast rate and reaches the desired value in a few seconds). The signal, for the molecular species, in the case of

the step atomization is 23% of the signal obtain while ramping up the temperature slowly.

Summary:

The data presented in this section demonstrate that the design of the instrument built is not adequate for the production of a device capable of ultra-trace multielemental analysis of small volume samples. Despite its potential ability to perform ppm level analysis on low boiling point analytes in μL size volume samples, its inability to transfer high boiling point elements from the graphite furnace to the mass spectrometer plus the rapid aging of the graphite tubes encountered at the lower pressures makes it inadequate for the purpose for which it was originally intended.

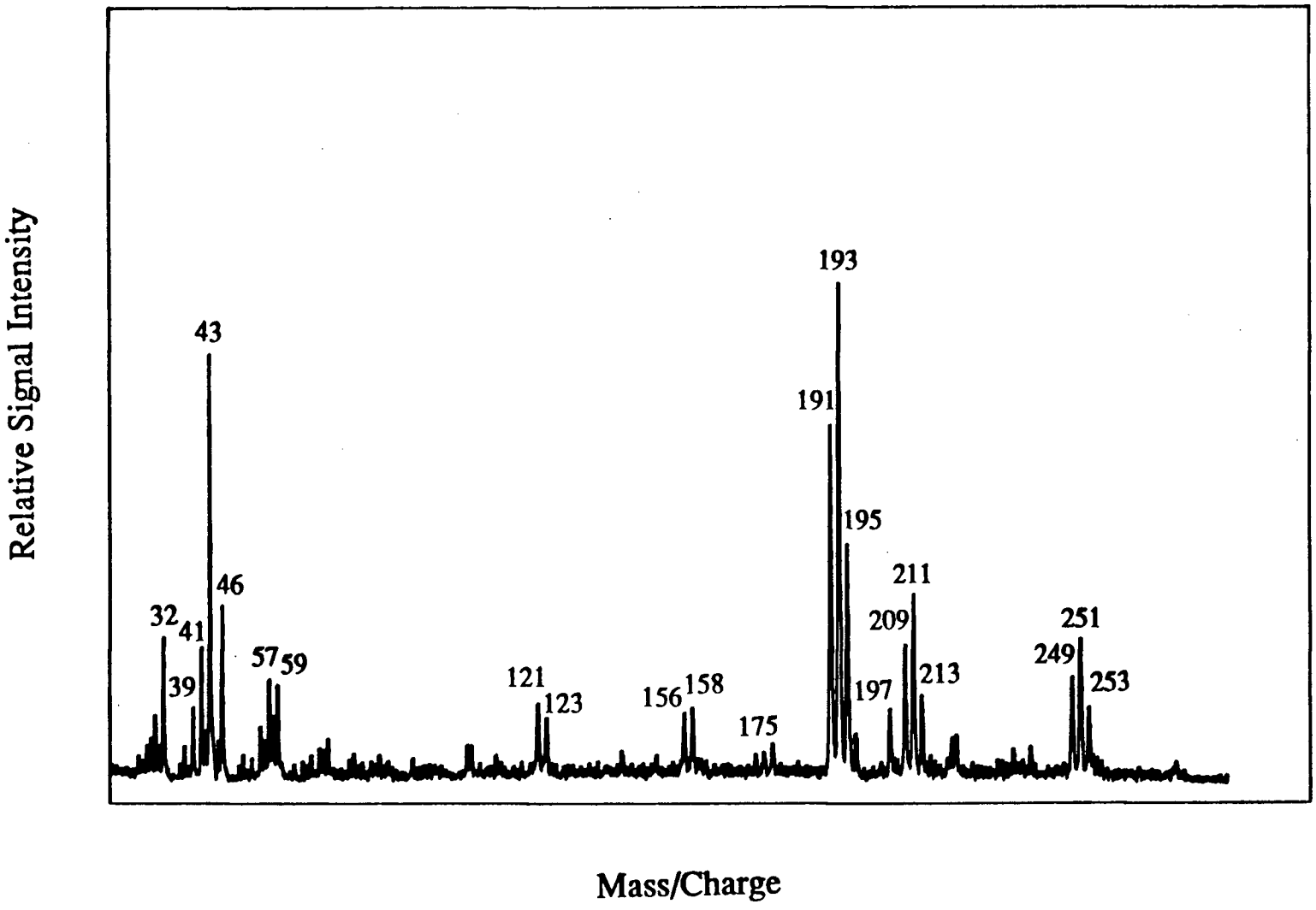

Figure 5.8: Spectrum of antimony trichloride solution obtained using a slow temperature increase rate.

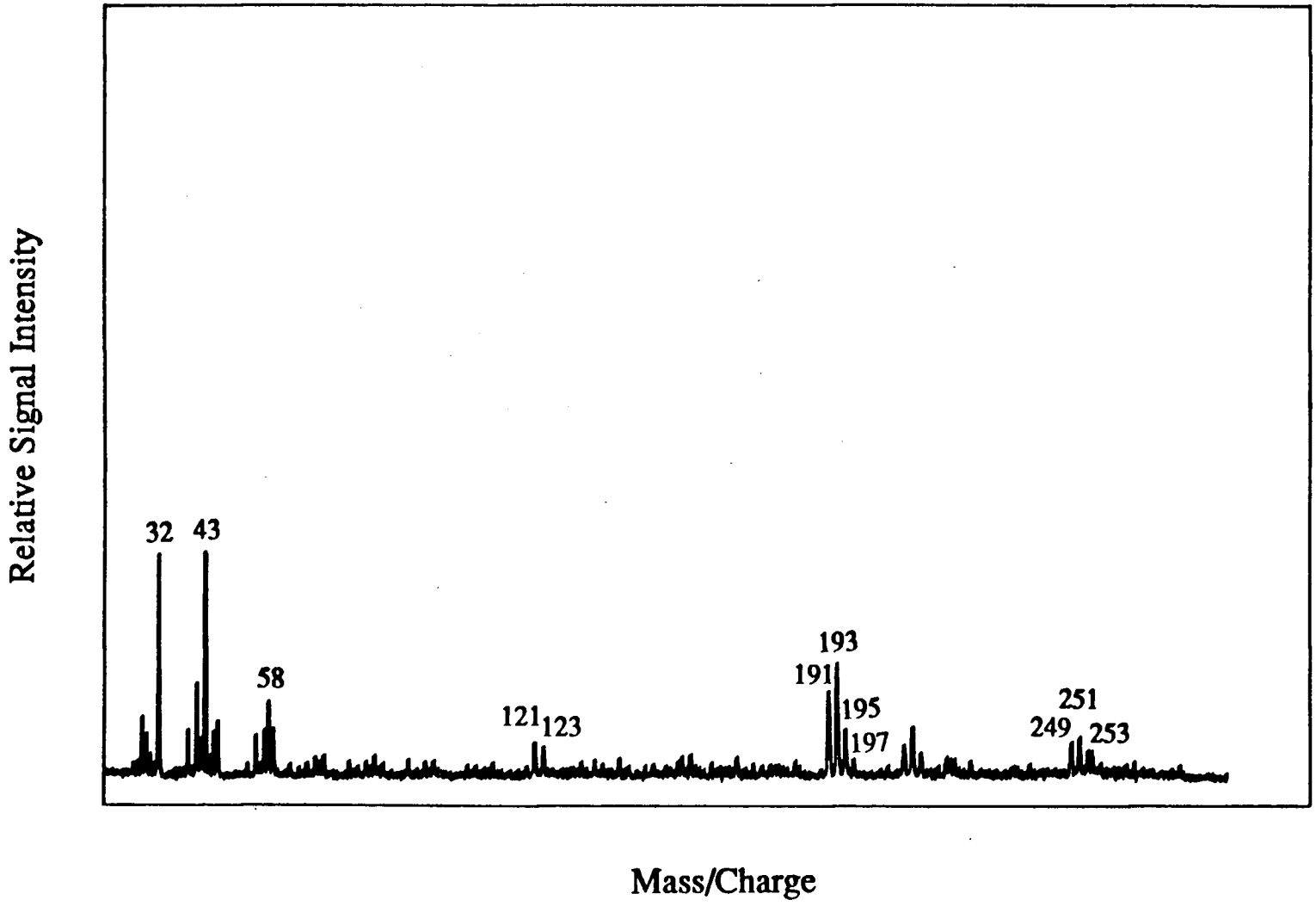

Figure 5.9: Spectrum of antimony trichloride obtained using step atomisation.

5.2 - Laser Ablation Ion Trap Mass Spectrometry:

5.2.1 - Introduction:

Mass spectrometry is a widely used technique to obtain information about the elemental composition of solid samples. It provides qualitative, quantitative and isotopic information about the elements of interest. Among the techniques used to perform inorganic mass spectrometry, laser ablation mass spectrometry is recognized to be a very powerful tool to study the elemental composition of solid samples both for bulk analysis and micro-analysis of the material. It does not require any chemical preparation of the sample and is relatively fast. Lasers are efficient instruments to vaporize solid samples and produce the atoms and molecules that will be analysed by mass spectrometry. When a laser pulse of sufficient energy density hits a solid surface, material is ejected from the surface into the gas phase. The ejected material may contain negative ions, clusters, particles and a significant number of positive ions. To analyse these positively charged species, TOF mass spectrometers and sector instruments are generally used. But the work done by B. S. Freiser on metal ion reactions in the gas phase using an ICR cell to trap metal ions created by laser ablation inside the cell opens the way to laser ablation/ion trapping mass spectrometric analysis. Although it was not their intention to produce an instrument capable of performing elemental analysis, they demonstrated the possibility of creating the laser induced plasma inside the trapping cell, trapping the ionized particles and detecting them to produce a mass spectrum of the metal ions present in the solid sample [96, 97].

The vaporization of solid samples by a normal mode laser is much different than the vaporization obtained with a Q-switched* laser. The laser pulse obtained with a normal mode laser is longer and has a higher energy than a Q-switched laser. This produces the vaporization of a larger amount of material from the sample. It also produces a higher amount of particles and clusters and a smaller amount of ionized atomic species than the Q-switched laser [98, 99]. The Q-switched laser has a lower energy but the much shorter pulse length (about 10^5 times shorter) provides for much higher power densities than with the normal mode laser. The result is that a smaller amount of material is being removed from the surface but at a higher temperature, producing a larger fraction of ionized atomic species than a normal mode laser does. It also produces very little molten material ejection.

The idea behind the development of a laser ablation mass spectrometer based on the ion trap is that the sampling efficiency of the vapour produced by the laser ablation directly inside the cavity of the ion trap could be much higher than in any other laser ablation mass spectrometer. The ion trap also offers the possibility of obtaining a mass spectrum covering a wide range of the mass-to-charge scale in a single laser pulse. Eventually the trapping capabilities of the ion trap could be used to accumulate the signal with low concentrations of analyte over multiple laser pulses to increase the signal intensity and obtain lower limits of detection with the instrument.

The problems that will be encountered with a laser ablation ion trap mass spectrometer for elemental analysis include both the problems of using a laser as a source of analyte and using the ion trap as a discriminator/detector system.

With laser ablation the efficiency of vaporization of material depends strongly on the laser power and the material composition. The reliability of the laser output is

---

* Q-switching is a technique by which the output of a laser is suppressed until it reaches very high intensities. Q-switching produces very short laser pulses that have a much higher power density than a normal mode laser pulse [98, 99].

therefore of prime importance for precision and accuracy of the results of a laser ablation analysis. Laser intensities will be affected by long term problems (such as flashtube deterioration, mirror coating deterioration) and short term problems (such as temperature changes of the lasing rod). Since the accuracy of an analysis is dependent on the reproducibility of the processes involved, laser ablation analysis will be particularly sensitive to statistical fluctuation in laser power output.

The interaction between the laser beam and the material to be analysed is also very much dependent on the composition of the material. The small size of the sampling spot of the laser can led to misleading results if the material is inhomogeneous. Homogeneity in the material studied is essential to obtain significant results from the instrument.

The most important limits that will be encountered with the ion trap are its low resolution and the troublesome ion-neutral reactions; a portion of the atomized atoms of interest could disappear from the trap through these reactions leading to a loss of sensitivity, an increase in detection limit and more complex mass spectra.

As far as we know, the data presented here constitute the first attempts at performing laser ablation inside the cavity of an ion trap. It only shows the possibility of performing this type of experiment and points out some of the problems encountered with the equipment used.

5.2.2 - Generalities:

We have developed a system in which the plasma created during the interaction of the laser beam with a solid sample is produced directly into the cavity of the ion trap. The ions produced by the laser plasma would be trapped and a mass spectrum covering the entire range of elements could be obtained. The laser used to perform our experiments was a 1J ruby laser having a pulse width estimated at 5 ms.

This laser is a normal mode laser (as opposed to a Q-switched laser). It was the only laser available for this study. This laser was very unreliable, spectra taken under the same experimental conditions would differ significantly; this is because the power supply and the flash lamp of the system do not operate reliably. The repetition rate of this laser is one pulse per minute: an increase in the repetition rate could cause over-heating and damage to the ruby crystal of the laser. Using a reproducible repetition rate also seems to be important since the capacitors storing the electricity used to power the flash lamp take a very long time to charge. Even if the settings on the power supply remain unchanged, a change in the repetition rate inevitably leads to differences in power output from the laser. To perform a complete study of the possibilities of this method, a quality laser system is required in order to have a good control on the power of the laser pulse used to vaporize the sample. The laser should also be Q-switched because of the higher amounts of ionized atomic species produced by Q-switched lasers. The problems encountered with the laser used include triggering problems (timing could vary by as much as ± 5 ms), power output variation (for a given setting of the power controls, different laser power levels would be obtained) and sensitivity to vibrations (vibrations will affect the setting of the rear mirror of the laser cavity).

5.2.3 - Results:

The results obtained with the four samples used (brass, copper, lead and silver) demonstrate the possibility of ablating material from a sample and creating the laser induced plasma directly into the cavity of the ion trap. Ions produced that way have been successfully trapped and mass spectra of these trapped ions have been obtained. However, none of the spectra obtained yielded conclusive evidence of the production of ionized atoms of the sample. This situation could be caused by a number

of things. The normal pulsed laser used may simply not produce the positively charged atomic species in high enough quantities to be distinguished in the mass spectra obtained. If atomic ions are being produced by laser ablation they may react very quickly with neutrals or negative ions and form higher mass ions or untrapped neutrals. Spectral interference can also mask the presence of atomic ions on our spectra.

The number of ions created is very high; on all the spectra there is at least one saturated peak. The saturated peaks often cover decades on the mass-to-charge scale indicating that enormous amount of material is being evaporated, ionized, trapped and detected. The amount of material taken from the sample by the laser pulse differs from one sample to the next. Undeniably lead was the material most affected by the laser: in 15 pulses the laser beam had drilled a hole 3 mm deep and 1 mm in radius through the lead sample. The other samples were not affected as much by the laser beam but physical damage to the sample could be observed after a few laser pulses. A large fraction of the material evaporated from the sample was found deposited on the surface of the electrodes of the ion trap. Some metal particles were also found outside the ion trap. The spectra obtained with different samples look very different from each other.

The use of the electron gun to ionize the vapour produced during the laser pulse is not required; the laser ablation process produces so many ions that there is no need to use the electron gun during these experiments. The utilization of the electron gun does not appear to affect either the signal intensities for the various peaks or the distribution of the ions. So in most of the experiments the electron gun was not used.

The possibility of forming molecular ions (as opposed to atomic ions) was investigated but no ions having structures such as M^+, M_2^+, M_3^+, M_3^{2+} were identified on our spectra.

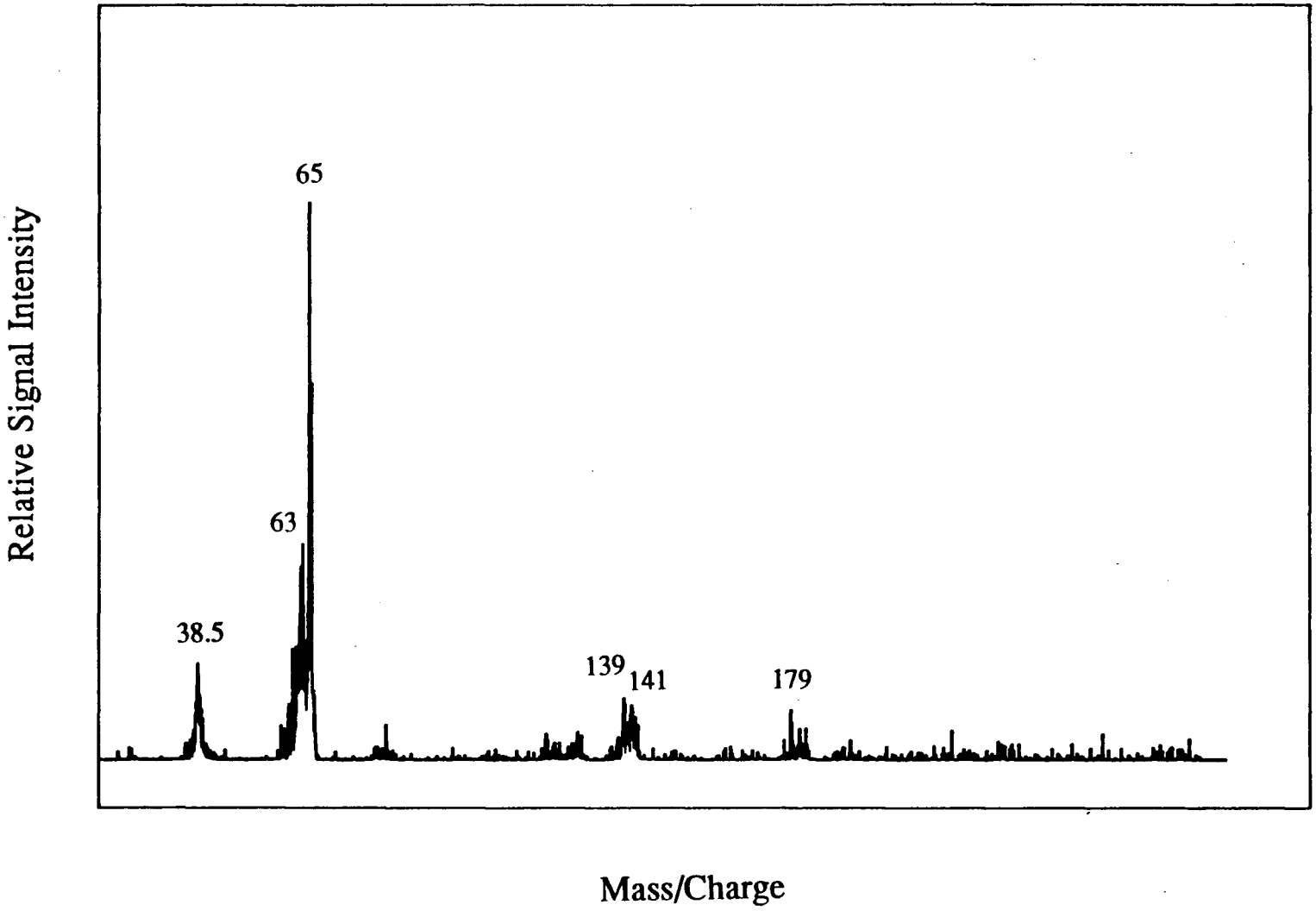

Figure 5.10: Laser ablation/ion trap mass spectrum of copper.

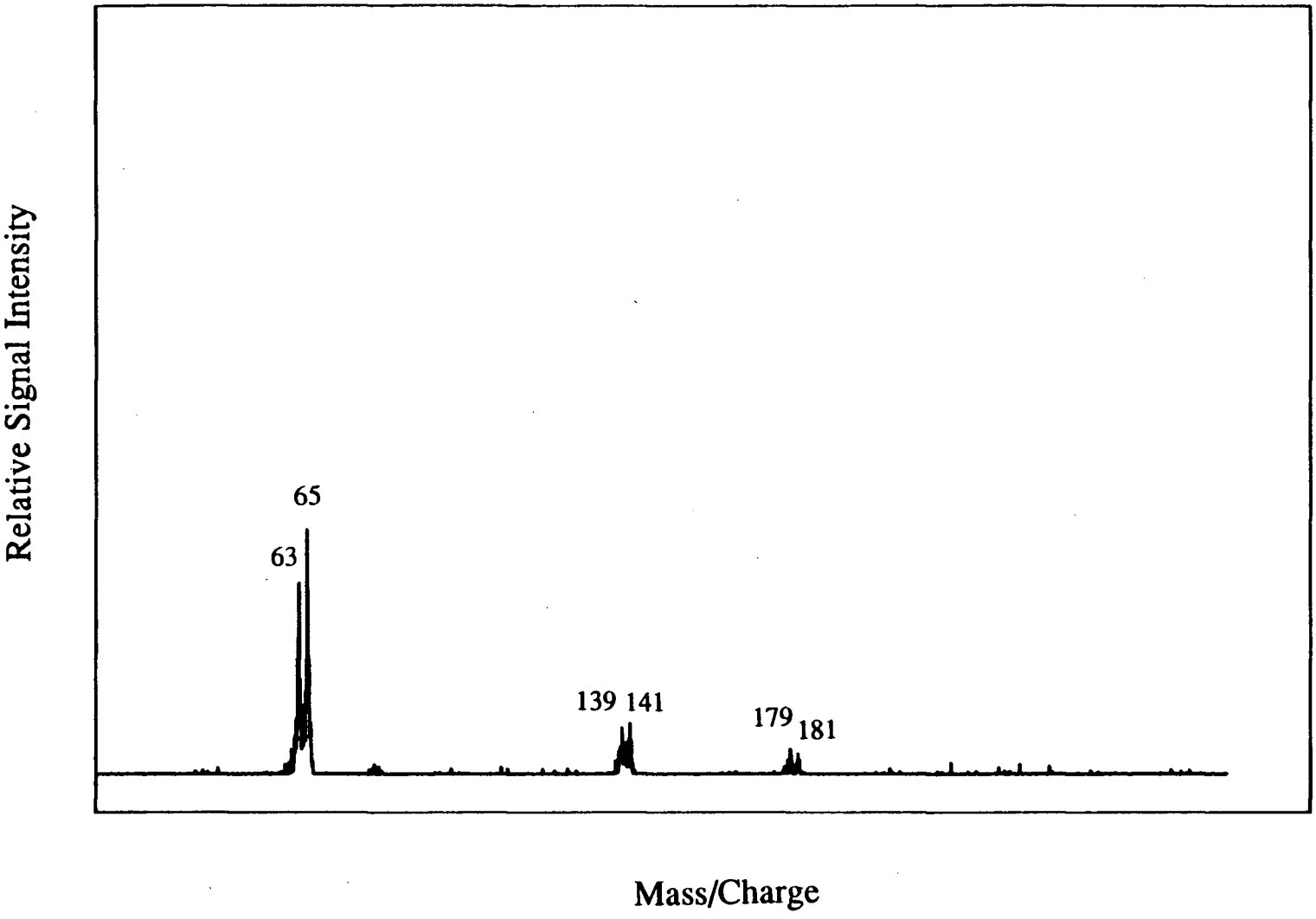

Figure 5.11: Laser ablation/ion trap mass spectrum of copper.

The reproducibility of the results obtained with our laser ablation system is very poor. The differences between the spectra are believed to be caused by instabilities in the laser power output. Despite the fact that the reproducibility of the results is poor, on a number of our spectra (for the same element) repetitive features can be found (see figures 5.10 and 5.11) which indicate that experiments done with proper equipment, under suitable operating conditions would likely produce interesting results.

The laser ablation experiments were performed using different pressures of background gas (helium). Total pressures ranging from $2.7 * 10^{-6}$ to $4.0 * 10^{-4}$ Torr were used. Despite the fact that instability in the laser power output prevents us from drawing definitive conclusions, it appears that an increase in helium pressure in the container produces an increase in the total number of ions detected which is consistent with the results presented in section 4.8.

Summary:

The preliminary results obtained with our laser ablation ion trap mass spectrometer suggest the possibility of performing direct elemental mass spectrometric analysis of solid samples. The use of a more reliable, Q-switched laser could greatly enhance the possibility of obtaining meaningful results with the system. From the work presented by Freiser [96, 97], it is believed that when a suitable laser will become available, these experiments will be successful.

CHAPTER VI

CONCLUSION

An ion trap mass spectrometer was designed and built in our laboratory in order to assess the possibility of developing a system capable of performing elemental analysis on small volume samples at trace concentration levels. The ability of the ion trap to accumulate ions at the centre of its cavity for relatively long periods of time and its ability to produce a mass spectrum of the trapped ions, covering a wide range of mass-to-charge values in a single scan was believed to be potentially very useful for the analysis of this type of sample. The ion trap built is capable of unit mass resolution with an upper mass limit of about 300 amu. Experiments showing the capability of our trap were reported. To perform these experiments the ion trap was interfaced to a source of volatile analyte. The effect of the presence of helium in the ion trap was found not to increase the maximum signal intensity obtainable from the system, but to shorten the storage time required to obtain this maximum intensity. The ion/neutral reactions that often make spectra obtained from the trap more complex than spectra obtained with a conventional quadrupole mass filter were found to be potentially useful for performing chemical ionization of the analyte on samples containing much lower quantities of material than required by the conventional chemical ionization systems: the ion trap mass spectrometer trades the high pressure found in conventional chemical ionization systems for longer reaction times. Using this technique, significant increases in signal intensity (compared to electron impact ionization) were obtained.

Elemental analysis of liquid or solid samples requires that the sample be first vaporized and atomized. To perform this function the graphite furnace atomizer was chosen due to its ability to handle small sample volumes, its high analyte transport efficiency and its low analyte ionization. A graphite furnace/ion trap mass spectrometer was built and it has been demonstrated that it is possible to transfer low boiling point analytes from the graphite furnace, through the interface, to the cavity of the ion trap mass spectrometer. However, transfer of higher boiling point analytes

proved to be impossible with the design adopted for this instrument. It was calculated that volatile compounds produced by the graphite furnace could be analysed at the ppm level with this set up. Mass spectra of mercury, tin chloride and antimony trichloride were successfully obtained using this instrument. The results produced with antimony show the kind of interference that can be encountered when an attempt is made at quantifying the amount of antimony present in a chloride containing solution using graphite furnace atomic absorption spectroscopy.

Another experimental set up was used to investigate the potential of the ion trap mass spectrometer in the field of elemental analysis. A laser ablation/ion trap mass spectrometer was built. The limited results obtained with this instrument show that this technique is a promising one for the direct mass spectrometric elemental analysis of solid samples. This set up offers the advantage that the ions generated by the laser pulse are produced directly inside the cavity of the trap allowing for a potentially higher efficiency of detection of these ions. The number of ions created by the laser pulse is high enough to saturate the ion trap mass spectrometer, so another source of ionization is not required to perform the analysis. Although the results presented are encouraging, more reliable equipment (specifically a Q-switched laser) is needed to complete a study of this system. The laser ablation experiments have also shown that, contrary to the information supplied by the manufacturer, the channeltron electron multiplier (used for the detection of the ions trapped in the device) can work under a much higher helium pressure than was originally believed. This will have a serious impact on the development of new technology for elemental analysis using the ion trap in our laboratory. The possibility of collisionally cooling the ions much more efficiently and much more quickly could improve the trapping efficiency significantly in some cases.

The future of the quadrupole radio-frequency ion trap is very promising. It has already shown its ability as a low resolution mass spectrometer capable of performing

tasks such as gas chromatography detection and MS/MS analysis that were previously reserved for bulkier, more expensive instruments. In the field of fundamental research, its ability to confine ions in its cavity for long periods of time has allowed the development of experiments leading to the observation of a single ion by laser fluorescence spectroscopy. Development of new applications for the ion trap could make the instrument one of the most versatile detection systems available on the market. This compact device has shown its ability to perform low resolution mass spectrometry of ions created through electron impact and chemical ionization (and could be used with photoionization). Detection of the ions, although generally performed by extracting the ions from the trap and detecting them with an electron multiplier, could gain much from developments in the field of in situ detection and eventually this research could lead to techniques which achieve lower limits of detection (trapped ion fluorescence spectroscopy) and higher resolution (Fourier transform mass spectrometry). Other improvements on the capabilities of the ion trap used as a mass spectrometer include the widening of the mass range covered by the instrument and the trapping of externally produced ions.

We believe that the approach taken during the course of our work on graphite furnace/ion trap mass spectrometry should be abandoned. The use of a small tube to interface the graphite furnace with the ion trap in conjunction with the use of a relatively large volume valve to stop the flow of gas between the two containers was a recipe for analyte loss through condensation on the walls of the interface. The graphite furnace could still be used as an analyte source if a proper interface is designed. An interface such as the one used in ICP-MS (skimmer) could be engineered to allow the sampling of the gas coming out of the graphite furnace at atmospheric pressure. But a different approach could also be taken. An electro-thermal vaporizer could be positioned much closer to the cavity of the ion trap in order to minimize analyte transport problems and maximize the transfer efficiency from the

sample in the liquid phase to the trapped analyte. A small electro-thermal vaporizer system of the type presented by Bukley and Boss* [100] could be positioned inside one of the electrodes of the trap, close to the hyperbolic surface, so that the vapour produced by the vaporizer could migrate quickly, with minimum obstruction, to the centre of the trap where ionization can take place. Such a system would likely eliminate the analyte transfer problem but could suffer from other difficulties because the electro-thermal vaporizer position inside a vacuum system: chemical interference could be a much greater problem with this set up than in a conventional graphite furnace system since it is believed that the hot gas inside the graphite tube (at atmospheric pressure) is largely responsible for dissociation of molecular compounds that escape from the graphite surface. At a lower pressure this effect would likely not be as significant. But this avenue should be seriously investigated.

The laser ablation set up will probably produce very interesting results as soon as a proper laser is made available for these experiments. A number of other experimental details should be improved in order to produce a better instrument. First, the laser alignment and focussing optics should be improved to allow a better control of the spatial sampling of the analyte. Second, the experimental set up should be redesigned in order to allow multiple firings of the laser on a fresh surface of the target without having to remove the target from the chamber to clean it. Third, a sample changing device should be installed to permit rapid changing of the sample with minimum disturbance of the vacuum in the ion trap container.

There is also a number of areas of methodology development which should be addressed in future research project. First, the addition of a DC potential applied

---

* In a new design, for an electro-thermal atomizer, Bukley and Boss[100] used a tungsten filament on which 1 μL of sample was deposited for analysis. The small size of such a vaporizer makes it ideal for its use in an electro-thermal evaporation/ion trap mass spectrometer.

between the electrodes of the trap should be a priority. This would permit the development of the potential of the instrument for accumulation of ions of similar mass-to-charge ratio over extended periods of time. The DC and RF voltages should be made independently controllable by the computer to allow for exploration in the fields of DC/RF scanning, DC only scanning, upper limit mass range cut off, etc. Second, the trapping of externally created ions is also an avenue to explore. One can imagine a system where it would be desirable to couple the capability of the ion trap to accumulate analyte with an analyte source that produces a high percentage of ionized species such as the ICP. Third, in situ detection of the analyte should be investigated. Trapped ion fluorescence could lead to very low limits of detection while Fourier Transform methods have the potential to give very high resolution. Fourth, the most interesting improvement that would make the ion trap much more interesting for routine analysis is likely to be its development as a multisource detector. Since the analyte can be brought into the trap from any side, it is possible to install many sources of analyte around the cavity of the trap. A single ion trap mass spectrometer could then be used as detector for a gas chromatograph, a liquid chromotograph, a source of atoms and a laser ablation set up. This coupled with the capability of the ion trap to use both electron impact ionization and chemical ionization, its capability to perform MS/MS analysis, its compactness, its mechanical simplicity, its versatility and its potential for high resolution (with the development of Fourier transform methods) could make the ion trap one of the most interesting devices in the analytical laboratory of the future. Inorganic analysis will gain greatly from taking advantage of the possibilities of this instrument.

REFERENCES

References

[1] - Brunée, C., "The ideal mass analyser: fact or fiction", International Journal of Mass Spectrometry and Ion Processes, 76 (1987), 125.

[2] - Comisarow, M. B., "Fundamental aspects and applications of Fourier-Transformed Ion-Cyclotron Resonance Spectrometry", Analytica Chimica Acta, 178 (1985), 1.

[3] - Comisarow, M. B., "Signal modeling for ion cyclotron resonance", J. Chem. Phys., 69 (1978), 4097.

[4] - Dehmelt H. G., "Radio Frequency Spectroscopy of Stored Ions I: Storage", Advances in Atomic and Molecular Physics, D. R. Bates and I. Estermann (Editors), Academic Press, New York, p. 53, 1967.

[5] - Courant, E. D., M. S. Livingtons and H. S. Snyder, "The stong focusing synchroton-A new high energy accelerator", Physical Review, 88 (1952), 1190.

[6] - Paul, W. and H. Steinwedel, "Ein neues Massenspektrometer ohne Magnetfeld", Zeitschrift für NaturForschung, 8A (1953), 448.

[7] - Zahn, U., "Monopole spectrometer, a new electric field mass spectrometer", Review of Scientific Instruments, 34 (1963), 1.

[8] - Fisher, E., "Die dreidimensionale Stabilisierung von Ladungsträgern in einen Vierpolfeld", Zeitschrift für Physik, 156 (1959), 1.

[9] - Wuerker, R. F., H. Shelton and R. V. Langmuir, "Electrodynamic Containment of Charged Particles", Journal of Applied Physics, 30 (1959), 342.

[10] - Wuerker, R. F., H. M. Goldenberg and R. V. Langmuir, "Electrodynamic containment of charged particles by three-phase voltages", Journal of Applied Physics, 30 (1959), 441.

[11] - Dehmelt, H. G., "RF Spectroscopy of trapped ions by a Selective Elimination-Collision Technique", Bulletin. American Physical Society, 7 (1962), 470.

[12] - March, R. E. and R. J. Hughes, Quadrupole Storage Mass Spectrometry, Chemical Analysis Vol. 105, Wiley-Intersciences Publication, New York, 1989, 471 p.

[13] -Bonner, R. F., G. Lawson and J. F. J. Todd, " A low-pressure chemical ionisation source: An application of a novel type of ion storage mass spectrometer", Journal, Chemical Society, Chemical Communication, 1972, 1179.

[14] - Wineland, D. J., W. M. Itano, R. S. Van Dyck Jr, Advances in Atomic and Molecular Physics, D. R. Bates (Editor), Academic Press, NY, 19 (1983), 135.

[15] - Neuhauser, W., M. Hohenstatt, P. E. Toschek and H. Dehmelt, "Visual observation and Optical Cooling of Electrodynamically Confined Ions", Applied Physics,17 (1978), 123.

[16] - Toschek, P. E., W. Neuhauser, "Spectroscopy on Lacalized and Cooled Ions", Atomic Physics, 7 (1981), 529.

[17] - Neuhauser, W., M. Hohenstatt, P. E. Toschek and H. Dehmelt, " Optical Sideband Cooling of Visible Atom Cloud Confined in Parabolic Well", Physical Review Letters, 41 (1978), 233.

[18] - Neuhauser, W., M. Hohenstatt, P. E. Toschek and H. Dehmelt, "Localized Visible Ba^+ Mono-Ion Oscillator", Physical Review A, 22 (1980), 1137.

[19] - Neuhauser, W., M. Hohenstatt, P. E. Toschek and H. Dehmelt, "Visual Observation and Optical Cooling of Electrodynamically Contained Ions", Applied Physics, 17 (1978), 123.

[20] - Wineland, D. J. and W. M. Itano, "Laser cooling of atoms",.Physical Review A, 20 (1979), 1521.

[21] - Plumelle, F., M. Desaintfuscien, M. Jardino and P. Petit, "Laser Cooling of Magnesium Ions: Preliminary Experimental Results", Applied Physics B, 41 (1986), 183.

[22] - Stafford,G. C., P. E. Kelly, J. E. P. Syka, W. E. Reynolds, J. F. J. Todd, " Recent Improvements in and Analytical Applications of Advanced Ion Trap Technology", International Journal of Mass Spectrometry and Ion Processes, 60 (1984), 85.

[23] - Blades, M. W. and B. Daigle, "Elemental Analysis using a Quadrupole Ion Storage Device", American Chemical Society, 193rd National Meeting, p. 38, 1987.

[24] - Heller, D. N., I. Lys, R. J. Cotter, "Laser Desorption from a Probe in the Cavity of a Quadrupole Ion Storage Mass Spectrometer", Analytical Chemistry,61 (1989), 1083.

[25] - Dawson, P. H., J. W. Hedman, N. R. Whetten, " A Simple Mass Spectrometer", The Review of Scientific Instruments, 40 (1969), 1444.

[26] - Benilan, M. and C. Audoin, "Confinement d'ions par un champ électrique de radio-fréquence dans une cage cylindrique", International Journal of Mass Spectrometry and Ion Processes, 11 (1973), 421.

[27] - Fulford, J. E., R. E. March, R. E. Mather, J. F. J. Todd, R. M. Waldren, Canadian Journal of Spectroscopy, 25 (1980), 85.

[28] - Nassiopoulos, A. G., P. A. Moller and A. Septier, "Confinement d'ions dans une cage cylindrique a champ quadrupolaire HF. Application à la spectrométrie de mass I. Partie théorique", Revue de physique appliquée, 15 (1980), 1529.

[29] - Nassiopoulos, A. G., P. A. Moller and A. Septier, "Confinement d'ions dans une cage cylindrique a champ quadrupolaire HF. Application à la spectrométrie de mass II. Partie expérimentale", Revue de physique appliquée, 15 (1980), 1543.

[30] - Mather, R. E., R. M. Waldren, J. F. J. Todd and R. E. March, "Some operational characteristics of a quadrupole ion storage mass spectrometer having cylindrical geometry", International Journal of Mass Spectrometry and Ion Processes, 33 (1980), 201.

[31] - Chun-Sing O and H. A. Schuessler, "Ion-storage in a radio-frequency trap with semi-spherical electrodes", International Journal of Mass Spectrometry and Ion Processes, 35(1980), 305.

[32] - Todd, J. F. J. and G. Lawson, "Quadrupole Mass Spectrometry", International Review of Science. Physical Chemistry, Series Two, A. D. Buckingham and A. Maccol (Editors), Butterworth and Co. (Publishers) Ltd, London, 5 (1983), 289.

[33] - Church, D. A., "Storage-ring ion trap derived from the linear quadrupole radio-frequency mass filter", Journal of Applied Physics, 40 (1969), 3127.

[34] - Dawson, P. H. (ed.), Quadrupole Mass Spectrometry, Elsevier Scientific Publishing Company, Amsterdam, 1976, 349 p.

[35] - Allison, J. and R. M. Stepnowski, "The Hows and Whys of Ion Trapping", Analytical Chemistry, 59 (1987), 1072A.

[36] - Comisarow, M. B., "Cubic trapped-ion cell for ion cyclotron resonance", International Journal of Mass Spectrometry and Ion Physics, 37 (1981), 251.

[37] - Wobschall, D., "Ion Cyclotron Resonance Spectrometer", The Review of Scientific Instruments, 36 (1965), 466.

[38] - Gross, M. L. and D. L. Rempel, "Fourier Transform Mass Spectrometry", Science, 226 (1984), 261.

[39] - Comisarow, M., "Fourier Transform Ion Cyclotron Resonance Spectroscopy", Advances in Mass Spectrometry, 7B (1978),1042.

[40] - Chattopadhayay, A. P. and P. K. Ghosh, "QUISTOR - A Study of Many Particle Systems", International Journal of Mass Spectrometry and Ion Physics, 49 (1983), 253.

[41] - Daigle, B. and M. W. Blades, "A study of storage time as an operation parameter in ion-trap mass spectrometry", FACCS. 15th annual meeting, Presentation #f34, p. 13, 1988.

[42] - Dawson, P. H., N. R. Whetten, "Ion Storage in Three-Dimensional, Rotationally Symetric, Quadrupole Fields II: A Sensitive Mass Spectrometer", Journal of Vacuum Science and Technology, 5 (1968), 11.

[43] - Bonner, R. F., G. Lawson, J. F. J. Todd, "Ion-Molecule Reactions Studies with a Quadrupole Ion Storage Trap", International Journal of Mass Spectrometry and Ion Processes, 10 (1973), 197.

[44] - Bonner, R. F., G. Lawson, J. F. J. Todd, R. E. March, "Ion Storage Mass Spectrometry: Applications in the Study of Ionic Processes and Chemical Ionization Reactions", Advances in Mass Spectrometry, 6 (1974), 377.

[45] - Turulski, J., J. Niedzielski and W. Stiller, "Simple theory of the charge transfer rate in ion/molecule reactions. Part 1. Derivation of the theory", International Journal of Mass Spectrometry and Ion Processes, 79 (1987), 189.

[46] - Turulski, J., J. Niedzielski and W. Stiller, "Simple theory of the charge transfer rate in ion/molecule reactions. Part 2. Experimental verification", International Journal of Mass Spectrometry and Ion Processes, 79 (1987), 203.

[47] - Louris, J. N., J. S. Brodbelt and R. G. Cooks, "Photodissociation in a quadrupole ion trap mass spectrometer using a fiber optic interface", International Journal of Mass Spectrometry and Ion Processes, 75 (1987), 345.

[48] - Lifshitz, C. and Y. Malinovich, "Time resolved photoionization mass spectrometry in the millisecond range", International Journal of Mass Spectrometry and Ion Processes, 60 (1984), 99.

[49] - Lifshitz, C., M. Goldenberg, Y. Malinovich and M. Peres, "Photoionization mass spectrometry in the millisecond range", Organic mass spectrometry, 17 (1982), 453.

[50] - Neuhauser, W., M. Hohenstatt, P. E. Toschek and H. Dehmelt, "Preparation, Cooling, and Spectroscopy of Single Localized Ions", Laser Spectroscopy IV, p. 73, 1979.

[51] - Nagourney, W., G. Janik and H. Dehmelt, "Linewidth of a Single Laser-Cooled $_{24}Mg^{+}$ Ion in a Radio Frequency Trap", Proceedings of the National Academy of Science, 80 (1983), 643.

[52] - Itano, W. M. and D. J. Wineland, "Laser Cooling and Double Resonance Spectroscopy of Stored ions", Laser Spectroscopy Y, Proccedings of the 5th International Conference, A. R. W. McKellar, T. Oka, B. P. Stoicheff, Eds, Spinger-Verlag, Berlin, p 360, 1981.

[53] - Dehmelt, H. G., "Mono-Ion Oscillator for Ultimate Resolution Laser Spectroscopy", Laser Spectroscopy Y, Proccedings of the 5th International Conference, A. R. W. McKellar, T. Oka and B. P. Stoicheff Editors, Spinger-Verlag, Berlin, 1981, p 353.

[54] - Larson, D. J. and R. M. Jopson, "Spectroscopy of Trapped Negative Ions", Laser Spectroscopy Y, Proccedings of the 5th International Conference, A. R. W. McKellar, T. Oka and B. P. Stoicheff, Editors, Spinger-Verlag, Berlin, 1981, p 369.

[55] - Church, D. A. and H. G. Dehmelt, "Radiative Cooling of an Electrodynamically Contained Proton Gas", Journal of Applied Physics, 40 (1969), 3421.

[56] - Ifflander, R., G. Werth, "Optical Detection of Ions Confined in a RF Quadrupole Trap", Metrologia, 13 (1977), 167.

[57] - Itano, W. M. and D. J. Wineland, "Laser Cooling of Ions Stored in a Harmonic and Penning Traps", Physical Review A, 25 (1952), 35.

[58] - Hoffnagle, J., R. G. DeVoe, L. Reyna and R. G. Brewer, " Order-Chaos Transition of Two Trapped Ions", Physical Review Letters, 61 (1988), 255.

[59] - Quint, W., W. Schleich and H. Walther, "Order and Chaos with Frozen Ions", Physics World, 2 (1989), 30.

[60] - Bergquist, J. C., R. G. Hulet, W. M. Itano and D. G. Winland, "Observation of Quantum Jumps in a Single Atom", Physical Review Letters, 57 (1986), 1699.

[61] - Adams, F., R. Gijbels and R. Van Grieken, "Inorganic Mass Spectrometry", Chemical Analysis ,Vol. 95, Wiley-Intersciences Publication, New York, 1988, 404 p.

[62] - Sturgeon, R. E.and S. S. Berman, "Analyte ionization in graphite furnace atomic absorption spectrometry", Analytical Chemistry, 53 (1981), 632.

[63] - Sturgeon, R. E. and C. L. Chakrabarti, "Recent Advances in Electrothermal Atomization in Graphite Furnace Atomic Absorption Spectrometry", Progress in Analytical Atomic Spectroscopy, C. L. Chakrabarti Editor., Paragon Press, Great Britain, p. 5, 1978.

[64] - Welz, B., Atomic Absorption Spectrometry, Second Edition, VCH Publisher, Germany, 1985, 506 p.

[65] - Bass, D. A. and J. A. Holcombe, "Mechanisms of lead vaporization from an oxygenated graphite surface using mass spectrometry and atomic absorption", Analytical Chemistry, 60 (1988), 578.

[66] - Bass, D. A. and J. A. Holcombe, "Mass spectral investigation of mechanisns of lead vaporization from a graphite surface used in electrothermal atomizers", Analytical Chemistry, 59 (1987), 974.

[67] - Styris, D. L. and J. H. Kaye, "Mechanismes of vaporization of vanadium pentoxide from vitreous carbon and tantalum furnaces by combined atomic absorptiion/mass spectrometry", Analytical Chemistry, 54 (1982), 864.

[68] - Sturgeon, R. E., D. F. Mitchell and S. S. Berman, "Atomization of lead in graphite furnace atomic absorption spectrometry", Analytical Chemistry, 55 (1983), 578.

[69] - Styris, D. L., "Elucidating atomization mechanisms by simultaneous mass spectrometry and atomic absorption spectrometry", Fresenius Zeitschrift fü Analitische Chemie, 323 (1986), 710.

[70] - Welz, B., Atomic absorption spectrometry, VCH Publisher, Federal Republic of Germany, 506 p, 1985.

[71] - Dong C. Liang and M. W. Blades, "Atmospheric pressure capacitively coupled plasma atomizer for atomic absorption spectrometry", Analytical Chemistry, 60 (1988), 27.

[72] - Jochum, K. P., L. Matus and H. M. Seufert, "Trace element analysis by laser plasma mass spectrometry", Fresenius Zeitschrift für Analitische Chemie, 331 (1988), 136.

[73] - Beske, H. E., "Comparison of the efficiency of spark sourcs, laser, glow discharge and secondary ion mass spectrometry for bulk analysis", Fresenius Zeitschrift für Analitische Chemie, 331 (1988), 150.

[74] - Dong C. Liang and M. W. Blades, "Atmospheric pressure capacitively coupled plasma spectral lamp and source for the direct analysis of conducting solid samples", Spectrochemica Acta, 44B (1989), 1049.

[75] - Dong C. Liang and M. W. Blades, "An atmospheric pressure capacitively coupled plasma formed inside a graphite furnace as a source for atomic emission spectroscopy", Spectrochemica Acta, 44B (1989), 1059.

[76] - McLachlan, Theory and Application of Mathieu Functions, Dover Publications, Inc., New York, 401 p, 1964.

[77] - Matter, R. E., R. M. Walden, J. F. J. Todd, "The Characterization of a Quadrupole Ion Storage Mass Spectrometer", Dynamic Mass Spectrometry, 5 (1978), 71.

[78] - Schuessler, H. A., "Stored Ion Spectroscopy", Physics of Atoms and Molecules, Progresses in Atomic Spectroscopy, W. Hanle and H. Kleinpoppen Editors, Plenum , NY, 1979, p 999.

[79] - Dehmelt, H., "Stored Ion Spectroscopy", Advances in Laser Spectroscopy, F. T. Arecchi, F. Strumia and H. Walther Editors, Plenum, NY, 1983, p 153.

[80] - Toschek, P. E., "Atomic Particles in Traps", New Trends in Atomic Physics, G. Grynberg and R. Stora Editors, North-Holland Physics Publishing, Amsterdam, 1 (1984), 383.

[81] - Armitage, M. A., J. E. Fulford, D. N. Hoa, R. J. Hughes, R. E. March, "The Application of Resonant Ion Ejection to Quadrupole Ion Storage Mass Spectrometry: A Study of Ion/Molecule Reactions in the QUISTOR", Canadian Journal of Chemistry, 57 (1979), 2108.

[82] - Dolnikowski, G. G., M. J. Kristo, C. G. Enke, J. T. Watson, "Ion Trapping Technique for Ion/Molecule Reaction Studies in the Center Quadrupole of a Triple Quadrupole Mass Spectrometer", International Journal of Mass Spectrometry and Ion Physics, 82 (1988), 1.

[83] - Lawson, G., R. F. Bonner, J. F. J. Todd, "The Quadrupole Ion Store (QUISTOR) as a Novel Source for a Mass Spectrometer", Journal of Physics E: Scientific Instruments, 6 (1973), 357.

[84] - Mosburg, E. R., M. Vedel, V. Zerega,F. Vedel, J. Andre, "A Time-of-Flight Method for Studying the Properties of an Ion Cloud Stored in an RF Trap", International Journal of Mass Spectrometry and Ion Physics, 77 (1987), 1.

[85] - Baril, M., A. Septier, "Piégeage des Ions dans un Champ Quadrupolaire Tridimensionnel à Haute Frequence", Revue de Physique Appliquée, 9 (1974), 525.

[86] - Todd, J. F. J., R. M. Waldren, R. E. Mather, G. Lawson, "On the Relative Efficiencies of Confinement of Ar^{+} and Ar^{2+} Ions in a Quadrupole Ion Storage Trap (QUISTOR)", International Journal of Mass Spectrometry and Ion Physics, 28 (1978), 141.

[87] - Todd, J. F. J., "Recent Developments in the Theory and Application of the Quadrupole Ion-Storage Trap", Dynamic mass spectrometry, 6 (1981), 44.

[88] - Todd, J. F. J., R. M. Waldren, R. E. Mather, "The Quadrupole Ion Store (QUISTOR). Part IX. Space-Charge and Ion Stability. A Theoretical Background and Experimental Results", International Journal of Mass Spectrometry and Ion Physics, 34 (1980), 325.

[89] - McIver, R. T., Jr., E. B. Ledford, Jr., J. S. Miller, "Proposed method for mass spectrometric analysis for ultra-low vapor pressure compounds", Analytical Chemistry, 47 (1975), 692.

[90] - Hunter, R. L., R. T. McIver, Jr., "Mechanisn of low-pressure chemical ionization mass spectrometry", Analytical Chemistry, 51 (1979), 699.

[91] - Ghaderi, S., P. S. Kulkarni, E. B. Ledford, C. L. Wilkins, M. L. Gross,"Chemical Ionization in Fourier Transform Mass Spectrometry", Analytical Chemistry, 5 (1981), 428.

[92] - Harrison, A. G., Chemical Ionization Mass Spectrometry, CRC Press Inc., 156 p, 1983.

[93] - Millard, B. J., Quantitative Mass Spectrometry, Heiden and Son Ltd., Printed inn Great Britain by Gaillard (Printers) Ltd., 171 p, 1978.

[94] - Moenke-Blankenbourg, L., "Laser Micro Analysis", Progress in Analytical Spectroscopy, 9 (1986), 335.

[95] - Adrain, R. S. and J. Watson, "Laser Microspectral Analysis: a Review of Principles and Applications", Journal of Physics D: Applied Physics, 17 (1984), 1915.

[96] - Cody, R. B., R. C. Burnier, W. D. Reents, Jr, T. J. Carlin, D. A. McCrery, R. K. Lengel and B. S. Freiser, " Laser Ionization Source for Ion Cyclotron Resonance Spectroscopy. Application to Atomic Metal Ion Chemistry", International Journal of Mass Spectrometry and Ion Physics, 33 (1980), 37.

[97] - Freiser, B. S., "Investigation of Reactions of Metal Ions and Their Clusters in the Gas Phase by Laser-Ionization Fourier-Transform Mass Spectrometry", Talenta, 32(1985), 697.

[98] - Piepmeier, E. H. (Ed.), Analytical Applications of Lasers, Wiley-Interscience Publication, 1986, 703 p.

[99] - Moenke-Blankenburg, L., Laser Microanalysis,Wiley-Interscience Publication, 1989, 287 p.

[100] - Buckley, B. T. and C. B. Boss, Private communication, (1989).

APPENDIX I

COMPUTER PROGRAMS PERFORMING THE CALCULATIONS TO PRODUCE THE END CAP ELECTRODES AND THE RING ELECTRODE

The following computer program calculates the motion required by the lathe to create the required shape of the hyperbole of the end caps electrodes of the ion trap. The electrode was machined in the Mechanical Engineering Shop of the Chemistry department at the University of British Columbia. The program is written in BASIC. The programs requires, as input, the radius of the ring electrode for the trap that will be produced. It then calculates the motion of the lathe at intervals of 0.025 mm along the "*r*" axis of the trap.

```
10 Z = 0
20 R = 0
30 INPUT "r0: ";R0
40 R20 = R0^2
45 PRINT R0
50 Z0 = SQR((R20/2))
60 LPRINT "r0 = ";R0;
70 LPRINT "z0 = ";Z0
80 FOR I = 1 TO 10:LPRINT:NEXT I
90 LPRINT "End caps"
100 FOR Z = Z0 TO Z0 + 16.875 STEP .025
120  R= SQR(((Z^2)*2)-R20)
130 LPRINT "r = ";R*2;TAB(20)"z = ";Z-Z0
140 NEXT Z
150 FOR J = 1 TO 10:LPRINT:NEXT J
160 END
```

The following computer program calculates the motion required by the lathe to create the required shape of the hyperbole of the ring electrode. The electrode was machined in the Mechanical Engineering Shop of the Chemistry department at the University of British Columbia. The program is written in BASIC. The motion of the lathe is calculated at 0.05 mm interval along the "*z*" axis of the trap.

```
10 Z = 0
20 R = 0
30 INPUT "r0: ";R0
40 R20 = R0^2
45 LPRINT R0
50 Z0 = SQR((R20/2))
60 LPRINT "r0 = ";R0;
70 LPRINT "z0 = ";Z0
150 FOR J = 1 TO 10:LPRINT:NEXT J
160 LPRINT "ring electrode"
170 FOR I = 0 TO 20.05 STEP .05
175 J = I
180 R = SQR(((2*(J^2))+R20))
185 R1 = R - R0
190 LPRINT "r = ";2*R1;TAB(30)"z = ";I
200 NEXT I
210 END
```

APPENDIX II

DATA ACQUISITION SUBROUTINE

This procedure is part of the program used to control the ion trap and to acquire the mass spectra of the traped ions. It is written in TurboPascal.

```
PROCEDURE ScanSpectrum (VAR darray : diodearraytype;
                        scans : INTEGER);


 PROCEDURE SetupISC16;
 {  Purpose : To set the ports on the ISC-16 board.}

  VAR
   i : INTEGER;

  BEGIN
    { disable ISC-16 during initialization }
   PORT[$030B] := 0;
   { load muxRAM to sample channel 1 only }
   FOR i:= 1 TO 16 DO
     PORT[$0310] := 0;
   { select external clock input }
   PORT[$0311] := 0;
   PORT[$0307] := $74;
   PORT[$0305] := LO(CLOCKTIME);
   PORT[$0305] := HI(CLOCKTIME);
    { select external trigger, positive polarity, trigger slope }
   PORT[$0308] := 11;
    { set burst to sample 1 channel on each clock pulse }
   PORT[$0307] := 50;
   PORT[$0304] := 1; PORT[$0304] := 0;
    { set post trigger delay for 4096 samples }
   PORT[$0307] := 178;
   PORT[$0306] := 0; PORT[$0306] := 16;
  END; { SetupISC16 }

 PROCEDURE GetAverageData (VAR specarray : diodearraytype;
```

```
                numscans : INTEGER);

TYPE
  byteArrayType = ARRAY[1..MaxArraySize] OF INTEGER;

VAR
 lobyte, hibyte                 : byteArrayType;
 i,j,k,A,B,C, V,D,E,S           : INTEGER;
 hibytefactor, lobytefactor     : REAL;
 ch                             : CHAR;

BEGIN
 (* SET UP PORTS FOR TRIGGERS *)
 PORT[$21B] := $80;
 C := $21A;
 B := $219;
 A := $218;
 (* TRIGGERS READY *)
 FOR i:= 1 TO 4096 DO
  BEGIN
   lobyte[i] := 0;
   hibyte[i] := 0
  END;
 GoToXY(20,12);
 ch := ' ';
 WRITE('Scanning Spectrum: ');
 FOR i := 1 TO numscans DO
  BEGIN
      IF Keypressed THEN
       BEGIN
        READ(Kbd,ch);
         IF Keypressed AND (ch = #27) THEN
          READ(Kbd,ch)
       END;
      IF NOT (ch = #27) THEN
       BEGIN
```

```
GoToXY(39,12);
ClrEol;
GoToXY(39,12);
WRITE(i);
 { select bank B manual ( data saved to bank A ) }
PORT[$0315] := 0;
 { reset bank A memory pointer and set buffer size to 4K }
PORT[$031B] := 04;
 {reset trigger to external, positive polarity, slope}
PORT[$0308] := $0B;
port[$030b] := 0;
 { enable trigger logic and start data acquisition  }
PORT[$030D] := 0;
 { wait for trigger status flag to indicate external trigger pulse }
(* START OF THE EXPERIMENT *)
V := 4095 - D;
OUTDAC12_S (0,V);
(* INITIAL VOLTAGE ON RING SET *)
DELAY(5);
(* TRIGGER FOR ELECTRON GUN *)
PORT[A] := $0;
PORT[A] := $FF;
DELAY(1);
PORT[A] := $0;  (* ELECTRON GUN PULSE OVER *)
PORT[B] := $0;
DELAY(STORTIME - 3);
(* TRIGGER FOR DATA AQUISITION *)
PORT[B] := $FF;
DELAY(1);
PORT[B] := $0;
DELAY(1);
FOR J := 1 TO FINVOLT DO
  BEGIN
    V := 4095 - (INITVOLT + J);
    OUTDAC12_S (0,V);
  END;  (* FOR *)
```

```
        FOR J := 10 TO 40 DO
          BEGIN
            V := J * 100;
            OUTDAC12_S (0,V);
          END;  (* FOR *)
        V := 4095;
        OUTDAC12_S (0,V);
        DELAY(50);
        (* EXPERIMENT OVER, VOLTAGE ON RING = 0 *)
        { select bank A manual }
        PORT[$0314] := 0;
        FOR j:= 1 TO 4096 DO
          BEGIN
            lobyte[j] := mem[$D000:0] + lobyte[j];
            hibyte[j] := mem[$D000:0] + hibyte[j]
          END { inside for loop }
        END { if not ESC key pressed }
      END;  { for loop }
      hibytefactor := 256/numscans;
      lobytefactor := 1/numscans;
      FOR k := 1 TO 4096 DO
        specarray[k] := hibyte[k]*hibytefactor + lobyte[k]*lobytefactor
    END; { GetAverageData }

BEGIN { ScanSpectrum }
  setupISC16;
   GetAverageData(darray,SCANS);

END;  { ScanSpectrum }
```